

JOURNAL OF THE
Electrochemical
Society

105, No. 2

February 1958

แผนกห้องสมุด กรมวิทยาศาสตร์
กระทรวงอุตสาหกรรม

LIBRARY
FEB 11 1958
NAV CERELAB





Making better cells

The skills and experience of the men who renew electrolytic cells are a major factor in their economical performance.

Other significant factors include the quality, design and machining of

GLC anodes, which are carefully "custom made" to the requirements of individual cells.

FREE — This illustration of cell building has been handsomely reproduced with no advertising text. We will be pleased to send you one of these reproductions with our compliments. Simply write to Dept. J-2.

ELECTRODE
GLC[®]
DIVISION

GREAT LAKES CARBON CORPORATION

18 EAST 48TH STREET, NEW YORK 17, N.Y. OFFICES IN PRINCIPAL CITIES

EDITORIAL STAFF

R. J. McKay, Chairman, Publication Committee
Cecil V. King, Editor
Norman Hackerman, Technical Editor
Ruth G. Sterns, Managing Editor
U. B. Thomas, News Editor
H. W. Salzberg, Book Review Editor
Natalie Michalski, Assistant Editor

DIVISIONAL EDITORS

W. C. Vosburgh, Battery
J. E. Draley, Corrosion, I
R. T. Foley, Corrosion, II
John J. Chapman, Electrical Insulation
Abner Brenner, Electrodeposition
H. C. Froelich, Electronics
D. H. Baird, Electronics—Semiconductors
Sherlock Swann, Jr., Electro-Organic
John M. Blocher, Jr., Electrothermics and Metallurgy, I
A. U. Seybolt, Electrothermics and Metallurgy, II
W. C. Gardiner, Industrial Electrolytic
C. W. Tobias, Theoretical Electrochemistry, I
A. J. de Bethune, Theoretical Electrochemistry, II

REGIONAL EDITORS

Howard T. Francis, Chicago
Joseph Schuelein, Pacific Northwest
J. C. Schumacher, Los Angeles
G. W. Heise, Cleveland
G. H. Fetterley, Niagara Falls
Oliver Osborn, Houston
Earl A. Gulbransen, Pittsburgh
A. C. Holm, Canada
J. W. Cuthbertson, Great Britain
T. L. Rama Char, India

ADVERTISING OFFICE

ECS
1860 Broadway, New York 23, N. Y.

ECS OFFICERS

Norman Hackerman, President
University of Texas, Austin, Texas
Sherlock Swann, Jr., Vice-President
University of Illinois, Urbana, Ill.
W. C. Gardiner, Vice-President
Olin Mathieson Chemical Corp., Niagara Falls, N. Y.
R. A. Schaefer, Vice-President
Cleveland Graphite Bronze Div., Clevite Corp., Cleveland, Ohio
Lyle I. Gilbertson, Treasurer
Air Reduction Co., Murray Hill, N. J.
Henry B. Linford, Secretary
Columbia University, New York, N. Y.
Robert K. Shannon, Assistant Secretary
National Headquarters, The ECS, 1860 Broadway, New York 23, N. Y.

Journal of the Electrochemical Society

FEBRUARY 1958

VOL. 105 • NO. 2

CONTENTS

Editorial

Automatic Cathodic Protection 17C

Technical Papers

- The Relation of the Conditions of Electrodeposition of Manganese Dioxide to the Discharge Characteristics. *A. Kozawa and W. C. Vosburgh* 59
- Cathodic Disintegration of Tin. *H. W. Salzberg and F. Mies* 64
- Oxidation of an Aluminum-3 Per Cent Magnesium Alloy in the Temperature Range 200°-550°C. *W. W. Smeltzer* 67
- Metallographic Manifestations of the Air Oxidation of Tantalum at 750°C. *R. Bakish* 71
- Cathodic Reduction of Oxide Films on Iron, II. Determination of α -Fe₂O₃ and Fe₃O₄. *K. H. Buob, A. F. Beck, and M. Cohen* 74
- Temperature Characteristics of Barium Strontium Lithium Silicate Phosphors. *A. H. McKeag* 78
- Zone Purification of Silicon. *E. A. Taft and F. H. Horn* 81
- A Fused Salt Bath for Electrodeposition of Molten Cadmium-Indium Alloy. *G. L. Schnable and J. G. Javes* 84
- The Relationship between Thermal Decomposition in Vacuum and the Macrostructure of Alkaline Earth Carbonates. *B. Wolk* 89
- Zone Melting and Crystal Pulling Experiments with AISb. *W. P. Allred, B. Paris, and M. Genser* 93
- Transport Numbers in Pure Fused Salts: Lead Chloride, Lead Bromide, Thallous Chloride, and Silver Nitrate. *R. W. Laity and F. R. Duke* 97
- Lead Dioxide Anode for Commercial Use. *J. C. Grigger, H. C. Miller, and F. D. Loomis* 100

Technical Notes

- Enhanced Surface Reactions, II. Oxygen Adsorption on Several Metals. *M. J. D. Low* 103
- Photodeposition of Luminescent Screens. *M. Sadowsky and P. D. Payne, Jr.* 105

Current Affairs

- Come to New York in April 19C
- International Symposium on Passivity 20C
- New United Engineering Center to be Erected in New York City 20C
- Division News 21C Book Reviews 26C
- Section News 21C Announcements from 27C
- New Members 22C Publishers 27C
- Personals 23C Employment Situations 28C
- News Items 24C Index (Vol. 104, 1957) i

Published monthly by The Electrochemical Society, Inc., from Manchester, N. H., Executive Offices, Editorial Office and Circulation Dept., and Advertising Office at 1860 Broadway, New York 23, N. Y., combining the JOURNAL and TRANSACTIONS OF THE ELECTROCHEMICAL SOCIETY. Statements and opinions given in articles and papers in the JOURNAL OF THE ELECTROCHEMICAL SOCIETY are those of the contributors, and The Electrochemical Society assumes no responsibility for them. Nonrefundable subscription to members \$5.00; subscription to nonmembers \$18.00. Single copies \$1.25 to members, \$1.75 to nonmembers. Copyright 1958 by The Electrochemical Society, Inc. Entered as second-class matter at the Post Office at Manchester, N. H., under the act of August 24, 1912.

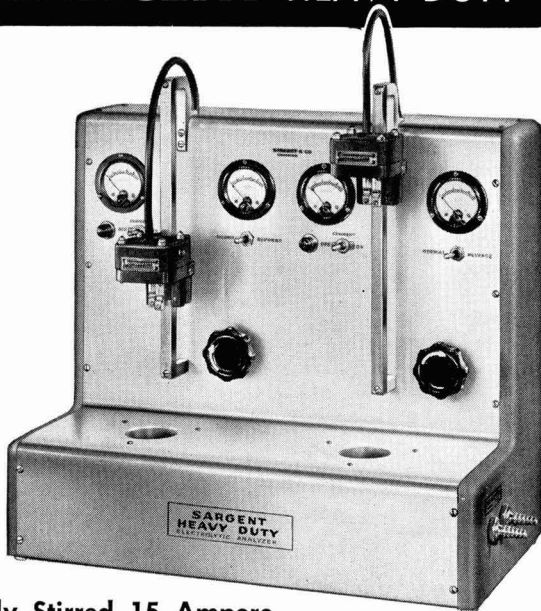
SARGENT SLOMIN



Motor-Stirred 5 Ampere

S-29465

SARGENT HEAVY DUTY



Magnetically Stirred 15 Ampere

Designed for continuous trouble-free performance, these electrolytic analyzers, manufactured by E. H. Sargent & Co., are durably constructed of the highest grade materials and component parts, including stainless steel front panel, cast aluminum end castings and stainless steel fittings.

Completely line operated, the Sargent analyzers employ self-contained rectifying and filter circuits. The deposition voltage between the electrodes is adjusted by means of auto-transformers, with meters indicating volts and amperes and controls on the panel. An easily replaceable fuse guards against circuit overload.

The Sargent-Slomin Analyzer stirs through a rotating chuck operated from a capacitor type induction motor, motor having a fixed speed of 550 r.p.m. with 60 cycle A.C. current or 460 r.p.m. with 50 cycle A.C. current. Motors are sealed against corrosive fumes; are mounted on cast metal brackets, sliding on 1/2" square stainless steel rods, permitting vertical adjustment of electrode position over a distance of 4". Pre-lubricated ball-bearings support the rotating shaft.

The Sargent Heavy Duty Analyzer provides efficient stirring by the interaction between the cell current and the field established by a permanent magnet, tubular in shape and coaxial with the cell holder.

The Heavy Duty has recessed wells to hold the sample beakers, wells being 6 1/4" deep, designed to contain 250 ml electrolytic beakers. The wall of each well serves as an inner wall of the water jacket, for use in either heating or cooling. Two serrated nipples for rubber tubing connections for cooling or heating water are mounted on the right end casting. In plain copper analysis, 1 gram of copper may be deposited in 15 minutes with an accuracy of approximately 0.05% without the necessity of special techniques.

All electrolytic analyzers accommodate electrodes having shaft diameters no greater than 0.059 inch. Stainless steel

spring tension chucks permit quick, easy insertion of the electrodes and maintain proper electrical contact. On the Heavy Duty Analyzer, the cathode chuck is eccentrically mounted, providing adjustability to accommodate electrodes up to 50 mm diameter. Special Sargent high efficiency electrodes are available for both analyzers.

Analyzers are complete with cord and plug for attachment to standard outlets. For operation from 115 volt, 50 or 60 cycle A.C. circuits.

	SARGENT-SLOMIN	HEAVY DUTY
Maximum D.C. current at each position	5 ampere	15 ampere
Maximum D.C. voltage at each position	10 volts	10 volts
Maximum power consumption	150* or 300 watts	400 watts
Height	18 inches	20 1/4 inches
Width	11 1/4* or 21 inches	21 inches
Depth	11 1/4 inches	11 1/4 inches
Net Weight	35* or 61 pounds	80 pounds
Shipping Weight	70* or 110 pounds	130 pounds

*One position unit

S-29459 ELECTROLYTIC ANALYZER — Motor Stirred, One Position, 5 Ampere, SARGENT-SLOMIN.....**\$300.00**

S-29460 DITTO. But with adjustable sub-surface heater**\$325.00**

S-29464 ELECTROLYTIC ANALYZER — Two Position, SARGENT-SLOMIN**\$490.00**

S-29465 DITTO. But with two adjustable heaters, pilot lights and control knobs.....**\$530.00**

S-29480 ELECTROLYTIC ANALYZER — Heavy Duty, Magnetically Stirred, Two Position, 15 Ampere, Sargent (illustrated top, right).....**\$610.00**

SARGENT

SCIENTIFIC LABORATORY INSTRUMENTS • APPARATUS • SUPPLIES • CHEMICALS

E. H. SARGENT & COMPANY, 4647 W. FOSTER AVE., CHICAGO 30, ILLINOIS
 MICHIGAN DIVISION, 8560 WEST CHICAGO AVENUE, DETROIT 4, MICHIGAN
 SOUTHWESTERN DIVISION, 5915 PEELER STREET, DALLAS 35, TEXAS
 SOUTHEASTERN DIVISION, 3125 SEVENTH AVE., N., BIRMINGHAM 4, ALA.



Automatic Cathodic Protection

CATHODIC protection has become a very important factor, indeed, in the never-ending war against corrosive deterioration. In recent years greatly improved knowledge of the requirements and of the mechanism of protection, as well as methods of testing the adequacy of performance, have made it possible to apply cathodic protection with economy and assurance of success. In some cases sacrificial anodes of magnesium or zinc, or of alloys, are eminently satisfactory if properly located and installed. In other cases it is preferable to supply current from power lines or from suitable generators. Both laboratory experiments and extensive field tests have shown that the main requirement is to keep the electrical potential of the metal which is to be protected, steel for example, at or beyond a given minimum value, with respect to a stable reference half-cell.

A long time ago the Canadian Navy found that more current is needed to maintain the proper potential of a ship's hull when it is idle in port, than when under way at sea. This led to the use of a dual protective system, with magnesium anodes to supply minimum current, plus additional current from the ship's generators when needed. In other instances, especially in marine installations, the necessary current varies with tidal flow, with winds, and other factors.

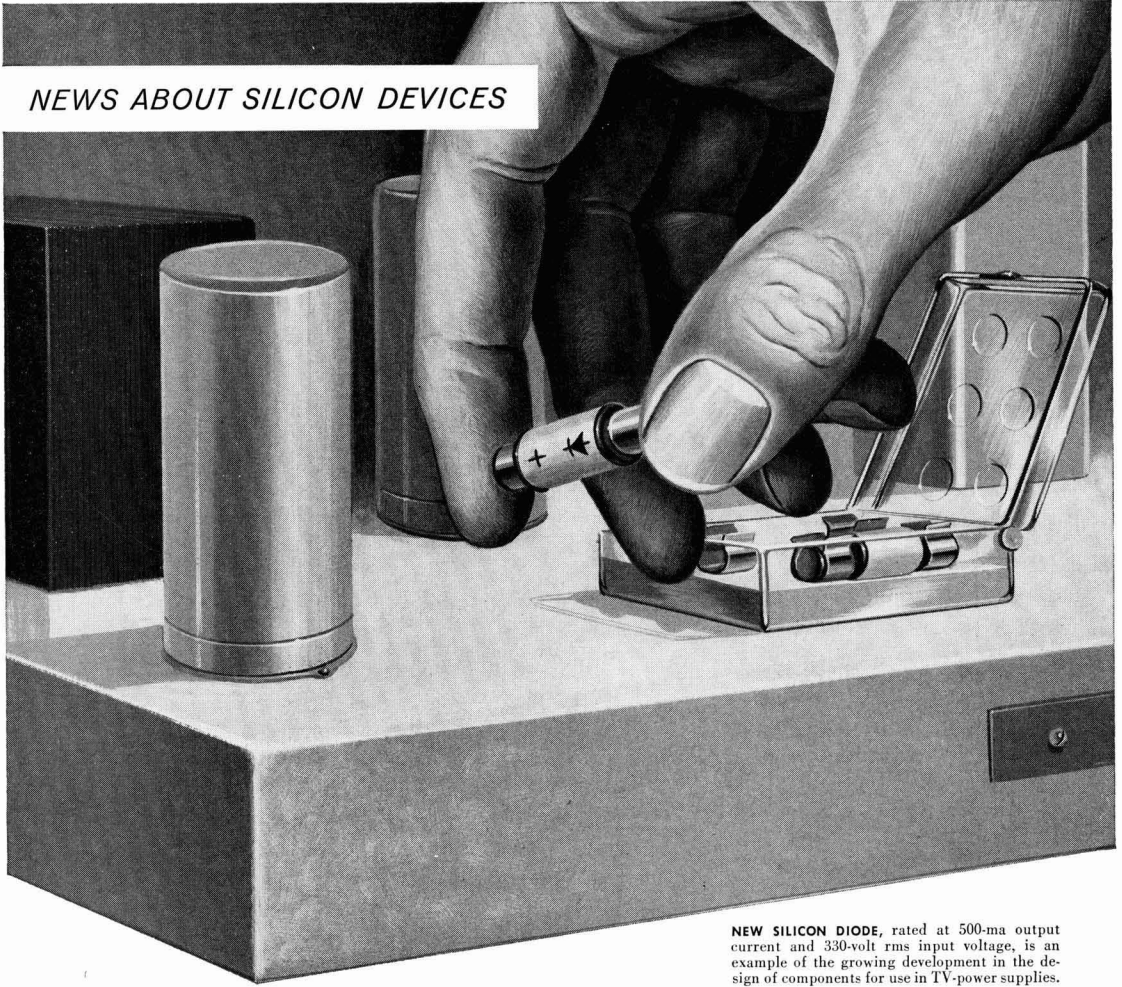
Such a system is an ideal one for use of automatic control. Modern potentiostats can maintain accurately the desired potential between a ship's hull, or other metal structure, and a reference half-cell, by supplying or by switching on and off varying amounts of current between the hull and an auxiliary anode. It was announced a few months ago that such automatic control systems, designed by Charles Engelhard, Inc., are in use on the Nautilus, the Sea Wolf, other vessels of the U. S. Navy, and a number of floating and stationary installations. A technical article describing some of the details may appear in this JOURNAL soon.

Of course, if a ship's hull could be covered with a completely flaw-free coating of paint or other protective material, cathodic protection would not be necessary. Unfortunately this is not the case. Only a few ma per square foot of hull gives maximum protection, but the exact current varies with the age and status of the paint, the position on the hull, composition and oxygen content of the water, speed of the ship, and other factors. It has been suggested, perhaps optimistically, that with adequate automatic cathodic protection, steel propellers, which would cost much less and be stronger than brass, might be used.

The Engelhard system uses noncorrosive platinum anodes, and this led to the appearance of the rather curious headline: "Platinum replaces magnesium to guard ships against corrosion on hulls and propellers."

—CVK

NEWS ABOUT SILICON DEVICES



NEW SILICON DIODE, rated at 500-ma output current and 330-volt rms input voltage, is an example of the growing development in the design of components for use in TV-power supplies.

Now... more efficient power supplies for radio-TV made possible with Du Pont Hyperpure Silicon

Actual test results as reported by various manufacturers indicate important advantages of silicon diodes and rectifiers. One TV manufacturer, for example, operated samples of silicon rectifiers under load continuously for 5,000 hours—with no noticeable drop in output voltage. Another manufacturer reports no voltage change after 500 hours in 95% humidity.

Silicon-equipped sets are relatively free of a decline in B+ voltage. Silicon diodes are up to 99% efficient in units operated at 60 cps—reverse leakage is as low as a few microamperes. Both rectifiers and transistors of silicon have temperature ratings far higher than those of other semiconducting materials... can operate continuously at -65° to 200°C .

Note to device manufacturers: You can produce silicon transistors, rectifiers and diodes of the highest quality with Du Pont Hyperpure Silicon. It's now available in three grades for maximum efficiency and ease of use... having a purity range of 3 to 11 atoms of boron per billion. Technical information is available on crystal growing from Du Pont... pioneer producer of semiconductor-grade silicon.



NEW BOOKLET ON DUPONT HYPERPURE SILICON

You'll find our new, illustrated booklet about Hyperpure Silicon helpful and interesting—it describes the manufacture, properties and uses of Du Pont Hyperpure Silicon. For your copy write to: E. I. du Pont de Nemours & Co. (Inc.), Silicon N-2496 -JE-2, Wilmington 98, Dela. (This offer is limited to U.S. and Canada.)

PIGMENTS DEPARTMENT



BETTER THINGS FOR BETTER LIVING
...THROUGH CHEMISTRY

The Relation of the Conditions of Electrodeposition of Manganese Dioxide to the Discharge Characteristics

Akiya Kozawa and W. C. Vosburgh

Department of Chemistry, Duke University, Durham, North Carolina

ABSTRACT

Electrodes were prepared by electrodeposition of MnO_2 at various temperatures and current densities or with NH_4^+ , K^+ , Zn^{++} , Mg^{++} , or Al^{3+} in the plating bath. The overpotential in acid electrolyte is largest when deposition is at high temperature and low current density. Variation in surface area seems to account for these effects. When NH_4^+ or K^+ is present in the plating bath, the MnO_2 contains NH_4^+ or K^+ and has a discharge curve in NH_4Cl electrolyte different from the normal. The other cations in the plating bath had only small effects. Heating at 140°C gave discharge curves resembling those of MnO_2 containing NH_4^+ in some respects.

In the preparation of electrodeposited electrodes in this laboratory the conditions generally have been approximately those of Nichols (1). Specifically, the bath contained about 50 g/l of $\text{MnSO}_4 \cdot \text{H}_2\text{O}$ and about 65 g/l of H_2SO_4 . The MnO_2 was electrodeposited on graphite rods at an apparent current density of 3.13 ma/cm² for 30 min with the bath at 80° or 90°C . The temperature of the plating bath affected the overpotential of the electrode when discharged in NH_4Cl solutions (2). In the present investigation the effect of variations of temperature and current density of electrodeposition, of the presence of certain foreign ions in the plating bath, and of heating the MnO_2 were studied.

Experimental

Preparation and discharge of electrodes.—Electrodes were prepared by electrodeposition of about 0.2 mmole of MnO_2 on 8 cm² of surface area of spectrochemical grade, 4.5 mm diameter graphite rods from a bath usually of the composition given above. The bath was maintained at constant temperature ($\pm 1.5^\circ\text{C}$) by a water bath and the current, furnished by dry cells and held constant manually, was measured by a milliammeter. The bath was not stirred. When not stated otherwise the temperature was 90°C , the current 25 ma, and the time 30 min. After electrodeposition electrodes were allowed to stand in water which was changed occasionally until no more acid was washed out. They were kept in water until used. Previous to discharge they were kept for several hours in the electrolyte to be used in the discharge.

Discharges (2) were carried out in vessels holding 250 ml of electrolyte with either clean lead or graphite anodes, the latter consisting of 5 rods surrounding the electrode to be discharged. Separation of cathode and anode was 2-3 cm. The cell was connected in series with four No. 6 dry cells and suitable resistance, and the discharge current was maintained constant manually. The electrolyte was stirred continuously during discharge by a magnetic stirrer. Air was not excluded. The potential of the discharg-

ing electrode was measured against a saturated calomel electrode by means of a recording potentiometer.

Effect of temperature and current density of electrodeposition on the overpotential in acid electrolyte.—Electrodes were made at 60° , 70° , 80° , 90° , and 97°C with a current of 25 ma for 30 min and at 90°C at current densities of 12.5, 25, 50, and 100 ma/electrode for 60, 30, 15, and 7.5 min, respectively. Overpotentials were measured in acid solutions as described previously (3). Briefly, an electrode was discharged for a short time with an electrolyte of 0.1M H_2SO_4 and 0.1M MnSO_4 , and when constant potential was attained the circuit was broken and the equilibrium open circuit potential was measured. The difference between the two was the overpotential. Several measurements could be made on a single electrode. With different electrodes the overpotentials at the same current agreed within 2 mv. Measurements were made with currents of 2, 4, and 6 ma/electrode of 8 cm² apparent surface. The iR drop was larger than previously (3) but probably did not exceed 2 mv. No correction was made. Results are shown in Fig. 1.

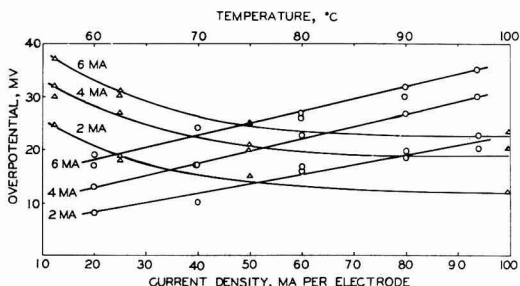


Fig. 1. Overpotentials in acid electrolyte (0.1M H_2SO_4 , 0.1M MnSO_4) of electrodes made by electrodeposition at various temperatures and current densities. The straight lines and upper scale of abscissas represent electrodes made at various temperatures and constant current (25 ma). The curves and lower scale of abscissas represent electrodes made at 90°C and various current densities, but with constant total MnO_2 .

Overpotential increases linearly with the temperature at which the MnO_2 was electrodeposited between 60° and 97°C. An increase of temperature of about 2° corresponds to an increase of overpotential of 1 mv. The overpotential decreases with increasing current at which the MnO_2 was electrodeposited. Between 12.5 and 50 ma/electrode (1.56-6.3 ma/cm²) the decrease is roughly 3 mv for 10 ma increase in electrodeposition current, but from 50 to 100 ma the change is much less than this.

A number of electrodes made at various temperatures and current densities were analyzed to see whether the above results could be correlated with changes in composition. Analyses were made by dissolution in FeSO_4 solution at room temperature for available oxygen¹ followed by potentiometric titration of the same samples for total manganese. Incomplete washing of the porous graphite rods after dissolution of the MnO_2 led to a positive error in x estimated as about 0.03. Between 80° and 97°C and at different current densities at 90°C the observed values of x in MnO_2 varied between 1.97 and 2.00 erratically and could not be correlated with the conditions of electrodeposition with any assurance. At 60° and 70°C x was appreciably lower, 1.94. Some other factor than composition of the MnO_2 must be responsible for the changes in overpotential.

Adsorption of zinc ion by MnO_2 .— Zn^{++} is adsorbed by MnO_2 from a slightly alkaline solution of ZnCl_2 and NH_4Cl . The amount of Zn^{++} adsorbed by electrodeposited MnO_2 electrodes from a particular solution increases as the overpotential of the electrodes decreases, and suggests that both phenomena are related to the same feature of the MnO_2 .

Previous to measurement of Zn adsorption an electrode was kept in 0.05M H_2SO_4 for 6 hr to remove any adsorbed Mn^{++} or lower oxide on the surface. Then it was washed and immersed for 12-15 hr at room temperature in 10 ml of Zn reagent, prepared by dissolution of 0.005 mole of ZnO in a liter of 0.5M NH_4Cl and having a pH of 7.2. Then the electrode was removed without washing and the excess Zn in the solution titrated with 0.01M ethylenediaminetetracetic acid disodium salt with eriochrom black T as the indicator. The difference between the amount of Zn in 10 ml of the original reagent and that in the reagent after removal of the electrode is the Zn adsorbed by the MnO_2 of the electrode. Because of the small quantities involved, errors may be 5-10%. The Zn adsorbed by a bare graphite rod was found to be negligible. The adsorbed Zn can be removed by keeping the electrode in 0.05M H_2SO_4 for several hours. After this a second trial leads to as much Zn adsorbed as in the first trial, or sometimes more.

The Zn adsorption must be dependent on the surface area of the MnO_2 and on the amount adsorbed per unit of surface. For MnO_2 samples sufficiently alike in structure the surface area is probably the more important. It will be assumed that, for similar samples of MnO_2 , Zn adsorption is proportional to surface area. The surface area of a sample of electrolytic MnO_2 was found to be 52.9 meter²/g by the

¹ This gives more nearly correct results than the method used previously (4). Details will be published.

B.E.T. method by Saito.² The same MnO_2 adsorbed 55.5×10^{-5} mole/g of Zn^{++} . Therefore, 1×10^{-5} mole of Zn^{++} is adsorbed by approximately 1 meter² of MnO_2 surface and one Zn^{++} occupies an area of 17 Å².

The surface area 25.4 meter²/g has been reported (5) for an electrolytic γ - MnO_2 in apparent disagreement with the value above. However, it is shown in Table II that even larger differences than this in electrolytic MnO_2 can be caused by differences in current density of electrodeposition.

Some representative data are shown in Table I. Four electrodes with different thicknesses of MnO_2 (plated on Karbate rods at 80°C and 25 ma for different times) were treated for 15 hr with the Zn reagent and the amount of Zn adsorbed measured by difference. The adsorbed Zn was then removed by standing in 0.05M H_2SO_4 for 6 hr after which a second and later a third measurement was made.

It is evident that the Zn adsorption is reversible and fairly reproducible. The increase in Zn adsorbed in successive trials may indicate a real increase of surface or greater accessibility to all parts of the surface as the result of the alternating treatment with NH_4Cl and acid solutions (4). The Zn adsorption by the two thinnest MnO_2 deposits is nearly proportional to the total MnO_2 , indicating a porous structure with all parts accessible to Zn^{++} . In the thicker layers the increase in adsorption with thickness is less, the inner part of the MnO_2 being less accessible than the outer portion.

It would be expected from these data that a thicker MnO_2 deposit would show a smaller overpotential on discharge than a thinner, if the apparent surface and the apparent current density are the same. A thicker deposit with its larger true surface would have a smaller true current density. This has been shown to be true previously (3).

Zinc adsorption data for electrodes prepared at different temperatures and at different current densities are shown in Table II, and in the last column

² H. Saito at Nagoya University.

Table I. Zinc adsorption by MnO_2 electrodes of varying thickness

Time of plating, min	1st Zn adsorption, mole $\times 10^5$	2d Zn adsorption, mole $\times 10^5$	3d Zn adsorption,* mole $\times 10^5$	Surface area, meter ²
60	1.72	2.32	2.40	1.7
30	1.40	1.70	2.00	1.4
15	1.05	1.19	1.18	1.1
7.5	0.59	0.60	0.55	0.6

* The Zn of the 2d adsorption was removed by 55 hr treatment with 0.05M H_2SO_4 , and 24 hr was allowed for the 3d adsorption.

Table II. Variation of overpotential with surface area as measured by Zn adsorption

Temp, °C	Plating conditions		Zinc adsorption, mole $\times 10^5$	Current calc'd, ma	Overpotential \bar{Y} and \bar{V} , mv	Obs. mv
	Current time, ma	min				
97	25	30	0.65	4.8	33	30
90	25	30	0.75, 0.80	4.0	29	27
80	25	30	0.87, 0.92	3.4 _s	26	23
90	12.5	60	0.50, 0.63	4.7	36	32, 30
90	50	30	1.05, 1.05	2.9 _s	25	20, 21
90	100	7.5	1.80, 1.76	1.7 _s	19	20

some overpotentials for similar electrodes, taken from the 4 ma data of Fig. 1. To test the relation between the two, the surface area of the electrode prepared at 90°C and 25 ma for 30 min was arbitrarily taken as unity, and relative surface areas for the other electrodes were calculated from the Zn adsorption data. The good reproducibility in overpotential of electrodes prepared under these conditions (3) shows that the surface area must be well controlled by the plating conditions. Then relative current densities were calculated by dividing the current per electrode, 4 ma in each case, by the relative surface area. Finally, overpotentials at the various relative current densities were interpolated from the data of Yoshizawa and Vosburgh (3) for their electrolyte No. 3. Their current per electrode is the same as the corresponding relative current density of Table II, because their electrodes were all prepared at 90°C and 25 ma for 30 min, assumed above to give unit surface. The overpotentials so calculated, given in the 7th column of Table II, are a little higher than the corresponding observed values of this investigation. Other experiments have shown that electrolyte No. 3 which contained 0.9M Na₂SO₄ in addition to 0.1M H₂SO₄ and 0.1M MnSO₄ gives overpotentials a few millivolts higher than without the Na₂SO₄. Correction of the Y and V values by subtracting 3 mv leads to as good agreement with the observed as can be expected. As far as these experiments can show, variations of overpotential with the current density and temperature of electrodeposition of the MnO₂ can be explained as the result of variations in surface area.

Discharge in ammonium-salt electrolyte.—Plating conditions have only a small effect in discharges in an ammonium-salt electrolyte of pH in the vicinity of 7.5. Four electrodes made like those described in Table II that were plated at 90°C and different current densities were discharged under carefully controlled conditions. The electrolyte was 2M NH₄Cl with enough NH₃ to give pH 7.65. The anode was five graphite rods surrounding the cathode, and the current passed was 2 ma for 100 min after which the electrode remained in the cell on open circuit for an additional 35 min. Under these conditions most of the Mn²⁺ passing into solution from the cathode in the discharge is deposited as an oxide on the anode rods. The amount so deposited was dissolved by H₂O₂ and H₂SO₄, and determined colorimetrically a HMnO₂. The small amount in the solution was determined also, and the sum of the two amounts is reported as Mn²⁺ formed.

The discharge curves were the same shape as the two lower curves of Fig. 2, or the upper one of Fig. 3, and showed small differences in closed-circuit potential such as would be predicted from Fig. 1. The Mn²⁺ formed was 0.33 × 10⁻² mmole for the 12.5-ma electrode, 0.28 × 10⁻² mmole for the 25-ma, and 0.19 × 10⁻² mmole for the 50 ma and 100 ma electrodes. The Mn²⁺ was 1-2% of the total Mn on the electrode and decreased a little with increasing surface area.

Electrodes plated at 70°, 80°, and 90°C also gave similar curves and the most Mn²⁺ for 90°-electrodes and the least for 70°C.

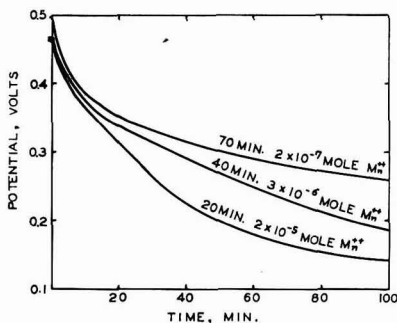


Fig. 2. Discharge curves for electrodes with different thicknesses of MnO₂; plating time at 25 ma for 8 cm² is a measure of thickness; Mn²⁺ passing into solution on discharge is given; discharges in 2M NH₄Cl and NH₃, pH 7.42.

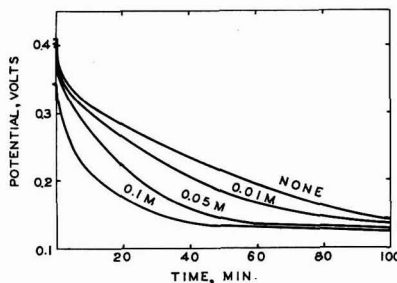


Fig. 3. Discharge curves for MnO₂ electrodes made with 0.01, 0.05, and 0.1M (NH₄)₂SO₄ in the plating bath compared with a curve for an electrode plated in the usual bath without (NH₄)₂SO₄.

Electrodes with different thicknesses differed more. Plated at 90° and 25 ma for 20, 30, 40, 50, and 70 min, five electrodes gave 2.3, 1.2, 0.3, 0.08, and 0.02 × 10⁻² mmole of Mn²⁺, respectively. The discharge curves at pH 7.56 for plating times of 20, 40, and 70 min are shown in Fig. 2. The two other curves fell in the expected places and were omitted for simplicity.

Comparison of Tables I and II shows that the variation of Zn adsorption with thickness is of the same order of magnitude as its variation with the current density of plating. However, the effect of thickness on the shape of the discharge curve and on the Mn²⁺ produced is much greater than the effect of current density. An increase in thickness not only brings about an increase in surface area, but also provides more MnO₂ for dilution of the lower oxide remaining on the electrode, if the latter diffuses into the interior of the oxide. Less lower oxide at the surface would lead to a higher closed-circuit potential and less Mn²⁺ going into solution. Both of these effects are observed, as Fig. 2 shows.

MnO₂ electrodeposited from solutions containing foreign cations.—MnO₂ electrodeposited from a bath containing (NH₄)₂SO₄ differs from that deposited in its absence and has been identified as α-MnO₂ (6, 7). Electrodes were prepared by electrodeposition from baths containing 0.01, 0.05, 0.10, and 1.0M (NH₄)₂SO₄ in addition to the usual MnSO₄ and H₂SO₄, and discharged in the usual manner in an electrolyte of 2M NH₄Cl and NH₃ with pH 7.8. In Fig. 3 the discharge

Table III. Zinc adsorption by electrodes prepared with 0.1 mole/l of foreign cation present and Mn^{2+} formed in the discharge

Foreign cation	NH_4^+	K^+	Mg^{++}	Zn^{++}	Al^{3+}
Zn^{++} ads., mole/electrode $\times 10^5$	1.15	1.17	0.62	0.42	0.67
Mn^{2+} formed, mmole $\times 10^2$	1.6	2.7	0.16	0.20	0.12

curves for electrodes plated in the presence of 0.01M, 0.05M, and 0.1M $(NH_4)_2SO_4$ are compared with the curve for one plated in absence of $(NH_4)_2SO_4$. The curve for 1M $(NH_4)_2SO_4$ was much like that for 0.1M. It is clear that NH_4^+ in the plating bath affects the shape of the discharge curve. The nearly flat portion of the lowest curve represents an approximately steady state in which the electrode surface is changing little with time, whereas there is no flat portion in the upper curve, which will arbitrarily be considered a normal curve.

The Mn^{2+} that went into solution during the five discharges was 0.38×10^{-2} mmoles for the normal and 0.95, 2.3, 3.4, and 3.3×10^{-2} mmoles for the four other electrodes in the order of increasing NH_4^+ concentration during preparation.

The lowest curve, for what was probably α - MnO_2 , falls much more steeply at the beginning than the normal. This may be explained as the result of slower diffusion of the lower oxide into the interior of the MnO_2 . An alternative explanation that the surface area of the α - MnO_2 is much smaller will be shown (Table III) to be improbable. With slower diffusion, the surface oxide becomes reduced to such a low potential that it can react with the electrolyte to give Mn^{2+} . When this reaction consumes the lower oxide as fast as it is produced a steady state results, with no further decrease of potential. This hypothesis can be checked by calculation of the electrical energy equivalent to the 3.4×10^{-2} mmoles of Mn^{2+} produced in the discharge represented by the lowest curve in Fig. 3. This calculation gives 110 ma-min to produce the Mn^{2+} , which may be compared with the 60 to 65-min period of constant potential with a current of 2 ma. The difference allows for production of a little lower oxide remaining on the electrode and accounting for the slight downward trend of the curve.

Electrodes were prepared from solutions containing K_2SO_4 , $ZnSO_4$, $MgSO_4$, or $Al_2(SO_4)_3$. When the concentration of the foreign cation was 0.1M the electrodes gave the discharge curves shown in Fig. 4. The curves for Zn^{2+} , Mg^{2+} , and Al^{3+} are little dif-

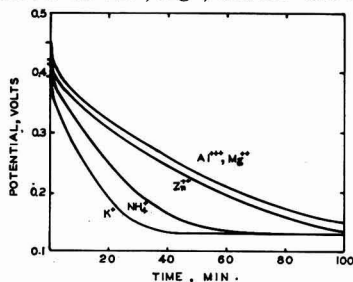


Fig. 4. Effect of a foreign ion present during the electro-deposition of the MnO_2 on the shape of the discharge curve; discharges in 2M NH_4Cl and NH_3 , pH 8.

ferent from the normal curve for electrodes made with no foreign cation present (compare with Fig. 3). The curve for K^+ resembles closely the curve for NH_4^+ . Data for Zn adsorption and the Mn^{2+} formed in the five discharges are given in Table III. Here also the NH_4^+ and K^+ electrodes are alike and different from the other three.

The effect of NH_4^+ and K^+ in the plating bath on the overpotentials in acid electrolyte of the resulting electrodes was within the limits of variability of the electrodes except when the NH_4^+ or K^+ concentration was 0.3 to 1M. At these higher concentrations the effect was a decrease in overpotential.

Analysis for NH_4^+ and K^+ .—Several electrodes prepared in the presence of NH_4^+ or K^+ were analyzed for these ions. The MnO_2 was dissolved by 10 ml of 1% H_2O_2 in 1M H_2SO_4 and the solution diluted to 100 ml. For NH_4^+ a 10 ml portion was treated with excess KOH and the resulting NH_3 distilled by heating in a slow current of air and catching in water. The NH_3 was then determined colorimetrically by Nessler's reagent. For K^+ a flame photometer was used. Both methods were checked by known solutions. Results are shown in Table IV.

The NH_4^+ or K^+ content of MnO_2 increases as the concentration of the foreign ion in the plating bath increases. The two ions are much alike in the relation of concentration to the mole ratio in the MnO_2 . The mole ratio of Mn:K in the formula for a typical cryptomelane (8) is 100:8.5, and this ratio is approached by the electrolytic MnO_2 .

Replacement of K^+ in MnO_2 by other ions.—It is of interest to inquire to what extent K^+ in MnO_2 can be exchanged for other ions, especially NH_4^+ , when the MnO_2 is placed in a suitable medium. Electrodes were made in a bath containing 0.1M K_2SO_4 , then

Table IV. NH_4^+ or K^+ content of electrodes made by electrodeposition in presence of $(NH_4)_2SO_4$ or K_2SO_4

$(NH_4)_2SO_4$ or K_2SO_4 M	NH_4^+ in MnO_2 mg/electrode	K^+ in MnO_2 mg/electrode	Moles/100 g-atoms Mn NH_4^+ K^+	
0	0.01	0.06	—	—
0.01	0.10	0.36	3.6	4.6
0.05	0.18	0.47	6.5	6.0
0.10	0.20	0.62*	7.3	7.9
0.30	0.22	0.62	7.8	7.9
0.5	—	0.65	—	8.3
1.0	0.24	—	8.6	—

* Average for 3 electrodes; 0.62, 0.63, 0.61.

Table V. Exchange of K^+ for other ions when MnO_2 containing K^+ is digested for 3 days with various solutions

Solution	K^+ after treatment mg/electrode	K^+ ex-changed %
H_2O , 0.1 and 1M $MgSO_4$	0.60, 0.60, 0.60*	0
0.1 and 0.3M NH_4Cl	0.32, 0.28	53, 48
1 and 4M NH_4Cl	0.25, 0.25	58
0.3 and 1M H_2SO_4	0.53, 0.48	12, 20
0.3 and 1M $ZnCl_2$	0.59, 0.58	3
0.1 and 1M $CuSO_4$	0.59, 0.57	3

* Compare 4th line of Table IV.

well washed and kept in solutions of NH_4Cl , H_2SO_4 , ZnSO_4 , ZnCl_2 , CuSO_4 , and MgSO_4 for 3 days at room temperature. They were then kept in water for a day to wash out salts and the K content determined. Results are shown in Table V.

Nearly 60% of the K^+ is replaced in 1M NH_4Cl whereas only 20% is replaced in 1M H_2SO_4 . The divalent cations have little or no effect.

The minimum in the discharge curve.—The discharge curve of a MnO_2 electrode often passes through a minimum potential (2, 3). The cause of the minimum is not clear and some observations on the effect of conditions of preparation of the electrodes on the minimum are recorded in the interests of its better understanding.

Electrodes plated at 90° and 97°C at 25 ma for 30 min and at 80° and 90°C at 12.5 ma for 60 min showed a pronounced minimum in the first discharge in 0.1M H_2SO_4 and 0.1M MnSO_4 . Electrodes plated at 60°–80°C at 25 ma for 30 min and at 90°C at 50 or 100 ma for 15 or 7.5 min showed no minimum. The conditions of the latter group lead to larger surface areas than the conditions of the former group.

Increasing amounts of K^+ in the MnO_2 led to decreasing depth of the minimum and an electrode made with 1M K_2SO_4 present gave no minimum. Amounts of NH_4^+ in MnO_2 resulting from the presence in the plating bath of 0.05–1M $(\text{NH}_4)_2\text{SO}_4$ gave no minima.

In discharges in 1M NH_4Cl buffered at pH 4 with an acetate buffer the minimum is usually much more pronounced than in acid electrolyte, 20–40 mv deep as compared with 9–14 mv in acid. Electrodes plated in solutions containing 0.1M $(\text{NH}_4)_2\text{SO}_4$, 0.1M K_2SO_4 , and 0.1M MgSO_4 gave no minima, although the overpotential was the same as for a normal electrode.

Effect of heating MnO_2 .—Heating some forms of MnO_2 decreases the electrode potential, reduces the discharge capacity, improves the crystal form, changes the iso-acidic point, and makes small changes in the available oxygen (9, 10). These changes were observed at temperatures above 100°C and mostly above 150°C. However, even below 100°C heating has an effect on the shape of the discharge curve and at 140°C a pronounced change takes place.

Electrodes after thorough washing were heated as in Table VI. They were then discharged for 100 min at 2 ma in 2M NH_4Cl and NH_3 with pH 7.8. The Mn^{++}

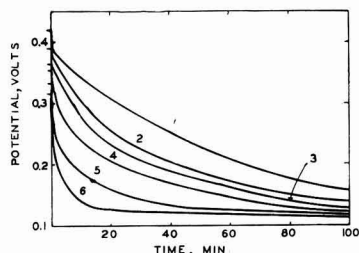


Fig. 5. Discharge curves for electrodes that were heated after preparation. The numbers refer to the electrode numbers in Table VI where the heating conditions and the Mn^{++} produced in the discharges are given.

which passed into the solution is shown in Table VI and the curves are shown in Fig. 5.

Heating, either in an oven or in hot water, has a progressively increasing effect as the temperature increases from 90° to 140°C. The discharge curve has a steeper initial portion, larger drop in potential, and is more nearly flat after the initial drop as the temperature increases. The amount of Mn^{++} formed increases as the curve drops to lower and lower potentials and becomes more nearly flat in the second portion.

The curve shapes for heated MnO_2 are very much like those for MnO_2 prepared in the presence of NH_4^+ . There is some difference between the two in discharges in 1M NH_4Cl buffered at pH 4, however. Under these conditions no minimum in the discharge curve was found for α - MnO_2 containing NH_4^+ whereas both normal MnO_2 and heated MnO_2 (150°C) gave pronounced minima. The α - MnO_2 had about the same overpotential as normal at pH 4, but heated MnO_2 had an overpotential about 30% larger than the normal.

Acknowledgment

This work was supported in part by the Office of Naval Research.

Manuscript received Aug. 26, 1957. This paper was prepared for delivery at the Buffalo Meeting, Oct. 6–10, 1957.

Any discussion of this paper will appear in a Discussion Section to be published in the December 1958 JOURNAL.

REFERENCES

- G. W. Nichols, *Trans. Electrochem. Soc.*, **62**, 393 (1932).
- A. M. Chreitberg, Jr., and W. C. Vosburgh, *This Journal*, **104**, 1 (1957).
- S. Yoshizawa and W. C. Vosburgh, *ibid.*, **104**, 399 (1957).
- S. Hills and W. C. Vosburgh, *ibid.*, **104**, 5 (1957).
- W. Buser and P. Graf, *Helv. Chim. Acta*, **38**, 828 (1955).
- S. Okada, I. Uei, and H. Chin, *J. Electrochem. Soc. Japan*, **15**, 79 (1947).
- I. Nakajima, *ibid.*, **21**, 369 (1953).
- J. W. Gruner, *Am. Mineralogist*, **28**, 497 (1943).
- J. Brenet and A. M. Moussard-Briot, *Rev. gén. élec.*, **61**, 405 (1952).
- A. Kozawa and K. Sasaki, *J. Electrochem. Soc. Japan*, **22**, 569 (1954).

Table VI. Conditions for heating electrodes and the Mn^{++} produced on discharge at pH 7.8

Electrode	Manner of heating	Temp., °C	Time of heating, hr	Mn^{++} mmole \times 10 ²
1	(None)	—	—	0.32, 0.50
2	Oven	90	14	0.59
3	Water	100	5	0.77
4	Oven	105	3	0.69
5	Oven	125	3	2.96
6	Oven	140	3	3.86

Cathodic Disintegration of Tin

H. W. Salzberg

City College, New York, New York

F. Mies

Brown University, Providence, Rhode Island

ABSTRACT

Disintegration of tin cathodes at high current densities was studied in neutral, acid, and alkaline solutions of sulfuric acid and alkali and ammonium hydroxides, sulfates, and chlorides. The tin left the surface as SnH_2 and the i_c 's were of the order of amp/cm^2 . Acid decreased the disintegration rate, salts added to acid increased the rate, salts added to neutral solution decreased the rate. The cation effect was specific, disintegration rates decreasing in the order sodium, potassium, lithium, ammonium, and hydronium ion.

Previous work on Pb (1,2) and Sb (3) indicated that cathode disintegration was the result of hydride formation via reduction of water molecules. The present investigation was undertaken in the expectation that tin hydride would be formed at low current densities and so give insight into the source of the hydrogen evolved at these low current densities. Instead, tin cathodes disintegrated only at extremely high current densities and this paper reports these anomalous results. The apparatus, materials, and method were the same as used previously (2,3).

Observations and Results

The disintegration rate was independent of time, as with Pb and Sb. Impurities seemed to have less of an effect. Critical current densities were much higher, the i_c 's being about an order of magnitude bigger, i.e., amperes per cm^2 , and the cation effect was very specific. In concentrated ammonium salt solutions, small amounts of ammonia gas were given off at about $0.5 \text{ amp}/\text{cm}^2$. The most striking observation, other than the magnitude of the current density, was the fact that even though tin hydride is a fairly stable compound at room temperature (5), most of the Sn lost to the cathode appeared as metallic Sn in the electrolysis cell. Only traces of Sn were picked up from the exit gas.

Figure 1 shows that for NaOH the slopes are less than theoretical for formation of SnH_2 , and that both slope and rate decrease as concentration increases. The rate in KOH was negligible in comparison to that in NaOH, and in NH_4OH there was no disintegration at all.

For neutral solutions (Fig. 2) the following was found:

(a) Disintegration rates decrease in the order Na^+ , K^+ , Li^+ . The rate in rubidium chloride was too small to be plotted and nothing at all was observed in either lithium chloride or ammonium sulfate.

(b) Increased Na_2SO_4 concentration decreased the rate. The intercept was increased but the slope was practically unchanged.

(c) Addition of KCl to Na_2SO_4 solution decreased the rate markedly but the reverse, adding Na_2SO_4 to KCl solutions, did not seem to have much of an effect.

(d) Adding LiCl to Na_2SO_4 did not seem to have any effect.

(e) Not shown on the graph are the results for addition of 0.02M RuCl_2 and 0.02M CsCl to 0.1M Na_2SO_4 . The disintegration was completely stopped up to at least $2.7 \text{ amp}/\text{cm}^2$ which was as far as the experiment went.

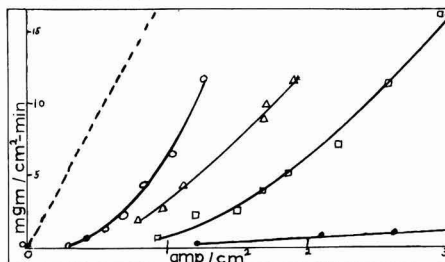


Fig. 1. Alkaline solution. Open circle represents 0.1M NaOH ; open triangle, 1M NaOH ; open square, 5M NaOH ; closed circle, 2M KOH .

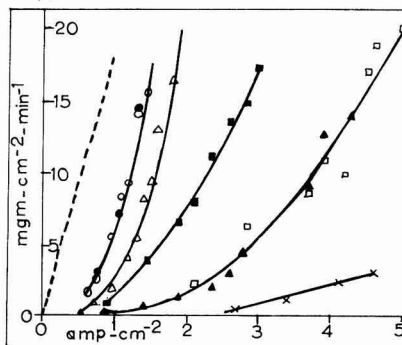


Fig. 2. Neutral solution. Open circle represents 0.1M Na_2SO_4 ; solid circle, 0.1M Na_2SO_4 plus 0.04M LiCl ; solid square, 0.1M Na_2SO_4 plus 0.04M KCl ; open square, 0.02M Na_2SO_4 plus 0.1M KCl ; open triangle, 1M Na_2SO_4 ; solid triangle, 0.1M KCl ; X, 0.2M LiCl .

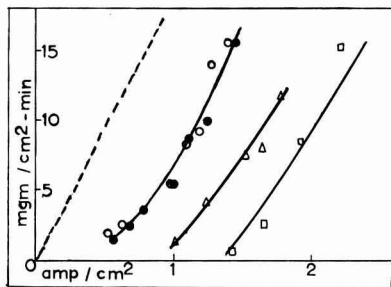


Fig. 3. 0.1M Na_2SO_4 . Open circle represents 0.0M H_2SO_4 ; solid circle, 0.01M H_2SO_4 ; open triangle, 0.1M H_2SO_4 ; open square, 0.2M H_2SO_4 .

In the presence of a constant amount of neutral salt, addition of acid decreased the rate sharply (Fig. 3). No decrease was noted in 0.1M Na_2SO_4 until the acid/salt ratio was greater than 1/10. Increased salt concentration at constant acidity increased the rates. Additional, ungraphed results showed that in more concentrated salt solutions rates were lower at the same acid/salt ratios and that the decrease began at lower acid/salt ratios. In other words, the rate depends on total ionic strength and total acidity as well as the acid/salt ratio. Also ungraphed, is the observation that in the absence of salt small amounts of acid lowered the rate drastically. For example, in 0.1M sulfuric acid the weight loss was only 0.4 $\text{mg}/\text{cm}^2\text{-min}$ at 4 amp/cm^2 .

Discussion and Conclusions

The disintegration is due to hydride formation since (a) the exit gas rapidly reduces silver nitrate; (b) the weight loss of the Sn is linear with current density and the slope of the curve corresponds to that required for formation of the known hydride, SnH_2 (at weight losses greater than 30 $\text{mg}/\text{cm}^2\text{-min}$ or 40 monolayers/sec the linearity disappears due to erosion as pieces fall off the surface); (c) the possibility of a tin-alkali alloy which reacts with water is ruled out because an increase in the concentration of any alkali cation either decreases the rate sharply or stops it completely. Even more to the point, disintegration was observed in dilute H_2SO_4 in the absence of alkali cations.

The SnH_2 is formed in a strained and unstable state. Since stannane is a tetrahedral molecule, it would have to be in a highly strained state (5,7) when formed at a planar surface. Even though unstrained stannane is stable at room temperature the strained variety should decompose rapidly, decomposition perhaps being catalyzed by cations in the double layer. This would explain the small amount of stannane found in the exhaust gas and the large amount of colloidal Sn found in the cell and also the low efficiency of electrolytic stannane production, reported by Paneth (6).

Figure 3 shows that the increase in hydronium ion concentration merely shifts the curve along the axis to higher current densities without change in slope. This indicates that the reaction is the same but that a higher current density is needed to start it, probably to remove the extra hydronium ions.

Also, if surface hydronium ions are displaced by sodium ions, i.e., if salt is added to acid, the rate increases. The lack of disintegration in acid solutions would therefore seem to be due to the reduction of hydronium ions at potentials too low for stannane formation. Only water molecule reduction would allow the potential to rise enough to form stannane. Certainly, at the extremely high current densities used here, there is not enough surface H_3O^+ ion to support the current (4) and the source of the hydrogen found in the stannane must be the water molecule.

The specificity of the cation effect must be explained on the basis of competing effects in the double layer. At first glance, this seems to be in accord with the alkali-alloy hypothesis, i.e., rates increase and E° decreases in the same order, Li, K, Na. However, in addition to the general evidence mentioned above the alkali-alloy hypothesis is not tenable because (a) disintegration rates in Li^+ solutions are much greater than in those of Cs^+ or Ru^+ , although Li has a higher E° ; (b) the deposition potential of Li is 0.10 v higher than that of K^+ and 0.3 v higher than that of Na^+ . Assuming a Tafel slope of 0.12 for the deposition of H_2 on Sn, the current density needed for Li^+ deposition would have to be about 7 times that for K^+ deposition and about 400 times that for Na deposition. Since, according to the alloy hypothesis, the disintegration rate would be proportional to the alkali deposition rate, the current densities at equal disintegration rates would have to be in the approximate ratio 400/57/1 for Li, K, and Na salt solutions, respectively. Figures 1 and 2 show that this is definitely not the case.

The formation of SnH_2 requires both a high potential and a surface largely covered by SnH_2 groups adjacent to each other. A large cation would not affect the potential particularly and would not be adsorbed strongly, but if adsorbed it would cover a large surface area. A small cation, with a more intense field, would cover a smaller portion of the surface but would be more strongly adsorbed and in addition have a greater effect in lowering the potential across the double layer.

Ion hydration decreases from Li to Cs and therefore so does the ionic radius. The area covered by the ion decreases in proportion to the square of the decrease in ionic radius. On the other hand, the force of attraction between the ion and the surface, and hence the adsorption, increases as the reciprocal of the square of the radius increases. These competing effects should cause a minimum to appear in the curve of surface coverage vs. ionic radius. If the minimum were in the neighborhood of the sodium ion radius, solutions of sodium salts should show maximum disintegration rates.

Some support is lent to this picture by the fact that mixtures of lithium and sodium salts show the disintegration rate expected of the smaller and more tightly held sodium ion and mixtures of sodium and potassium salts show the rates expected of the potassium salt solution.

The effect of ammonium ion is not covered by this explanation. Here, the evidence indicates that the ammonium ion is itself reduced, probably at a lower potential than that needed for stannane formation. This statement is based on the facts that (a) addition of ammonium salts to a sodium salt solution almost completely stops disintegration; (b) small quantities of ammonia gas are observed to be given off from the solution, even in 0.1M sulfuric acid; (c) the surface of the tin darkens during this process, losing its metallic luster.

At current densities above i_0 , the surface is probably saturated with unstable SnH_2 molecules. The reasoning for this is as follows.

Since the 4 hydrogen atoms needed for SnH_4 are almost certainly not produced by consecutive reductions at the same site, at least 2 sites and therefore 2 tin atoms are involved, with some sort of disproportionation following the electrochemical reduction. The most probable disproportionation would be the one involving two tin atoms each with two hydrogen atoms. The hydrogen atoms would not be in the form of an adsorbed molecule, since at the high current densities of this reaction the molecules would be formed in such a high energy state that they could desorb immediately on formation. Instead, the two hydrogen atoms would have to be associated with the tin atom as a complex or hydride. This SnH_2 hydride would have to be non-volatile, and unstable, the first because the slope of the curve shows that tin leaves in the tetravalent state, the second because no SnH_2 has been reported. This molecule would decompose to tin and hydrogen molecules unless it reacted with an adjacent SnH_2 to form SnH_4 and a tin atom. Since at and above i_0 most of the current goes into removal of tin from the surface, (one equivalent of tetravalent tin for each faraday) the surface would have to be saturated with SnH_2 molecules.

Below i_0 , the surface is unsaturated and the large current densities are required to saturate the surface with the unstable SnH_2 molecules. This statement is based on the following considerations.

The over-all disintegration rate is determined either by the reactions involved in forming the SnH_2 or by the disproportionation between two SnH_2 groups. If the former, the rate-determining step will be either electrochemical or a chemical combination of two atoms. If the rate-determining step is electrochemical, both disintegration and the over-all current density will be semilog functions of poten-

tial and therefore linear with each other at i_0 . However, the graphs show that the intercept at i_0 is curved, which eliminates an electrochemical step as the rate-determining factor. If the rate is determined by the chemical combination of two hydrogen atoms, to form an SnH_2 complex, the rate will be proportional to the square of the hydrogen atom concentration. Since until stannane is evolved all the hydrogen leaves the surface as H_2 , $i = k\text{H}^2$, so that the disintegration rate should be linear with current. Since the figures are definitely curved, at the intercept, this possibility is also eliminated.

Finally, if the disintegration is determined by the rate of combination of two SnH_2 groups, each of which would have to be in equilibrium with two hydrogen atoms, the over-all rate would be proportional to the fourth power of hydrogen atom concentration and therefore proportional to the square of the current density. The graphs seem to support this possibility, within experimental error.

This picture of an over-all rate being determined by the combination of adjacent unstable complexes would explain (a) the very high current densities needed, (b) the relative insensitivity of the reaction to high overvoltage poisons such as mercury and lead, and (c) the relatively inefficient production of stannane even at high overvoltage cathodes.

Acknowledgment

This work was done under a research contract with the Office of Naval Research. The authors wish to thank J. C. White and Sigmund Schuldiner of the Naval Research Laboratory for their encouragement and technical assistance and Saul Berman of the Office of Naval Research for his administrative assistance.

Manuscript received Nov. 15, 1956.

Any discussion of this paper will appear in a Discussion Section to be published in the December 1958 JOURNAL.

REFERENCES

1. H. W. Salzberg, *This Journal*, **100**, 146 (1953).
2. L. Gastwirt and H. W. Salzberg, *ibid.*, **104**, 701 (1957).
3. A. Andreaitch and H. W. Salzberg, *ibid.*, **101**, 528 (1954).
4. S. Schuldiner, *ibid.*, **99**, 488 (1952).
5. D. Hurd, "Chemistry of the Hydrides," John Wiley & Sons, Inc., New York (1952).
6. F. Paneth and E. Rabinowitch, *Ber.*, **57B**, 1877 (1924).
7. J. W. Mellor, "Reference Book of Inorganic Chemistry," Vol. 1, p. 324, Longmans, Green and Co., London (1922).

Oxidation of An Aluminum-3 Per Cent Magnesium Alloy in the Temperature Range 200°-550°C

W. W. Smeltzer¹

Aluminium Laboratories Limited, Kingston, Ontario, Canada

ABSTRACT

A study of the oxidation and magnesium evaporation kinetics has been carried out on an aluminum-3% magnesium alloy. A metallographic examination of the surface oxide films produced was included. The alloy was oxidation resistant to 200°C. At temperatures greater than 350°C the oxidation rate was initially inversely proportional to the oxide film thickness, transforming to a constant rate for long exposures. Selective oxidation of magnesium caused formation of aluminum inclusions in the surface oxide. These inclusions imparted a black discoloration to the alloy surface. Magnesium evaporated from the alloy in a vacuum at temperatures greater than 350°C after an induction period, the duration of which was dependent on the temperature. A comparison of the magnesium evaporation and alloy oxidation rates demonstrated that the oxide film offered resistance to oxidation of the metal.

It has been shown in previous investigations that oxide film structures on alloys containing up to 10% Mg are dependent on the mode of heating, and final temperatures attained as amorphous oxide formed at room temperature may crystallize into γ -alumina or $MgAl_2O_4$ and MgO (1, 2). Magnesia forms rapidly on these alloys if they are exposed to steam (3-6). The surface of the Al-Mg alloy is discolored gray to black by high temperature oxidation and it has been suggested that this effect is associated with the MgO content of the oxide film (2). This discoloration is decreased by volatilization of NaBF₄ into the oxidizing atmosphere (7), pre-exposure of the alloy to HF (3), or small additions of Be to the metal (5, 8).

Although Al forms an oxide film highly resistant to oxidation (9, 10), Al additions increase the oxidation rates of Mg (11, 12). For the converse case, additions of Mg to Al, information is not available. Hence, in this investigation the oxidation rates of an Al-3% Mg alloy in pure oxygen have been investigated. Some results of studies on Mg evaporation rates from the alloy and metallographic examination of the oxide films are also included.

Experimental

The alloy used in this investigation was prepared from high purity Al and Mg and contained 2.87% Mg and impurities of 0.002% Cu, 0.03% Fe, and 0.001% Si. The 0.063 in. gauge sheet as received was cold-rolled to 0.013 in., annealed for 30 min at 400°C, and further cold-rolled to 0.010 in. Specimens, 0.6800 g, were prepared from sections of this sheet after they had been polished to 000 emery under kerosene and then on a dry Selvyt cloth. All specimens were stored in a desiccator after preparation and prior to use.

A vacuum microbalance assembly, which has been described previously (9, 13), was employed for the measurement of the oxidation and Mg evaporation

rates. Oxidation rates were determined from specimen weight increases in oxygen at 7.6 cm oxygen pressure and Mg evaporation rates were determined from specimen weight losses in a vacuum of 10^{-6} mm. Each specimen was suspended on the microbalance and degassed at room temperature in a vacuum for 5 hr prior to further experimentation. For oxidation tests at 200° and 350°C each specimen was degassed 30 min at 400° and 12 hr at 350°C, respectively. At higher temperatures oxygen was admitted to the specimens before the initiation of Mg evaporation.

Results of oxidation tests in the temperature range 200°-550°C for short and long exposures are illustrated in Fig. 1 and 2. These results show that the alloy was relatively oxidation resistant at a temperature of 200°C. As the temperature was elevated, the oxidation rate increased. However, rapid oxidation did not occur until a temperature

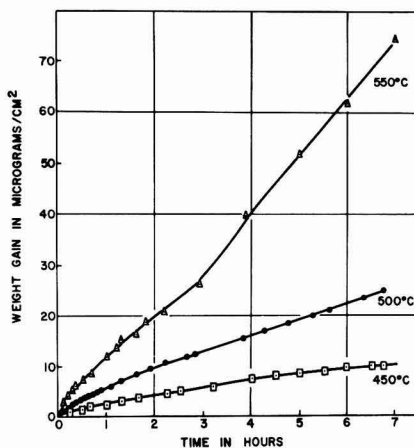


Fig. 1. Oxidation of metallographically polished Al-3% Mg alloy in the temperature range 450°-550°C.

¹ Present address: Metals Research Laboratory, Carnegie Institute of Technology, Pittsburgh, Pa.

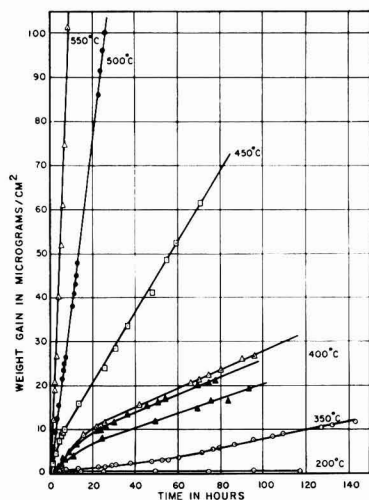


Fig. 2. Oxidation of metallographically polished Al-3% Mg alloy in the temperature range 200°-550°C.

of 400°C was exceeded. The initial rate of oxidation decreased with time but gave way to an approximately constant rate at oxygen weight gains less than $10 \mu\text{g}/\text{cm}^2$ (less than 1000Å film thickness) over the temperature range 350°-550°C. Thus an increase in film thickness beyond a certain range did not increase oxidation resistance. The reproducibility of the measurements is illustrated by the three 400°C curves in Fig. 2.

Results of the Mg evaporation tests in the temperature range 350°-500°C are illustrated in Fig. 3. There was an initial weight loss of approximately $10 \mu\text{g}/\text{cm}^2$ because of loss of gas as each specimen was heated in vacuum to the evaporation test temperature. This was followed by an additional weight loss due to Mg evaporation after an induction period which was dependent on the temperature. For example, this period was 200 min at 375°C and was of such short duration at 500°C that it could not be determined accurately. Magnesium evaporation measurements were reproducible to 10%.

Marked discoloration of the Al-3% Mg alloy occurred on exposure to oxygen above 400°C. Conversely, metallographically polished specimens and a specimen with a thick oxide layer (100μ) were

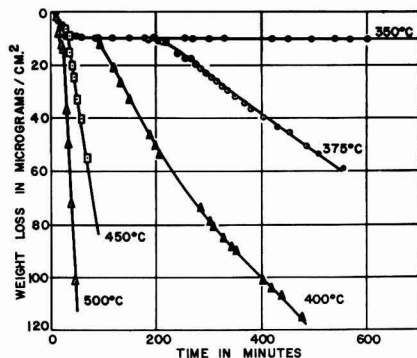


Fig. 3. Evaporation of Mg from metallographically polished Al-3% Mg alloy in the temperature range 350°-500°C.

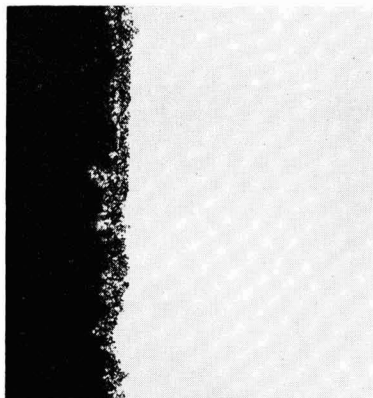


Fig. 4. Oxide film on Al-3% Mg alloy, in cross section at magnification of 500X before reduction for publication; Metal—white, oxide—black.

not discolored by vacuum anneals at 500°C. The photomicrograph in Fig. 4 illustrates the cross section of a black oxide film formed on the alloy after a 40-hr exposure at 550°C. The oxide was non-uniform in thickness ($3\text{-}15\mu$) and contained small metal particles. Further, the metal/oxide interface was serrated with many small metal inclusions nearly surrounded by oxide. Examination of metal cross sections revealed oxide penetration along grain boundaries and directly into grains.

It was doubtful if these metal inclusions resulted from metal entrainment during polishing. To confirm this, oxide films were stripped from the metal substrate and then examined. The surface of an oxidized specimen was backed with Formvar plastic by brushing on a 3% solution of Formvar in $\text{C}_2\text{H}_5\text{O}_2$. Sections, 1 cm^2 , were outlined with razor scratches and the film stripped with a 3% solution of Br in anhydrous methanol. A section was prepared for microscopic examination by placing it between two pieces of 1/16 in. Lucite sheet and placing this sandwich vertically in a Lucite plastic mount for metallographic polishing. Such an oxide cross section is illustrated in Fig. 5. Particles of a second phase less

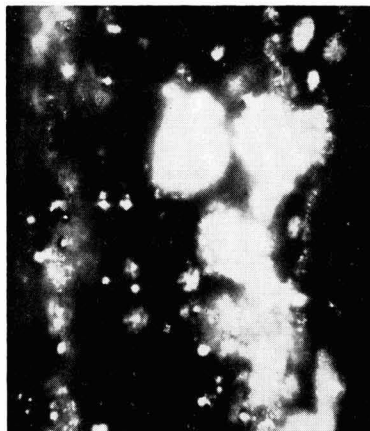


Fig. 5. Stripped oxide film from Al-3% Mg alloy at magnification of 1000X with oil immersion objective before reduction for publication; metal inclusions—small white spots.

than 2μ in diameter were scattered throughout the oxide. Also, powder x-ray analyses were taken of oxide stripped from an alloy which had been exposed 60 hr in dry oxygen at 500°C . All powders gave an Al diffraction pattern and the oxides identified were MgO and MgAl_2O_4 . One powder contained silica in trace amounts. Two powders, which gave the best Al diffraction patterns, were heated 18 hr in air at 900°C . The powders changed color from black to white; x-ray analyses showed only MgO and MgAl_2O_4 .

Discussion

Alloy Oxidation

Due to the complexity of the oxidation kinetics, quantitative conclusions cannot be deduced from the oxidation characteristics of this Al-Mg alloy. However, qualitative conclusions may be drawn by approximating the results to parabolic and linear oxidation rate equations. That is, the rate constants for the initial varying and final constant oxidation rates may be expressed, respectively, as,

$$K_p = \lim_{t \rightarrow 0} \left[\frac{d(\Delta m/A)}{dt} \right]^2 \quad (\text{I})$$

$$K_L = \lim_{t \rightarrow \infty} \left[\frac{d(\Delta m/A)}{dt} \right] \quad (\text{II})$$

where K_p and K_L are the parabolic and linear rate constants, respectively, and $\Delta m/A$ is the amount of oxygen per unit area at time t . The initial weight increments were plotted according to the parabolic equation: $(\mu\text{g}/\text{cm}^2)^2$ oxygen vs. time. These curves and linear sections of the oxidation curves illustrated in Fig. 2 show that the oxidation rates obey parabolic and linear relationships to a first approximation over the temperature range 350°C - 500°C . Parabolic and linear rate constant values determined from tangents to the initial and final sections of the parabolic and linear oxidation curves are recorded in Table I.

The temperature variation of these oxidation rate constants over part of the temperature range examined may be expressed by the Arrhenius relation

$$K = A \exp - E/RT \quad (\text{III})$$

where A is the frequency factor, E is the energy of activation, R is the gas constant and T is the absolute temperature. This is illustrated by plots of log

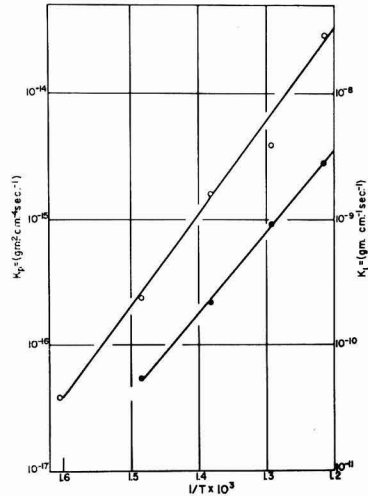


Fig. 6. Arrhenius plots of parabolic and linear oxidation rate constants; open circle = parabolic constants; solid circle = linear constants.

K vs. $1/T$ in Fig. 6; the expressions for the constants are:

$$K_p (\text{g}/\text{cm}^2 \text{sec})^2 = 2 \times 10^{-5} \exp - 33,000/RT \quad (\text{IV})$$

$$K_L (\text{g}/\text{cm}^2 \text{sec}) = 0.2 \exp - 29,000/RT \quad (\text{V})$$

It has been suggested by Evans (14) and Loriers (15) that transition from a parabolic to a linear oxidation rate relationship occurs for pure metals if porous oxide forms over compact oxide. The inner compact layer tends to a limiting thickness y_{max} when its formation rate is equal to its transformation rate to porous oxide. Webb, Norton, and Wagner (16) express this thickness as,

$$y_{\text{max}} = f K_p / 2K_L \quad (\text{VI})$$

where f is the ratio of oxygen content per gram atom metal in the compact and porous oxide.

From electron diffraction results, De Brouckère (3) has suggested that the oxide on Al-Mg alloys, containing up to 8% Mg, consists of an inner γ -alumina or magnesium aluminate compact layer and an outer porous magnesia layer upon high temperature oxidation. If this is valid, it follows to a first approximation from Eqs. (IV), (V), and (VI) that

$$y_{\text{max}} = 5 \times 10^{-5} \exp - 4000/RT \quad (\text{VII})$$

The calculated oxygen values of 3 to $5 \mu\text{g}/\text{cm}^2$ for compact layer formation over the temperature range 400°C - 550°C are of the same magnitude as the experimental values of less than $10 \mu\text{g}/\text{cm}^2$ before the onset of constant oxidation rates.

Other evidence may be advanced to support the view that the oxide film offers resistance to the reaction of metal with oxygen. Studies of Leontis and Rhines (11) and Gulbransen (17) have shown that the oxidation and evaporation kinetics of pure Mg may be represented by linear rate equations. Table II contains three different ratios: the evaporation

Table I. Oxidation and Mg evaporation rates for the Al 2.87% Mg alloy

Temp, $^\circ\text{C}$	Linear oxidation rate ($\text{g}/\text{cm}^2/\text{sec}$)	Parabolic oxidation rate ($\text{g}/\text{cm}^2/\text{sec}$) ²	Mg evaporation rate ($\text{g}/\text{cm}^2 \text{sec}$)
350		3.8×10^{-17}	
375			2.6×10^{-9}
400	4.7×10^{-11} 5.6×10^{-11} 5.9×10^{-11}	9.2×10^{-17} 2.4×10^{-16} 3.8×10^{-16}	6.0×10^{-9}
450	2.2×10^{-10}	1.6×10^{-15}	1.6×10^{-8}
500	9.2×10^{-10}	3.9×10^{-15}	5.6×10^{-8} 6.8×10^{-8}
550	2.8×10^{-9}	2.9×10^{-14}	1.3×10^{-7}

Table II. Comparison of oxidation and Mg rates for pure Mg and the Al 2.87% Mg alloy

Temp. °C	Mg oxid. rate ^(11, 17) (g/cm ² sec)	Mg evap. rate ⁽¹⁷⁾ (g/cm ² sec)	Mg evap.		Alloy oxid.		Mg oxid.	
			Alloy evap.	Alloy evap.	Alloy evap.	Alloy oxid.		
400	4.7×10^{-11}				7×10^{-8}	1.2×10^{-2}	1.1	0.7
450	5.6×10^{-10}	3.6×10^{-8}	2.3	2.8	2.8×10^{-2}		1.9	
500	6.3×10^{-9} 2.0×10^{-8}	2.2×10^{-8} 1.9×10^{-8}	1.4	0.3	2.5×10^{-2}		4.5	

rate of pure Mg to its evaporation rate from the alloy, the oxidation rate of the alloy to the evaporation of Mg from the alloy and, finally, the oxidation rate of pure Mg to the oxidation rate of the alloy. These ratios show, first, that the oxidation rate of the alloy is very nearly the same as for pure Mg and, second, the oxidation rate of either the alloy or pure Mg is much smaller than Mg evaporation rates. This suggests that the oxide film on the alloy offers resistance to oxidation of the metal at all stages of exposure.

Although parabolic and linear rate equations give an excellent approximation to the reaction kinetics, oxidation does not proceed simply by formation of porous magnesia over a compact oxide layer of constant thickness. The oxidation mechanism is more complex as the metal/oxide interface is highly serrated and metal inclusions occur in the oxide. Perhaps, this composite film forms according to the type of alloy oxidation mechanism proposed by Wagner (18). In the temperature range of this investigation, Al oxidizes rapidly for exposures not exceeding 10 hr and after this formative stage the oxidation rate decreases to a negligible value at film thicknesses of the order of 2000Å (9, 10). On the other hand, the alloy oxidizes at a constant rate similar to Mg after the initial formative oxidation stages. Thus, the oxidation rate of the base component, Mg, exceeds that of the noble component, Al, for long exposures. Selective oxidation of Mg would produce the serrated alloy/oxide interface and inclusions of the alloy depleted with respect to Mg as the oxide moves inward to fill the space of consumed metal.

Magnesium Evaporation

The weight loss curves of Fig. 3 for specimens suspended in vacuum at elevated temperatures have shown three characteristic features: (a) an initial weight loss due to outgassing; (b) an induction period; and (c) the onset of Mg evaporation. Values for the initial Mg evaporation rate (Table II) increase exponentially with temperature according to the Arrhenius relation:

$$K_{\text{Evap.}} (\text{g/cm}^2 \text{ sec}) = 0.6 \exp - 25,000/RT \quad (\text{VIII})$$

Magnesium may evaporate at an initial constant rate after the induction period by two possible mechanisms: it may diffuse through the oxide film upon establishment of a concentration gradient or evaporate from the metal/vacuum interface if the compact oxide film breaks down to porous oxide. These two mechanisms may be differentiated by a calcu-

lation based on equations for the induction period and diffusion rate of a substance through a semi-permeable membrane given by Barrer (19). The diffusion rate P of a substance through a semi-permeable membrane of thickness l is to a first approximation

$$P = \frac{lc}{\delta L} \quad (\text{IX})$$

if L is the period required to establish a concentration gradient for concentrations of c and zero at the interfaces. The concentration c , which in this case represents the solubility of Mg in the oxide at the metal/oxide interface, may be estimated from the experimental data. The electron diffraction studies of De Brouckère (2) indicate that the air-formed oxide film on the alloy at room temperature does not exceed 100Å at 400°C; the initial Mg evaporation rate is 6×10^{-9} g/cm² sec after an induction period of 200 min. Hence, $c = 432$ g/cm³. This very high value indicates that Mg evaporates from the metal/vacuum interface through porous oxide which may be produced by chemical reaction or mechanical breakdown of compact oxide. Since the duration of the induction period is strongly dependent on temperature, alumina may be reduced by Mg to give magnesia and the film would be porous as the volume ratio products/reactants for this reaction is 0.7. Consequently, the decreasing Mg evaporation rate from the alloy illustrated by the curve for vacuum exposure at 400°C is determined by its diffusion rate in the alloy and by partial resistance of porous oxide.

Surface Discoloration

Different views as to the origin of the discoloration of Al-Mg alloys by oxidation have been expressed. De Brouckère (2) has shown by electron diffraction that black films contain magnesia which was assumed to cause discoloration. Guminski and Hines (20) have suggested that metal in atomic or particle form in the surface oxide may be the cause of discoloration as hydrogen is evolved from black oxide when it is treated with acid. This investigation indicates that metal particles embedded in the oxide are a primary cause of discoloration as microscopic and x-ray examinations have shown the occurrence of Al inclusions. Thus, the black oxide became white when exposed at 900°C, as Al was completely oxidized. Metal particles of colloidal dimensions are often colored black. However, it is not known if discoloration is caused by this effect or by multiple reflection and absorption of light by irregular surfaces of larger particles. The view that discoloration is associated with the lattice defect structure of magnesia has not been disproven in this investigation. Leontis and Rhines (11) have shown that gray magnesia, presumably due to its non-stoichiometric composition, occurs next to the metal surface of magnesium. That this effect is a primary cause of alloy discoloration is doubtful as metallographically polished specimens or a specimen with a thick anodic film were not discolored by vacuum anneals of sufficient duration to allow Mg evaporation.

General

In the preceding discussion, the oxidation kinetics at temperatures greater than 350°C have been approximated to parabolic and linear rate equations. A comparison of oxidation and Mg evaporation rates demonstrated that the oxide film offered resistance to oxidation at all stages of exposure. Metallographic and x-ray examinations have shown that depletion of Mg by selective oxidation resulted in formation of Al inclusion in the oxide. These inclusions, in turn, caused a gray to black discoloration of the surface. Many of the views which have been expressed must remain speculative because chemical compositions and structures of the oxides in the composite film, and determinations of Mg activities and diffusivities for the alloy and oxides are required to elucidate the oxidation and Mg evaporation behavior.

Acknowledgments

The author wishes to express his thanks to former colleagues, especially J. S. Kirkaldy and H. P. Godard, at Aluminium Laboratories, for helpful discussions.

Manuscript received Nov. 26, 1956.

Any discussion of this paper will appear in a Discussion Section to be published in the December 1958 JOURNAL.

REFERENCES

1. S. Dobinski and M. Niesluchowski, *Nature*, **144**, 510 (1939).
2. L. De Brouckère, *J. Inst. Metals*, **71**, 131 (1945).
3. R. Eborall and C. E. Ransley, *ibid.*, **71**, 525 (1945).
4. O. Kubaschewski and H. Ebert, *Metallforschung*, **2**, 232 (1947).
5. M. Whitaker and A. R. Heath, *J. Inst. Metals*, **82**, 107 (1953).
6. A. J. Swain, *ibid.*, **80**, 125 (1951).
7. P. T. Stroup, "Controlled Atmospheres," A.S.M. (1941).
8. E. A. Smith, Jr., *Light Metal Age*, **12**, 24 (October, 1954).
9. W. W. Smeltzer, *This Journal*, **103**, 209 (1956).
10. M. S. Hunter and P. Fowle, *ibid.*, **103**, 483 (1956).
11. T. E. Leontis and F. N. Rhines, *Trans. Am. Inst. Mining Met. Engrs.*, **166**, 265 (1946).
12. I. A. Makolkin, *Zhur. Priklad. Khim.*, **24**, 460 (1951).
13. E. A. Gulbransen, *Rev. Sci. Instr.*, **15**, 201 (1944).
14. U. R. Evans, *Trans. Am. Inst. Mining Met. Engrs.*, **166**, 292 (1946).
15. J. Lories, *Compt. rend.*, **231**, 522 (1950).
16. W. W. Webb, J. T. Norton and C. Wagner, *This Journal*, **103**, 107 (1956).
17. E. A. Gulbransen, *Trans. Electrochem. Soc.*, **87**, 589 (1945).
18. C. Wagner, *This Journal*, **103**, 571 (1956).
19. R. M. Barrer, "Diffusion in and Through Solids," Cambridge University Press, p. 19 (1951).
20. R. D. Guminski and R. A. Hines, Private communication.

Metallographic Manifestations of the Air Oxidation of Tantalum at 750°C

Robert Bakish¹

Sprague Electric Company, North Adams, Massachusetts

ABSTRACT

The crystallographic and structural factors involved in the air oxidation of tantalum at 750°C are presented. The role of the {100} planes in the oxidation process is discussed, and a tentative mechanism for the conversion of metal to oxide under these conditions is proposed.

The oxidation of Ta has been studied by a number of investigators with emphasis on the type and structure of the oxide formed (1-4) or on the kinetics of oxidation (5-9). Work on the solubility of oxygen in Ta has also been reported (10). In all these investigations, the nature of the oxide-metal interface has been completely disregarded, and no mention of the crystallographic dependence of the tantalum oxygen reaction has been made.

Pure Ta (Ta 99.9 + Fe 0.03 max and C 0.03 max) supplied by Fansteel Metallurgical Corporation was used for this investigation.

Experimental Procedure

It has been shown that tantalum oxide exists in a stable modification in the temperature range 650°-1300°C (3). The tantalum oxide used in the most recent structure determination was prepared by

oxidation of the metal at 700°C (4). In order to avoid possible complications introduced by working with an unknown oxide, an oxidation temperature was selected on the basis of the above references. All specimens in this investigation were subjected to 45-min oxidation in air at 750°C, followed by quenching in air at room temperature.

X-ray powder technique was used to identify the oxide formed. The single crystals used in this study were grown by standard strain anneal technique and their orientations determined using Greninger's method (11). The identification of the plane of oxidation was carried out as follows: two surfaces with known angular relations were ground on crystals of known orientation, and the angles made by the planes of preferred oxidation with the common edge were measured. This information was then plotted stereographically and analyzed using a standard cubic projection, in accordance with standard procedures (12).

¹ Present address: Ciba Limited, Rare Metals Division, Basle, Switzerland.

Standard metallographic techniques were applied in this study, and a solution consisting of H_2SO_4 (96%), HNO_3 (70%), and HF (48%) in ratio (2:1:1) was used as the etching reagent.

In oxygen embrittled Ta, both inter- and trans-crystalline fracture can be observed. Intergranular failure is predominant in relatively small grain size material (about 0.1 mm). The oxide distribution on grain surfaces obtained by fracturing small grained metal were examined in order to gain additional information regarding the sites of preferred oxidation. These observations were made on freshly fractured wires without any subsequent surface preparation.

Experimental Results

Air oxidation of Ta leads to surface oxidation and crystallographically dependent internal oxidation. The latter proceeds at higher rates along certain planes and directions in the Ta lattice. The oxide-metal interface in polycrystalline Ta oxidized in air at $750^\circ C$ is shown in Fig. 1. Observe here the surface oxide and the spear-like orientation-dependent platelets of the oxide. Note that no preferential oxidation exists at the grain boundary. This type of interface is typical of the large number of oxide-metal interfaces examined and is unaffected by longer oxidation treatments which only moves this interface into the metal.

X-ray study by application of powder technique indicates that the oxide formed under these conditions is Ta_2O_5 , of the same variety as commercially produced material of this formula. The structure of this oxide has recently been reevaluated (4). X-ray lines characteristic of the oxide pattern were also detected after removal of the surface oxide in specimens which, by metallographic examination, were shown to have internal preferential oxidation.

The oxide formed on polycrystalline Ta is of very fine particle size, as indicated by diffuse x-ray patterns. This oxide has a high degree of porosity which can be detected on careful microscopic examination of the polished oxide. The same type of polycrystalline oxide seems to be formed on single crystal surfaces.

X-ray analysis of the internal oxidation occurring in single crystals shows that, within the accuracy

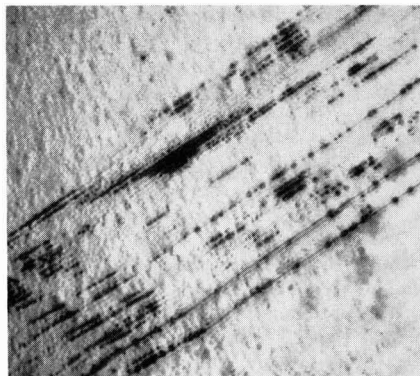


Fig. 2. Details of early stage internal oxidation. 2000X before reduction for publication.

of the measurements of about 2° , the planes of internal oxidation are parallel to the $\{100\}$ planes of the bcc lattice. On successive lapping and polishing of single crystal surfaces normal to the oxidized surface, and in several cases normal to the $\langle 100 \rangle$ directions, it was found that quite often the solid platelet profile of $\{100\}$ planes was substituted at a greater depth by a bead profile and eventually with discrete sites of oxidation. See Fig. 2 for the appearance of $\{100\}$ traces at some depth from the oxide metal interface. (Observe both "bead" profile and discrete oxidation sites.) These oxide platelets do not grow appreciably in thickness normal to the $\{100\}$ planes after they reach a thickness of about 0.002 mm (see Fig. 3). Heavier oxidation is characterized by the presence of a greater number of more narrowly spaced platelets. The porous oxide is but a thorough oxidation of the volume of the metal by oxidation along $\{100\}$ planes. Figure 4, which is a taper section of an oxidized surface of a single crystal, supports this contention. Observe the islands of porous oxide, the high density of platelets in their immediate vicinity, and the relatively smaller density of platelets as the distance from the oxidized surface is increased. That this appears to be the nature of oxidation seems to be also supported by examination of polished oxide surfaces

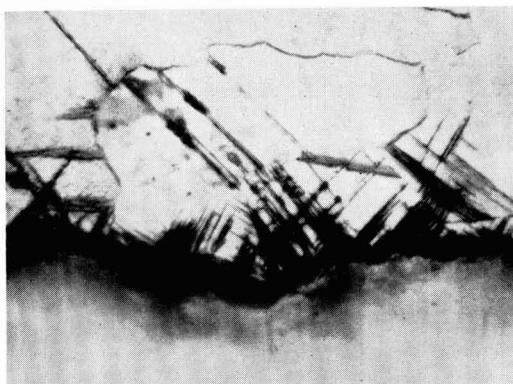


Fig. 1. Oxide metal interface, cross section normal to oxidized surface. 2000X before reduction for publication.



Fig. 3. Traces of the $\{100\}$ planes. 2000X before reduction for publication.



Fig. 4. Taper section of oxidized single crystal surface. 500X before reduction for publication.



Fig. 7. Fractograph showing sites of nucleation of oxygen metal reaction on a grain surface. 500X before reduction for publication.

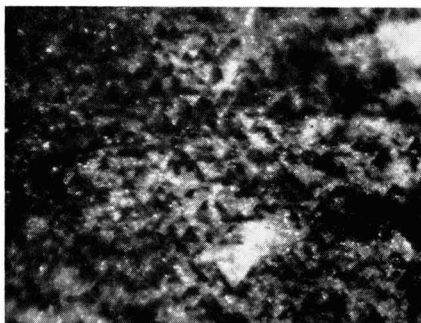


Fig. 5. Polished oxide surface (polarized light). 500X before reduction for publication.

under polarized light (see Fig. 5). This reveals a fine structure with elements parallel to the traces of the $\{100\}$ planes of the substrate.

Another aspect in which the crystallographic dependence of oxidation manifests itself is the formation of steps bound by $\{100\}$ substrate planes on the oxide-metal interface of single crystals. Figure 6 shows the appearance of such an interface as viewed on a (112) plane. When such single crystals were subjected to oxidation, it was possible to observe that the $\langle 100 \rangle$ directions in the $\{100\}$ planes were the directions of a higher rate of oxidation. This observation and the occurrence of the $\{100\}$ step formation, tend to show that the $\langle 100 \rangle$ directions

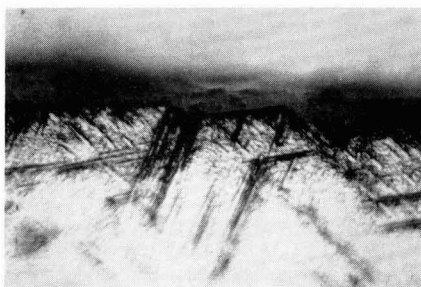


Fig. 6. Crystallographic $\{100\}$ steps on oxide metal interface plane of photomicrograph parallel to (112) . 2000X before reduction for publication.

in the $\{100\}$ planes are the directions of preferred oxidation.

In addition to oxidation within the grains, evidence of internal oxidation was found on grain surfaces. This information was obtained by microscopic examination of fractured, fine grained, oxidized Ta wire. Figure 7 shows a distribution typical of those observed.

Discussion of Results

The findings of this investigation show the presence of a set of high activity planes in the $\{100\}$ planes of the Ta lattice.

Two alternatives are offered as possible explanations of the high activity of the $\{100\}$ planes: it can be due either to the inherent high activity of this plane; or it can be the result of the presence of favorably oriented imperfections which could act as short circuiting paths for diffusion and oxidation. It is on these imperfections that the metal-oxide reaction appears to nucleate. No preferential grain boundary oxidation was observed in this study. The oxidation process seems to proceed by nucleation of oxidation at highly localized sites along the traces of the $\{100\}$ planes, leading to the growth of oxide platelets parallel to the $\{100\}$ planes. These platelets grow in thickness until they reach about 0.002 mm. Further oxidation proceeds by nucleation and the growth of additional platelets until all the metal is consumed in the reaction. The high activity usually associated with grain boundaries in oxidation reactions is not apparent from examination of metal-oxide interfaces in this study. No satisfactory explanation for this behavior can be advanced at present. Oxide-metal reaction, however, was found to nucleate at discrete sites on grain surfaces, and discrete oxide particles can be seen on observation of these surfaces. The exact nature of the sites which act as nucleating centers for the oxide-metal reaction is not known. Their appearance and distributions suggest the possibility that they are dislocations. This, however, cannot be asserted at present.

Conclusions

On the basis of this study, it is proposed that oxidation of Ta proceeds by preferential oxidation

along the {100} planes in the $\langle 100 \rangle$ direction. The complete conversion of the metal to oxide is effected by the nucleation and growth of {100} plates, which eventually fill the volume of the metal. The individual plates do not exceed 0.002 mm in thickness.

On examination of tapered sections, the Ta_2O_5 shows clearly the crystallographic dependence of its growth process and the orientation of the traces of the {100} planes of the substrate. Lattice imperfections, believed to be dislocations, seem to act as sites for the nucleation of the metal-oxide reaction.

Acknowledgment

The author wishes to acknowledge the assistance of D. Rogers and N. Harvin in the course of this work. Thanks are also due to W. Bernard for reading the manuscript.

Manuscript received April 22, 1957. This paper was prepared for delivery before the Buffalo Meeting, Oct. 6-10, 1957.

Any discussion of this paper will appear in a Discussion Section to be published in the December 1958 JOURNAL.

REFERENCES

1. G. Brauer, *Z. anorg. u. allgem. Chem.*, **248**, 1 (1941).
2. S. Lagergren and A. Magneli, *Acta. Chem. Scand.*, **6**, 444 (1952).
3. R. J. Wasilewski, *J. Am. Chem. Soc.*, **75**, 1001 (1953).
4. L. K. Frevel and H. W. Rinn, *Anal. Chem.*, **27**, 1329 (1955).
5. E. Gulbransen and K. F. Andrews, *This Journal*, **99**, 6 (1949).
6. E. Gulbransen and K. F. Andrews, *Trans. Am. Inst. Mining Met. Engrs.*, **186**, 586 (1950).
7. R. C. Petersen, *et al.*, *ibid.*, **200**, 1038 (1954).
8. J. T. Waber, *J. Chem. Phys.*, **20**, 734 (1952).
9. J. T. Waber, *et al.*, *This Journal*, **99**, 121 (1952).
10. E. Gebhardt and H. Preisendanz, *Plansee Proceedings*, 254 (1956).
11. A. B. Greninger, *Trans. Am. Inst. Mining Met. Engrs.*, **17**, 61 (1935).
12. C. S. Barrett, *Structure of Metals*, 40 (1952).

Cathodic Reduction of Oxide Films on Iron

II. Determination of α - Fe_2O_3 and Fe_3O_4

K. H. Buob, A. F. Beck, and M. Cohen

National Research Council, Ottawa, Ontario, Canada

ABSTRACT

A study of the cathodic reduction of α - Fe_2O_3 on iron has been made with the object of using the technique for the accurate determination of both the α - Fe_2O_3 and Fe_3O_4 formed during the oxidation of iron. The films were examined after oxidation and after various stages of cathodic reduction. Examination was made by weight change, electron diffraction, x-ray diffraction, and chemical analysis of the films. Some evidence for the existence of a thin layer of γ - Fe_2O_3 between the layers of Fe_3O_4 and α - Fe_2O_3 was found. A standard pattern for Fe_3O_4 was obtained.

When Fe is oxidized in oxygen at temperatures up to about 450°C a duplex film of Fe_3O_4 next to the metal and α - Fe_2O_3 is formed. The over-all growth of the oxide film should be related to the rates of growth of these two layers. In a previous paper (1) there was described a technique for the cathodic reduction of α - Fe_2O_3 . In this paper the application of this technique to the determination of α - Fe_2O_3 and Fe_3O_4 is described.

The method proposed was to weigh the oxidized specimen and to reduce it cathodically until the potential of the Fe indicated a change in the cathodic process. The specimen was reweighed and the Fe_3O_4 determined by difference. The Fe_2O_3 was calculated from the total weight gained and the weight of Fe_3O_4 .

To check on the validity of this method, reflection electron diffraction identification of the oxide was made during various stages of the cathodic reduction process. Films were stripped for identification by both diffraction and chemical analysis, and the effect of cathodic reduction on magnetite films was determined.

Experimental

Preparation of oxidized specimens.—The specimens measuring 5 x 1 cm with a handle 2.5 x 0.2 cm were cut from rolled Armco Iron sheet 0.150 mm thick. The Fe contained 0.113% total impurities. The specimens were degreased in benzene, wiped dry with Kleenex, stored in a desiccator for 1 hr, and weighed on a microbalance to $\pm 2 \times 10^{-6}$ g. They were then supported in a quartz tube over which a

furnace could be drawn. The temperature of the furnace was regulated to $\pm 0.5^\circ\text{C}$. The Fe surface was reduced in purified hydrogen at 400°C for 1 hr. The hydrogen was pumped off and the Fe outgassed for 3 hr, during which time the desired oxidation temperature was set. Oxygen was admitted to the oxidation chamber to a pressure of 20 mm Hg. At the end of the desired oxidation time, the furnace was removed, the outside of the quartz tube was cooled rapidly with water, the specimens placed in a desiccator for 1 hr, and reweighed on the microbalance.

Cathodic reduction of $\alpha\text{-Fe}_2\text{O}_3$.—The cathodic reduction was carried out in the cell described by Oswin and Cohen (1). Optimum results were obtained in a borate-HCl buffer of pH 7.65, with a current density of $15 \mu\text{a}/\text{cm}^2$. The specimens were dried and weighed after cathodic reduction.

Isolation of oxide films.—A modified version of the film stripping apparatus of Vernon, Wormwell, and Nurse (2) was used. This was of all-glass construction and employed a vacuum and purified nitrogen for deoxygenation and movement of solutions. A solution of 12% iodine in methanol was used. All reagents were well dried and free of oxygen. The time of treatment varied from 30 to 90 min, depending on the nature of the films. It was found that the duplex film or a film of Fe_3O_4 alone could be stripped equally well.

After treatment the film was washed and floated on methanol. This film could then be used for chemical analysis or examination by diffraction.

Electron diffraction.—For electron diffraction examination the oxide film was mounted on a 12 mesh grid supported by a thin Formvar film. This film was prepared by spreading one drop of a 0.3% w/v Formvar in ethylene dichloride solution on water, and mounting on the grid. This combination forms a tough mounting substrate for the somewhat brittle oxide film, yet the Formvar film is thin enough to be practically transparent to the electron beam. The "hole" area of the 12 mesh grid is larger than the area of the electron beam, hence eliminating interference by the grid. Reflection electron diffraction examination was also made on the specimens at various stages of reduction.

Chemical analysis.—The thin stripped films were thoroughly washed with water and then dissolved in 1:1 HCl. The magnetite dissolved readily while the Fe_2O_3 dissolved only very slowly. Ferrous ion was determined by the α' dipyridyl method (3) and total Fe by the thioglycolic acid method (4).

Results and Discussion

A series of specimens were oxidized in quadruplicate. These were then reduced cathodically and the amounts of $\alpha\text{-Fe}_2\text{O}_3$ and Fe_3O_4 determined. A typical set of results is shown in Table I. As can be seen from the table the deviation from the average is less than 7%. The Fe_3O_4 value, of course, is obtained by difference. As pointed out in the previous paper, the current efficiency estimated from either weight loss or Fe in solution is about 95%.

A cathodic reduction curve is shown in Fig. 1. The normal points at which the specimens are weighed

Table I. Iron oxidized at 320°C

Time min	Total wt gain $\mu\text{g}/\text{cm}^2$	Weight loss on C.R.* $\mu\text{g}/\text{cm}^2$	O_2 as $\alpha\text{-Fe}_2\text{O}_3$ $\mu\text{g}/\text{cm}^2$	O_2 as Fe_3O_4 $\mu\text{g}/\text{cm}^2$
2413	21.0	45.1	13.5	7.5
2413	21.3	46.8	14.0	7.3
2413	23.1	50.7	15.1	8.0
2413	21.8	50.8	15.2	6.6
Average	21.8	48.4	14.4	7.4

* Cathodic reduction.

Table II. Effect of cathodic reduction on Fe_3O_4

Reduction time min	Weight loss $\mu\text{g}/\text{cm}^2$	Current efficiency %
53 (Point A)	39.2	98
+5	0.60	—
+5	0.66	—
+10	0.73	—
+20	0.60	—

are at the beginning and at Point A, just after completion of the inflection. Reflection electron diffraction showed that the surface was composed of $\alpha\text{-Fe}_2\text{O}_3$ at the end of the oxidation. After cathodic reduction up to Point A only Fe_3O_4 was present.

A series of experiments was made to determine whether Fe_3O_4 was reduced under the conditions used in the cathodic reduction. A specimen was reduced to Point A and weighed. It was then reduced under the same conditions for further periods of 5, 5, 10, and 20 min, with weighings between each reduction period. The results on a specimen which had been heated for 24 hr at 320°C are shown in Table II. It was also shown that cathodic reduction for periods up to at least 1 hr past Point A did not change the Fe_3O_4 diffraction pattern.

It can be seen that, once the $\alpha\text{-Fe}_2\text{O}_3$ has been removed at Point A, there is a small but constant

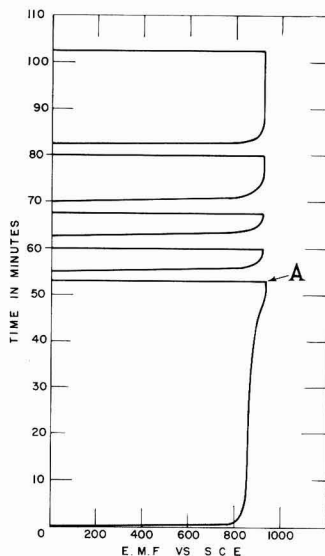


Fig. 1. Repetitive cathodic reduction of a single specimen. Complete reduction is usually assumed at Point A.

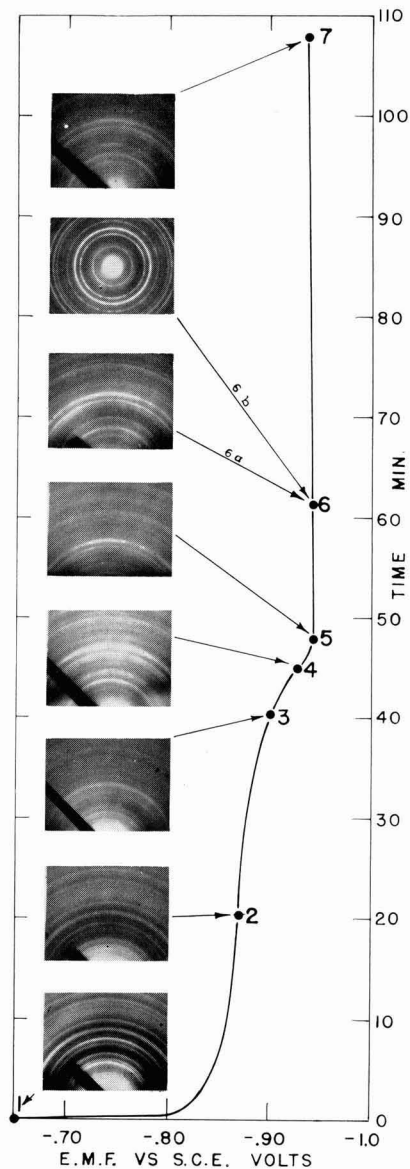


Fig. 2. Diffraction patterns of specimens removed at various stages of cathodic reduction.

weight loss on re-exposing the specimen to further reduction. This is probably caused by corrosion loss in the short period that the specimen is first immersed until it is cathodically protected. A part of the weight loss may be due to a small amount of oxidation of Fe_3O_4 to Fe_2O_3 on exposure to air with subsequent reduction of this Fe_2O_3 . In a continuous run, the weight change after Point A should be negligible. It would thus appear that Fe_3O_4 is not reduced under the conditions used in these experiments.

As a further check on the process, reflection patterns were obtained from specimens which had been

cathodically reduced to the points indicated in Fig. 2. In Table III typical interplanar spacings and the estimated intensities of the patterns are tabulated. Only those spacings, and their intensities, unique to the particular oxide are tabulated.

Reduction curve.—The specimen at point 1 in Fig. 2 gave a reflection pattern only of hexagonal $\alpha\text{-Fe}_2\text{O}_3$, indicating the thickness of this oxide to be greater than the depth of penetration of the electron beam. At point 2 enough of the $\alpha\text{-Fe}_2\text{O}_3$ had been removed to allow the beam to diffract from a cubic oxide beneath, producing a pattern of $\alpha\text{-Fe}_2\text{O}_3$ plus a trace of cubic oxide. The pattern from point 3 was similar to that from point 2. Of these last three patterns, the intensity of the characteristic 2.69 line has been decreasing as the reduction progresses, being absent at point 4. No material, other than the cubic oxide, was detected during the reduction, indicating that no intermediate product was formed by the reduction. Reflection diffraction patterns from thicker oxide films showed no Fe_3O_4 until point 4 was reached, thus eliminating the possibility of formation of Fe_3O_4 as a reduction product of $\alpha\text{-Fe}_2\text{O}_3$.

The pattern from point 4 did not contain the characteristic $d = 2.69\text{\AA}$ reflection, indicating almost total disappearance of $\alpha\text{-Fe}_2\text{O}_3$. The pattern, however, differed from that of Fe_3O_4 by extra reflections not possible by a true Fe_3O_4 structure. This pattern is very similar to Brindley's (5) $\gamma\text{-Fe}_2\text{O}_3$. Davies and Evans (6) find that $\gamma\text{-Fe}_2\text{O}_3$ can be distinguished from Fe_3O_4 by the presence of these and other additional lines; also that the $\gamma\text{-Fe}_2\text{O}_3$ pattern appears in adjacent layers of $\gamma\text{-Fe}_2\text{O}_3$ and Fe_3O_4 when the ratio of these oxides is approximately 4:1, respectively. The presence of these extra lines, and the slight shift of the remaining lines in point 4 toward the higher angle of diffraction indicate a high probability of the presence of $\gamma\text{-Fe}_2\text{O}_3$.

The patterns from specimens at points 5, 6, and 7, (there is also a transmission pattern at point 6) all give a strictly Fe_3O_4 pattern, with no anomalies. It would appear that if $\gamma\text{-Fe}_2\text{O}_3$ is present, it is only present as a very thin layer.

Chemical analysis.—Stripped films were dissolved in HCl and analyzed for both ferrous and total Fe. Pure Fe_3O_4 would have a total Fe/Fe^{++} ratio of 3/1, while mixtures of Fe_3O_4 and Fe_2O_3 would have a ratio greater than 3/1.

Films which had been stripped without initial reduction gave ratios greater than 3, indicating the presence of both ferric and ferrous ions. Specimens which had been cathodically reduced before stripping gave ratios of 2.73 ± 0.10 . This would indicate too high a concentration of ferrous ion for pure Fe_3O_4 . X-ray diffraction of these films showed the presence of small amounts of $\alpha\text{-Fe}$ and Fe_3C , which probably consisted of particles which adhered to the stripped film. Approximately 5% of extraneous Fe in the film would account for this lowering in ratio.

Some specimens were oxidized in the ordinary way and then annealed in vacuum until only an Fe_3O_4 pattern was obtained. Films stripped from

Table III

d	$1/I_0$														
2.69	100	2.72	80	2.70	5	3.00	40	2.97	40	2.97	33	2.97	40	2.98	50
						[1]*									
						2.64	20								
2.50	50	2.50	100	2.50	100	2.50	100	2.54	100	2.52	100	2.53	100	2.51	100
						[2]*									
2.20	35	2.20	65	2.19	33	2.19	20								
						2.09	40	2.09	20	2.08	33	2.09	20	2.09	50
								1.87	14	1.88	3	1.87	4		
1.85	25	1.85	33	1.84	17										
						[3]*									
						1.81	13								
1.68	80	1.69	65	1.68	33	1.70	17	1.70	17	1.70	10	1.71	13	1.69	25
1.60	8	1.61	25	1.60	13	1.61	40	1.61	50	1.61	50	1.62	33	1.60	65
						1.09	33	1.08	40	1.09	25	1.09	20	1.09	30

* Spacings [1] and [3] belong neither to α -Fe₂O₃ nor Fe₃O₄. The γ -Fe₂O₃ pattern, as given by Brindley, however, contains these 2 lines, as well as line [2]. The absence of the 2.70 spacing of α -Fe₂O₃ in the pattern reduces the probability of line [2] being that of α -Fe₂O₃.

these specimens gave a total Fe/Fe²⁺ ratio of 2.93 ± 0.05 . X-ray diffraction of these specimens showed only a trace of the Fe lines. This lowering in ratio would be accounted for by about 1% of extraneous Fe.

Fe₃O₄ standard.—The annealed specimens described above gave extremely good Fe₃O₄ patterns both by reflection and transmission. Some of the film was mounted on a glass fiber with C.I.L. Duco cement for x-ray diffraction. The patterns obtained contained more lines than those reported by Brindley (5) or any other source. The electron diffraction patterns are shown in Fig. 3 and the tabulated spacings are given in Table IV. It can be seen that there is very good agreement between the reflection and transmission patterns. This indicates that there is

no significant change during the stripping of the film. The transmission pattern gives the more accurate values, because the diameters of whole cir-

Table IV. Standard Fe₃O₄ Patterns

hkl	Reflection d	$1/I_0$	Transmission d	$1/I_0$	X-ray d	$1/I_0$
111	4.93	20	4.81	25	4.78	20
200			4.20	4		
220	2.95	40†	2.97	40	2.95	70
					2.70	10
311	2.53	100	2.53	100	2.53	100
222	2.42	5	2.43	20	2.42	5
400	2.09	33	2.09	25	2.09	75
					2.04*	10
331	1.91	10	1.92	8		
420			1.87	6	1.85	2
422	1.72	20	1.71	25	1.71	20
511						
333	1.62	50†	1.62	40	1.61	70
440	1.48	80†	1.48	50	1.48	80
531	1.42	10	1.42	13		
620	1.34	10	1.32	13	1.33	10
533	1.28	20	1.28	20	1.28	20
444	1.22	10	1.21	17	1.21	7
711						
551	1.18	10	1.17	13		
642	1.12	20	1.12	20	1.13	5
731						
553	1.10	25	1.09	25	1.09	25
800	1.05	17	1.05	8	1.05	10
820						
644			1.02	6		
822						
660	0.986	20	0.983	8	0.985	2
751						
555	0.966	25	0.966	17	0.970	20
840	0.938	20	0.938	13	0.938	5
842			0.917	10		
664			0.892	5		
931	0.877	17	0.877	13		
844						
(10)00 860	0.854	25	0.854	20		
			0.839	5		
(10)20 862			0.821	5		
951						
773	0.815	17	0.810	13		

* Strongest Fe line.
† Broad.

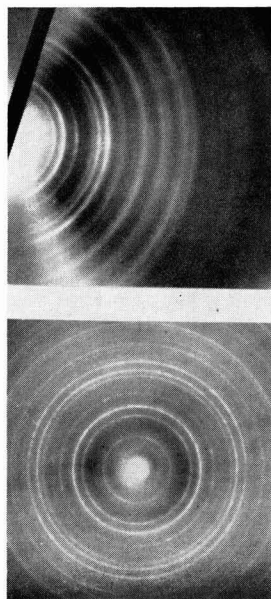


Fig. 3. a. (top) Reflection diffraction pattern of Fe₃O₄; Fig. 3b. (bottom) transmission diffraction pattern of Fe₃O₄.

cles can be measured more accurately than the radii of semicircles.

The lattice parameter of Fe_3O_4 was calculated from the x-ray data and was found to be $8.394 \pm 0.002\text{\AA}$.

Summary

It has been shown that the cathodic reduction technique can be used to obtain an accurate measure of the amounts of Fe_3O_4 and $\alpha\text{-Fe}_2\text{O}_3$ found in a two scale layer on Fe. Positive identification of the two layers has been made. There is some diffraction evidence for the existence of a very thin layer of $\gamma\text{-Fe}_2\text{O}_3$ between the two layers which is also reduced and measured as $\alpha\text{-Fe}_2\text{O}_3$.

In the course of the work a standard pattern for Fe_3O_4 was obtained.

Manuscript received May 29, 1957. This paper was prepared for delivery before the Buffalo Meeting, Oct. 6-10, 1957.

Any discussion of this paper will appear in a Discussion Section to be published in the December 1958 JOURNAL.

REFERENCES

1. H. G. Oswin and M. Cohen, *This Journal*, **104**, 9 (1957).
2. W. H. J. Vernon, F. Wormwell, and T. J. Nurse, *J. Chem. Soc.*, **1939**, 621.
3. E. Schulek and I. Floderer, *Z. anal. Chem.*, **117**, 176 (1939).
4. J. W. Swank and M. G. Mellon, *Ind. Eng. Chem., Anal. Ed.*, **30**, 7 (1938).
5. G. W. Brindley, "X-ray Identification and Crystal Structure of Clay Material," The Mineralogical Society, London (1951).
6. D. E. Davies and U. R. Evans, *J. Chem. Soc.*, **1956**, 4373.

Temperature Characteristics of Barium Strontium Lithium Silicate Phosphors

A. H. McKeag

Research Laboratories, General Electric Company, Ltd., Wembley, England

ABSTRACT

The changes in spectral emission, efficiency, and temperature stability are discussed which result from changes in the following variable parameters in phosphor preparation: the barium: strontium ratio, lithium content, base: acid ratio, activator concentrations, and firing conditions. For practical application in jacketed high pressure mercury vapor lamps, compositions within a critical base: acid ratio of 3R0 : 1.8 to 1.9 SiO_2 have produced the best results.

The temperature dependence of the luminescence of various phosphors has been studied by a number of workers (1,2). The wide variation in behavior between the same activator in different matrices and between different activators in the same matrix suggests that temperature dependence characteristics are determined by the nature of the matrix-activator combination. The effect of activator concentration has also been studied and Fonda has shown that in Willemite high Mn concentrations produce a lowering of the quenching temperature (2). Similar effects have also been observed when certain harmful impurities, such as Fe, are added to sulfides and silicates. Kroeger (1) has also noted that phosphors which are badly crystallized have a low quenching point.

Recently, attention has been directed to the improvement in both color rendering and efficiency of high pressure Hg vapor lamps by the application of improved phosphors to the outer glass envelopes of these lamps. As a result of this work (3-8), a number of new phosphors have been found which maintain their fluorescence at high temperatures. The present paper gives details of the preparation of improved barium strontium lithium silicate phosphors for use at high temperatures and shows that the method of preparation can have a marked effect on the temperature characteristics of the phosphor.

Barium Strontium Lithium Silicates—Activated with Cerium and Manganese

This family of phosphors have been described previously (6,7). Trivalent Ce, produced by firing in reducing conditions, gives a characteristic blue emission by itself, and acts as a sensitizer for the secondary activator, Mn. The broad excitation spectrum and freedom from appreciable body color makes these "triple silicate" phosphors attractive for use in color-corrected high pressure Hg vapor (H.P.M.V.) lamps.

A marked improvement in the temperature characteristics of these phosphors, obtained by the methods described below, has led to a corresponding improvement in the color rendering properties of commercial H.P.M.V. lamps utilizing these phosphors.

Preparation Conditions, Barium to Strontium Ratio

As Ba is replaced by Sr in these phosphors, the color of the fluorescence changes from orange-yellow to red with a given Mn content and this change is also associated with a decrease in the response to short u.v. radiation. The brightest phosphors have not been obtained with a pure barium lithium silicate composition, as might be expected from color considerations, but with phosphors containing an appreciable proportion of Sr corresponding to an

approximate molar ratio of $4\text{BaO} \cdot 1\text{SrO}$. This effect may be associated with differences in ionic size between Ba and activator ions which would tend to make substitution of activator ions more difficult in phosphors of pure barium lithium silicate composition.

Lithium Content

The lithium oxide content is not critical and can be varied over a wide range without altering the color or intensity of the fluorescence markedly. The most useful range lies between one fifth and one half the combined molar proportions of the alkaline earth oxides, and within this range x-ray examination shows that the crystal structure is basically unchanged. At higher Li contents, a phase of different crystal structure can be formed (7) and the spectral emission becomes modified; these phosphors show poorer temperature characteristics as the lithium oxide is increased. Although Li may be regarded as a major constituent of the complex silicate lattice, it is interesting to note that Klasens (5) has observed an improvement in the temperature characteristics of magnesium arsenate phosphors, following the addition of Li.

Silica Content

Silica content appears to exercise a marked effect on both chemical stability and temperature response characteristics of these phosphors. Phosphors can be prepared in the range $3\text{RO} : 1.7\text{SiO}_2$ to $3\text{RO} : 2.3\text{SiO}_2$ (where RO represents the combined basic radicals), but the best results have been obtained within the much narrower range $3\text{RO} : 1.8\text{SiO}_2$ to $3\text{RO} : 1.9\text{SiO}_2$. These ranges, which are modified by the activator content, refer to phosphors containing 0.25 additional moles of the combined oxides of Ce and Mn.

With this proportion of activators the range of silica from 1.8 to 1.9 moles appears to cover a critical balance point in the chemical stability of these phosphors. At ambient temperatures, the brightest phosphors are obtained with silica contents ranging from 1.8 to 1.85 moles of silica (Fig. 1) and these phosphors are initially somewhat whiter in body color than those with higher silica ratios. If, however, a range of phosphors with varying silica contents are heated in air to about 400°C , a marked discoloration occurs in phosphors containing about 1.8 moles of silica or less, whereas much smaller changes take place with higher silica ratios. As might be expected phosphors with low silica contents are more susceptible to lamp processing conditions.

Changes in body color, which occur when phosphors with low silica content are heated, begin to develop markedly at temperatures slightly higher than the temperature break point and are thought to be associated with displacement of activator atoms from the phosphor lattice followed by surface oxidation. X-ray examination shows that, after prolonged heating at 400°C , small amounts of a second phase may be formed. This second phase, referred to later, is believed to correspond to a triple silicate which is deficient in Ce.

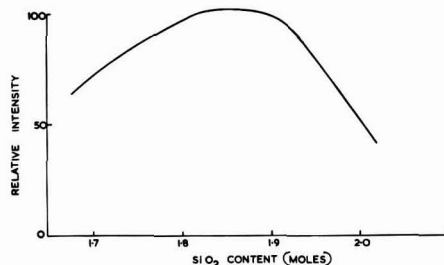


Fig. 1. Variation of brightness of triple silicate phosphor with silica content (at ambient temperature).

The temperature response curves of phosphors prepared with a range of silica contents also show a marked progression in properties as the silica content is increased (Fig. 2). At low temperatures (below 200°C) phosphors with lower silica ratios are brighter, but as the silica content is increased the maximum is reached at progressively higher temperatures. The temperature break point for phosphors with lower silica content corresponds roughly to the temperature at which darkening sets in and suggests that the silica content (base to acid ratio) may determine the readiness with which the activators are displaced from the lattice, evidenced by the discoloration produced by heating in air.

Effect of Activator Concentration

In common with calcium orthophosphate phosphors activated with Ce and Mn (9), comparatively large quantities of Ce of the order of 10% by weight of the matrix, give the brightest fluorescence at ambient temperatures. Although the temperature characteristics of these phosphors are not critically dependent on the Ce content, increase in Ce lowers the temperature at which optimum brightness occurs while the rate of depreciation beyond this point is reduced. Results are similar to those observed by Kroeger (1) for lanthanum silicate activated by Ce.

Manganese content influences the color and intensity of fluorescence but, even in amounts which

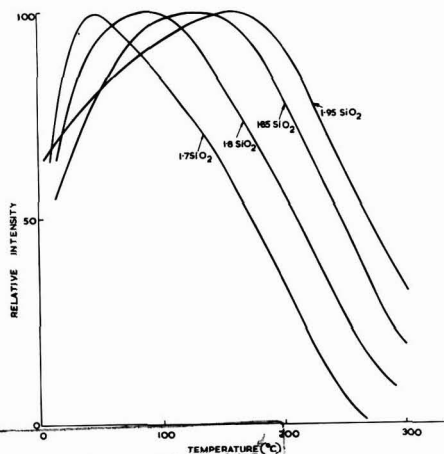


Fig. 2. Temperature response curves of triple silicate phosphor with varying silica content.

reduce the initial brightness, does not alter markedly the shape of the temperature dependence curves, provided optimum silica ratios are maintained.

Cerium also appears to assist in the formation of the crystalline phase associated with fluorescence (7). Nonfluorescent materials, prepared without Ce, are usually of a distinct crystal structure.

Effect of Firing Treatment

Triple silicate phosphors are fired in a reducing atmosphere to retain Ce in the cerous state necessary for activation. The optimum firing temperature is fairly critical and the best results have been obtained at temperatures close to the sintering temperature which may vary between 800°-900°C for compositions described earlier. As the firing time is increased a marked improvement in temperature dependence occurs. This effect is illustrated in Fig. 3, which compares phosphors with the same initial composition fired for 3 hr and 100 hr, respectively. X-ray examination shows that the only crystal phase in these two samples is that normally associated with the barium strontium lithium silicate phosphors. The crystal size of the material fired for the longer period ranged from 5 to 30 μ , while the 3-hr firing period gave a crystal size range of approximately 1-10 μ . These results confirm those of Kroeger (1), that the temperature characteristics depend on the perfection of the crystal lattice.

Effect of Temperature on Spectral Emission Characteristics

The triple silicate phosphor shows a marked change in color of fluorescence as its temperature is raised. This is due to a shift in the position of the Mn emission band toward shorter wave lengths, which occurs most markedly below about 150°C (see Fig. 3). This shift also accounts, at least partly, for the observed increase in brightness of fluorescence between these temperatures (Fig. 2). At higher temperatures, modification of the color is less marked and is due mainly to a relative decrease in the blue emission band due to Ce.

At liquid air temperatures there may be some tendency to a head in the red emission band which occurs at 6,400Å for a phosphor containing equimolecular proportions of Ba and Sr.

Performance in Lamps

Color corrected H.P.M.V. lamps were first introduced in Great Britain in 1937 using zinc cadmium sulfide phosphors. These lamps gave a red ratio of about 5% where red ratio is defined as the percentage of the total lumens from the lamp passing through an orange Wratten No. 25 filter. In 1953, triple silicate phosphors were introduced in place of the sulfide phosphors in 125-w quartz lamps. Red ratios of about 6-7% were obtained with these early phosphors which had relatively poor temperature response characteristics. Improvements in temperature characteristics of these phosphors, of the type described above, have led to an improvement in red output of some 20%, so that red ratios of about 8% are now obtained. The improvement in color rendering over sulfide-coated lamps is not

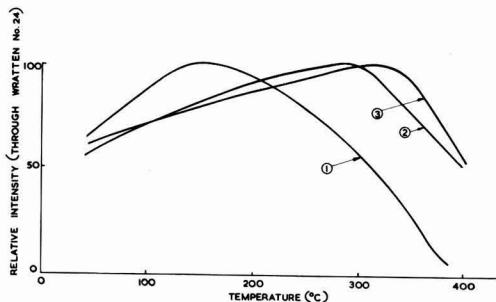


Fig. 3. Effect of firing time on temperature response of triple silicate phosphor. Curve 1, triple silicate (3-hr firing); curve 2, triple silicate (100-hr firing); curve 3, 3 MgO·1 MgF₂·GeO₂(Mn).

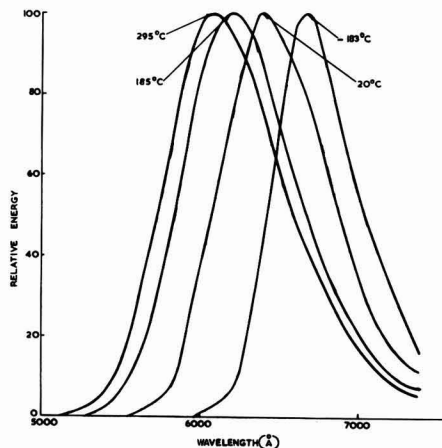


Fig. 4. Change of spectral energy distribution of triple silicate phosphor (Mn band) with temperature.

fully reflected by the increase in red ratio measurements. The blue emission from the silicate phosphor together with its relative freedom from body color gives a marked improvement in the blue and blue-green regions of the spectrum. The luminous efficiency and lumen maintenance characteristics of these lamps follow closely that of the lamp without fluorescent coating and lamps of 125 w rating give 100 hr efficiencies of about 40 lpw.

These results are obtained with triple silicate phosphors having equimolecular proportions of Ba and Sr. If phosphors with higher Ba to Sr ratios are used, additional yellow light is added and efficiencies some 10% higher can be obtained. Although the color rendering properties are slightly degraded, the red ratio figures are not materially reduced. This may be due to the increased sensitivity of these phosphors to short u.v. radiation, which results in a higher proportion of fluorescence emission in lamps coated with these phosphors.

Discussion

The addition of comparatively minor constituents to improve the temperature characteristics of several phosphor systems is well known. Froelich and Margolis (9), for example, have shown that certain

alkali metals can improve the temperature characteristics of calcium phosphates activated with Ce and Mn, and have suggested that these additives may produce a lattice with fewer vacancies or defects. Klasens (5) has observed similar improvements with Mn-activated magnesium arsenate phosphors containing Li. The effect of silica content, in the triple silicates, represents a further example of the importance of small changes in phosphor composition on temperature characteristics.

As described above, increase in silica content improves temperature dependence characteristics and reduces the tendency to discolor during low temperature air bake. The onset of marked discoloration in phosphors with low silica content appears to occur at temperatures somewhat higher than those at which peak brightness of fluorescence is attained. This discoloration is believed to correspond to a displacement of activators from lattice positions at elevated temperatures which is followed by a superficial oxidation. Such conditions may be expected to obtain in a lattice which is constrained and the function of additional silica may be to relieve such constraints. It may, for example, provide more readily for the incorporation of activators into the lattice or indirectly by creating lattice vacancies by the incorporation of additional Li ions into the lattice. In either case, conditions may be created in the

lattice equivalent to a lowering of activator concentration, and which might, therefore, be expected to give improved temperature characteristics. The results thus lend some support to the views of Klement (10) that in a given phosphor system temperature quenching is dependent on the degree of isomorphism of the activator and the matrix lattice.

Manuscript received June 3, 1957. This paper was prepared for delivery before the Washington Meeting, May 12-16, 1957.

Any discussion of this paper will appear in a Discussion Section to be published in the December 1958 JOURNAL.

REFERENCES

1. F. A. Kroeger, "Some Aspects of the Luminescence of Solids," Chap. VI, Elsevier Publishing Co., Amsterdam (1948).
2. G. R. Fonda, *J. Phys. Chem.*, **43**, 561 (1939).
3. L. Thorington, *J. Opt. Soc. Amer.*, **40**, 579 (1950).
4. M. Travniczek, F. A. Kroeger, Th. P. J. Botden, and P. Zalm, *Physica*, **18**, 33 (1952).
5. H. A. Klasens, *Philips Research Repts.*, **9**, 377 (1954).
6. H. G. Jenkins and A. H. McKeag, *Lux*, **21**, 87 (1953).
7. A. H. McKeag and E. G. Steward, *Brit. J. Appl. Phys.*, Suppl. No. 4, p. S26 (1954).
8. M. J. B. Thomas, K. H. Butler, and J. M. Harris, *Illum. Eng. Soc. Conf.*, 1956, Preprint No. 30.
9. H. C. Froelich and J. M. Margolis, *This Journal*, **98**, 400 (1951).
10. F. D. Klement, *Izvest. Akad. Nauk. S.S.S.R. Ser. Fiziol.*, **15**, 651 (1951).

Zone Purification of Silicon

E. A. Taft and F. H. Horn

Research Laboratory, General Electric Company, Schenectady, New York

ABSTRACT

A procedure is described for the zone purification of high purity silicon using thin-walled quartz boats. Data are given that show that improved lifetime and more uniform electrical resistivity result from the zone purification of commercially available silicon.

The zone purification (1) of high purity Si in a boat presents problems not encountered in processing the less chemically reactive Ge for which zone refining is almost a routine purification procedure. It is not necessary to use a boat as in floating zone purification (2); however, in such a case one is limited to one molten zone per pass. It is the purpose of this report to (a) describe a procedure that has been used successfully to zone refine high purity Si in quartz, (b) present data to indicate what is accomplished thereby, and (c) suggest some of the present limitations to the process.

In order to work out a process one is faced with a certain number of variables that after some exploration must be arbitrarily fixed. In the case of zone refining these are (a) materials for the boat and related apparatus, (b) working atmosphere, (c) source of heat, and (d) the form of starting material.

Experimental

Tests using selected refractory sulfides, nitrides, carbides, and oxides indicated that because of direct attack by molten Si and/or because of the impurities in the refractories obtainable, fused clear quartz was the best available material for the boat. There are certain chemical limitations to the use of quartz that are discussed later. The first serious difficulty involved in the use of quartz is mechanical. Molten Si wets quartz. If molten Si is allowed to freeze in boats of quartz of commercially available thickness, cracking of the quartz and Si takes place on cooling the solid Si since the coefficient of thermal expansion of quartz is considerably smaller than that for Si. Nevertheless quartz may be employed for handling Si if use is made of the plastic properties of quartz and Si. At and above the freezing point of Si, quartz is plastic; below the freezing point of Si to about 1000°C (3), in which temperature range

quartz is negligibly plastic, solid Si itself is plastic. The solution to the problem of using quartz to handle molten and solid Si is to use as thin quartz as possible, in practice from 5 to 15 mils thickness¹ depending on the size of equipment, and to maintain the temperature of the solid Si in the plastic range throughout a process. This latter requirement may be met by a proper distribution of heat.

No very marked differences in the final product have been observed whether the Si during zone refining is maintained in a vacuum or in atmospheres of H, He, or A. The use of A requires less power than H or He for heating. A lower power input may be reflected in a somewhat lower temperature of the molten silicon-quartz interface. This is important as is discussed below. The use of A is preferred for this reason.

Induction heating has been used throughout this work. The source of power has been a 15-kw 450-kc General Electric Induction heater. The power output was filtered to remove low frequency components that cause agitation of the liquid zones. It is not essential to do this in order to zone melt the Si; however, crystal grains grow to a significantly larger size if the agitation is removed by the use of a filter.

High purity Si is obtainable in either small crystalline aggregate or "densified" form.² With direct induction coupling the fusion of aggregates or densified material in a boat is very difficult to accomplish. It is easier to have a single solid rod of Si to place in the boat. Such rods were prepared by melting together the crystalline aggregates.

Premelting is carried out in a thin wall quartz tube in the apparatus shown schematically in Fig. 1. The molten Si is blanketed by argon gas. As the Si is added, the heating coils are moved upward keeping about 1 in. of molten Si on top of the solid. The quartz tube adheres to the Si and must be removed (HF solution) before proceeding with the zone refining. Typical premelt rods are shown in Fig. 2, both before and after removing the quartz tube.

¹ Available through General Electric Company, Cleveland Quartz Works, Cleveland, Ohio.

² E. I. du Pont de Nemours Company, Pigments Division, was the major supplier of the high purity Si used in these experiments.

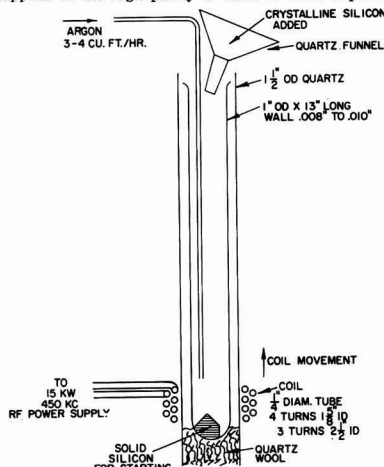


Fig. 1. Schematic arrangement for premelting Si crystals

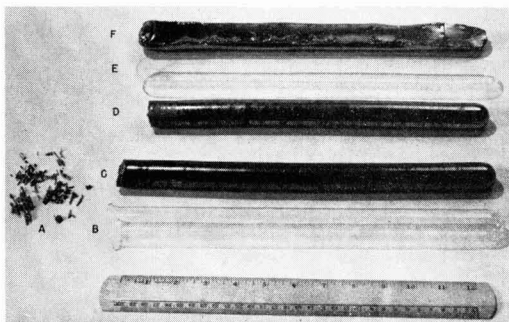


Fig. 2. Photograph of (A) crystalline aggregate of Si; (B) thin quartz premelt tube; (C) premelt rod of Si with quartz tube adhering to surface; (D) premelt rod of Si with quartz removed; (E) thin quartz zone melt boat; (F) zone melted billet of Si.

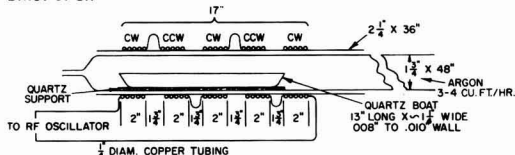


Fig. 3. Schematic arrangement for zone refining Si

The arrangement for zone refining Si is shown schematically in Fig. 3. Approximately 400 g of Si is handled at a time and five zones are carried through the solid in one pass. Movement of the zones at the rate of about 5 1/2 in./hr has been found satisfactory. The appearance of a zone refined billet is shown in the photograph of Fig. 2. Before use, the quartz adhering to the Si must again be removed by solution in HF.

Discussion

In order to assess what is accomplished by the zone purification, single crystals were grown from quartz crucibles using portions of the zone refined ingot. Lifetime and resistivity measurements were made along the length of the single crystal. Some of these data are given in Tables I and II. The con-

Table I. Lifetime and resistivity of crystals grown from zone refined Si ingot

Crystal No.	Description	Type	Resistivity ohm cm*		Lifetime μ sec		
			ρ_{10}	ρ_{90}	τ_{10}	τ_{50}	τ_{90}
91	Premelt only	P	80	56	90	50	—
82	Zone melt—front	P	90	40	200	400	150
83	2nd—10%	P	90	40	>1000	750	400
84	3rd—10%	P	90	40	800	150	—
85	4th—10%	P	90	40	200	100	60
86	Zone melt—50%	P	90	40	140	100	60

* Subscript denotes percentage of grown crystal.

Table II. Lifetime and resistivity of crystals grown from separate zone refined ingots from same lot of Si

Crystal No.	Description	Type	Resistivity ohm cm*		Lifetime μ sec	
			ρ_{10}	ρ_{90}	τ_{10}	τ_{90}
127	Densified Si	n	20	2	100	100
193	Zone melt 133	P	76	34	300	200
195	Zone melt 134	P	90	50	300	200
198	Zone melt 135	P	—	—	300	150

* Subscript denotes percentage of crystal grown.

clusions reached based on these data are valid for all of the work done on zone refining.

All data in Table I are derived by using the same lot of Si. Crystals grown directly from the crystal aggregates of this lot contain barriers which make resistivity measurements unreliable as an index of purity. The lifetime as determined for regions of the crystals not including a barrier was less than 20 μ sec. It is seen that the premelting operation alone improves the quality of the Si. A more significant improvement is obtained after zone purification. In particular, the concentration of impurities that shorten the lifetime of the crystal appears to be reduced. The resistivity is not appreciably altered. The resistivity profiles of the crystals are consistent with an assumption of the presence in the crystals of an acceptor impurity with a segregation coefficient near unity such as is the case for boron. If no B is introduced during the processing of the Si, the results suggest that the donors originally present are either volatile or are readily segregated during growth of the evaluation crystal. This situation is more apparent from the results of Table II.

The data in Table II are all for the same lot of Si but the evaluations were made on crystals grown from the Si taken from the same region of different zone melt ingots. These data are compared with those from an evaluation crystal grown from densified Si (without zone refining) from the same lot. The dominant impurity in the densified material was a donor, the dominant impurity after premelting and zone refining was an acceptor. Processing apparently removes the donor impurities. Lifetime is again seen to improve. The consistency of the results from separate operations suggests that the final resistivity level results from an impurity whose segregation coefficient is near unity.

These results of Si quality are indicative of what is accomplished by zone refining, namely (a) increased lifetime resulting from a substantial reduction in the concentration of lifetime suppressors in Si, and (b) reduction of the concentration of donors with resultant increased uniformity of material from an ingot, or a lot, and even among lots.

It was considered desirable to learn, particularly with respect to boron, the extent to which the use of commercially available quartz may control the results of zone purifying Si. In order to assess this possible limitation it is necessary to know the rate of attack of fused quartz by molten Si. This was done by determining the loss in weight from cubes of fused quartz left in contact with molten Si at several temperatures. The area of contact between the quartz and Si is clearly indicated by the reaction. The weight loss per cm^2 per hour is plotted as a function of the Si temperatures in Fig. 4. Using the value of 5 $\text{mg}/\text{cm}^2/\text{hr}$ for the rate of reaction between quartz and molten Si it is estimated that about 10^{14} boron at./cc of Si may be dissolved dur-

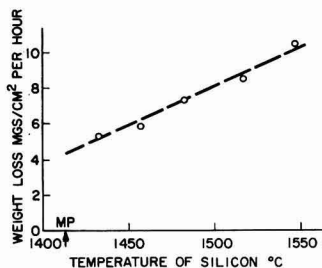


Fig. 4. Removal of quartz by molten Si

ing zone melting for each part per million of B in the quartz. The B concentration in the quartz used is of the order of tenths of parts per million. In practice, material with a resistivity in excess of 300 ohm cm, or less than 5×10^{13} carriers/cc has been realized. The reaction between the quartz and molten Si can be kept at a minimum by keeping the liquid Si at a temperature as near the melting temperature as is consistent with conducting the process.

In addition to the problem of possible B contamination by the quartz, Si melted in quartz apparatus also contains some oxygen (4). In this respect the Si zone refined in quartz differs from the material obtainable by a procedure such as the floating zone. If Si relatively free from oxygen is required, the Si zone refined in quartz represents a convenient form of starting material for applying the floating zone technique.

Summary

1. A procedure for zone refining Si in thin-walled quartz is described.
2. Zone refining Si has been found to improve lifetime.
3. Silicon of more consistent resistivity is realized within an ingot or within a lot after zone purification. The remaining impurity behaves like B.
4. The use of commercially available quartz does not necessarily constitute a limitation on the purity of the zone refined Si if the initial concentration of the poorly segregating impurity in the Si (presumed B) is larger than approximately 5×10^{13} carriers/ cm^3 (300 ohm cm). It should be borne in mind, however, that Si processed in quartz is not free of oxygen.

Manuscript received Aug. 19, 1957.

Any discussion of this paper will appear in a Discussion Section to be published in the December 1958 JOURNAL.

REFERENCES

1. W. G. Pfann, *Trans. Am. Inst. Mining Met. Engrs.*, **194**, 747 (1952).
2. P. H. Keck, W. Van Horn, J. Soled, and A. MacDonald, *Rev. Sci. Instr.*, **25**, 331 (1954).
3. C. J. Gallagher, *Phys. Rev.*, **88**, 721 (1952).
4. W. Kaiser, P. H. Keck, and C. F. Lange, *ibid.*, **101**, 1264 (1956).

A Fused Bath for Electrodeposition of Molten Cadmium-Indium Alloy

George L. Schnable and John G. Javes

Philco Corporation, Lansdale Tube Company Division, Lansdale, Pennsylvania

ABSTRACT

A fused salt bath for electrodeposition of molten cadmium-indium alloy is described, from which ellipsoidal beads of molten alloy are plated onto wires used as leads to emitter and collector electrodes of transistors. Electrodeposition of molten metals can be very rapid, and the deposits are smooth, dense, and nonporous. The fused salt bath, containing 6% cadmium chloride, 56% indium monochloride, and 38% zinc chloride, by weight, is operated at about 260°C. Tungsten anodes are used. With 6 v d.c. applied, a 2 mg ellipsoidal bead of cadmium-indium alloy of approximately eutectic composition can be deposited on a 0.5 mm wire that is immersed a depth of 1.5 mm into the plating bath in about 4 sec. Under these conditions, current density is of the order of 40 amp/cm². The effect of bath composition and of plating conditions on alloy composition and plating rate is discussed.

In the fabrication of transistors, for example, alloyed-junction and surface-barrier types, electrical connections must be made to the emitter and collector electrodes. If the transistor electrodes are indium metal, In cannot be used as a solder since it is not desirable to melt the electrodes during soldering. Cadmium-indium eutectic alloy (25% Cd, 75% In, by weight) melts at 123°C. The molten alloy readily wets In in the presence of a suitable flux and can be used to solder whisker wires, ribbons, stem leads, or other electrical connections to the emitter and collector electrodes without melting the In electrodes (mp 157°C). The soldering operation is performed in a few seconds at 140°C in the presence of a mild flux. The alloy is harder than In metal, with the result that joints soldered with it are considerably stronger than joints soldered with In alone. Transistors having In electrodes soldered with Cd-In alloy, in contrast to those soldered with Sn-In alloy, can be clean-up etched in acids such as aqueous solutions containing HNO₃ and HF. Cd⁺⁺ and In⁺⁺⁺ ions do not deposit chemically on the Ge during the clean-up etching process. Since both Cd and In are more negative than Ge in the electromotive series (1-3) (less noble), chemical deposition would not be expected.

Electrodeposition of Molten Cd-In Alloys

Several milligrams of Cd-In alloy are required on the ends of emitter and collector leads of transistor stems. (The stem consists of three lead wires hermetically sealed in an equilateral triangular configuration in a glass base.) Because of the sensitivity of transistors to contaminants, the Cd-In solder must be free of entrapped fluxes, plating solutions, or other impurities. A rapid process was required for production line use.

Experiments indicated that hot dip "tinning" of stems in molten Cd-In alloy produced coatings too

thin to be satisfactory. Electrodeposition of solder was considered the most suitable approach. With electrodeposition any or all of a group of lead wires simultaneously immersed in the plating solution can be plated and different amounts can readily be plated on emitter and collector leads.

Electrodeposition of Cd-In alloys from aqueous solutions resulted in rough, porous deposits. Plating rates were too low for production use.

Electrodeposition of molten metals results in smooth, dense, nonporous deposits which are free of plating bath constituents (occlusions). The high surface tension of the molten deposits in plating baths having a fluxing action tends to affect the surface area and location of the molten metal or alloy deposit. For example, on wires held vertically during plating, the molten deposit flows downward, forming a smooth ellipsoidal bead of molten metal or alloy at the end of the wire.

Since molten deposits in an effective flux are characterized only by composition and temperature, plating quality is unaffected by many of the variables which must be carefully controlled in ordinary aqueous plating processes. For example, the limiting current density which can be employed is not determined by plating quality as with aqueous plating baths, where dendritic growths are formed at higher current densities.

A number of methods have been developed at this laboratory for electrodepositing molten metals and alloys from plating baths operated at temperatures above the melting point of the metal or alloy.

Baths developed for electrodeposition of molten Cd-In alloys are of two general types: (a) Cd and In salts dissolved in high-boiling polar organic solvents such as glycerol; (b) fused salt solutions containing Cd and In salts.

In general, the plating baths developed are effective fluxes for base metals such as Ni as well as for

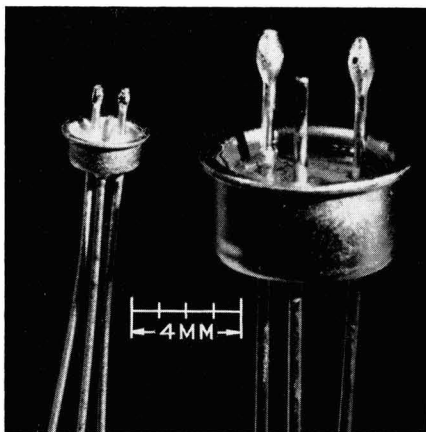


Fig. 1. Typical transistor stems having leads plated with Cd-In alloy.

the deposited metals and alloys. Thus good wetting of the base metals is obtained.

Typical Operating Conditions

The fused salt bath is particularly suitable for plating wires 5-40 mils in diameter, where a few milligrams of Cd-In alloy are desired on each wire or lead. The preferred bath, containing 6% CdCl₂, 56% InCl₃, and 38% ZnCl₂ by weight, plates molten Cd-In alloy several hundred times as fast as aqueous baths. Under typical operating conditions the plating bath is maintained at 255°±5°C; a plating potential of 6 v d.c. is applied between the cathode and a tungsten anode. For 60 mil immersion of stem leads 20 mils in diameter (1.5 mm immersion of leads 0.5 mm in diameter), plating times of roughly 2 and 4 sec are suitable for electrodeposition of 1 and 2 mg of Cd-In alloy on emitter and collector leads, respectively. Plating current averages about 2 amp/lead. Under these conditions, current density is of the order of 40 amp/cm².

Typical plated whiskers and stems are shown in Fig. 1.

No Zn has been detected in Cd-In alloys plated from CdCl₂-InCl₃-ZnCl₂ fused salt baths.

Experimental Results

Cadmium-Indium Alloys

The Cd-In system has been investigated by Betteridge (4), Carapella and Peretti (5), Valentin (6), and Wilson and Wick (7). Cadmium (mp 321°C) and indium (mp 157°C) form a eutectic alloy containing 25% Cd and 75% In by weight, melting at 123°C. Cadmium-indium alloys in the range from nearly 100% Cd to about 18% Cd-82% In by weight have structures showing the eutectic, and thus have a solidus temperature of 123°C; liquidus temperatures vary from 321° to 123°C. Alloys containing less than about 18% Cd by weight have solidus temperatures from 123° up to 157°C as In content increases. Alloys in the approximate range from 50% Cd-50% In to 20% Cd-80% In have been found to flow at temperatures below 130°C. Although some of these alloys have a liquidus temperature above 130°C, all have a solidus tem-

perature of 123°C and all would consist of at least 67% liquid phase at 130°C. Therefore, any alloy in this composition range flows below 130°C and is considered a satisfactory solder for In metal.

The temperature at which deposited alloys flow was determined by flattening ellipsoidal beads of alloy plated on the ends of wires and immersing them in a heated flux bath which was stirred vigorously. Alloys were considered to flow if the flattened alloy returned to an ellipsoidal bead of molten alloy within 3 sec after immersion in a flux bath at the particular temperature chosen. A flux consisting of 2% by volume concentrated HCl (37%) in glycerol is suitable.

Breaking load experiments have indicated that Cd-In eutectic alloy at any temperature from 25° to 110°C has a greater tensile strength than In metal at the same temperature; indeed the alloy has a greater tensile strength at 110°C than In metal at room temperature. Cadmium-indium alloys might be expected to have a greater tensile strength than In metal since binary alloys of In with Pb, Ag, Cd, Bi, and Sn have been reported to have tensile strengths greater than that of In at room temperature (8-10).

Hundred-hour creep strength measurements made at 100°C have shown that Cd-In eutectic alloy has a somewhat higher creep strength than In metal at 100°C.

Fused Salt Bath for Electrodeposition of Molten Cadmium-Indium Alloys

The requirements of a fused salt bath for electrodeposition of molten Cd-In alloys on Ni wires are rapid plating rate, practical operating temperature, freedom from objectionable crust formations, reasonable bath life, minimum evolution of fumes, and ability to act as a satisfactory flux for Ni as well as for molten Cd-In alloy.

The most obvious choice as a source of In ions for a fused salt bath is InCl₃, which melts at 586°C but sublimes below 400°C. The only alkali or alkaline earth chloride system which could serve as a solvent for InCl₃ was the LiCl-KCl eutectic, mp 352°C. A solution of InCl₃ in molten LiCl-KCl eutectic fumed too much to be practical.

Indium trichloride was found to dissolve in molten ZnCl₂. However, electrolysis of a molten solution of InCl₃ in ZnCl₂ at 320°C resulted in cathodic reduction of In³⁺ to In²⁺ and/or In⁺ (indicated by formation of In metal by disproportionation when an electrolyzed bath was treated with water) but no In metal (or Zn) was deposited on the cathode. This is in agreement with the work of Coyle (12), who, upon electrolysis of a fused solution of InCl₃ in ZnCl₂, obtained no deposit of In metal at the cathode.

Molten InCl₃, mp 225°C, was found to deposit molten In metal upon electrolysis. However, InCl₃ is a relatively poor solvent for anhydrous CdCl₂, tends to form crusts (oxides), and was a relatively poor flux for Ni.

Molten InCl₃ (mp 225°C) and molten ZnCl₂ (mp 275°C) are miscible in all proportions. Cooling curves run on fused salt solutions of InCl₃ and ZnCl₂,

containing 50, 57, and 60% by weight InCl, indicated that the InCl-ZnCl₂ system forms a eutectic containing about 55-60% InCl by weight, melting at roughly 145°C.

Cadmium chloride appears to be more soluble in molten solutions containing both InCl and ZnCl₂ than in either of these alone. A solution containing 60% InCl and 40% ZnCl₂ dissolves roughly 10% by weight of CdCl₂ at 200°C, and dissolves more than 15% CdCl₂ at 260°C. [Molten ZnCl₂ dissolves only 15% by weight CdCl₂ at 305°C (11).]

The presence of ZnCl₂ in the fused salt plating bath minimizes crust formations and makes the bath a more effective flux for base metals such as Ni as well as for the molten Cd-In alloy.

A CdCl₂-InCl-ZnCl₂ bath containing 6% CdCl₂, 56% InCl, and 38% ZnCl₂, by weight, may be operated at temperatures from 200° to about 320°C. At temperatures above 300°C fuming may be objectionable.

Electrolysis of molten CdCl₂-InCl-ZnCl₂ solutions at 250°C results in electrodeposition of molten Cd-In alloys at the cathode; no Zn has been detected in spectrographic analyses of the electrodeposited alloys. Thus, in the solutions investigated, Zn⁺⁺ is sufficiently negative in the electromotive series compared to Cd⁺⁺ and In⁺ (or In⁺⁺ and In⁺⁺⁺) that ZnCl₂ is capable of serving as an inert solvent for CdCl₂ and InCl without any reduction of Zn⁺⁺ ions to Zn metal occurring during electrolysis. This might be expected from the data of Hamer, Malmberg, and Rubin (13), who calculated the theoretical decomposition voltages of fused metal chlorides at various temperatures.

Preparation of Plating Baths

The InCl used in the plating solution is prepared by reacting anhydrous InCl₃ with an excess of In metal at 300°C in an inert atmosphere to form molten InCl (mp 225°C). Indium monochloride prepared by this method has a monovalent In content, as determined by the disproportionation method, averaging 96-98% of theoretical. Minimum assay for acceptable InCl is 95%.

Some InCl has also been prepared by reaction of anhydrous HCl gas with excess molten In metal at about 300°C.

It is necessary for fused salt baths which are operated at high current densities to be essentially anhydrous. Otherwise excessive bubbling occurs at the cathode, caused by evolution of water vapor as a result of local heating at the cathode during electrolysis and/or by evolution of hydrogen gas at the cathode. A considerable amount of water was found to be present in CdCl₂-InCl-ZnCl₂ baths prepared by heating the constituent salts to 250°C. The principal source of the water is the ZnCl₂; reagent-grade zinc chloride has an assay of about 95% ZnCl₂.

While water can be removed from fused salt baths by heating to about 450°C, this procedure results in the formation of some insoluble material since in the presence of water the metal chlorides are to some extent converted to oxides and/or oxychlorides with evolution of HCl. It was found that completely clear, anhydrous CdCl₂-InCl-ZnCl₂ fused salt solu-

tions could be prepared by bubbling anhydrous HCl gas through the molten bath at about 360°C. Any excess HCl in the treated melt is removed by bubbling dry nitrogen through the fused salt solution.

The InCl is treated with anhydrous HCl during preparation. Cadmium chloride and zinc chloride in the proper proportions are heated to 360°C and treated with anhydrous HCl to remove water, at which time the correct amount of InCl is added, and the CdCl₂-InCl-ZnCl₂ solution at 360°C is treated with anhydrous HCl for a short time.

The fused salt bath, analyzed for monovalent In content by disproportionation, should assay not less than 93% of the theoretical amount of InCl.

Plating Apparatus

Stirring of fused salt baths during rapid electrodeposition of Cd-In alloy is essential in order to insure reproducible plating of the correct amount of alloy of suitable composition. Stirring minimizes local depletion of ions at the electrodes and minimizes local heating at the cathode during electrolysis. It also enables immersed wires, which are to be plated, to attain bath temperature quickly. This is especially important when immersion depth is only slightly greater than the diameter of the wire to be plated.

A magnetic stirring apparatus was used during all plating experiments described below. The magnetic stirring bar was sealed in a Pyrex tube. Average velocity of plating bath past cathodes and anodes was estimated to be of the order of 10 cm/sec. Baths were contained in Pyrex vessels.

Inert anodes are used in the fused salt bath for electrodepositing molten Cd-In alloy. Carbon anodes (spectroscopic graphite) may be used at low currents but disintegrate rather rapidly at high currents, and, therefore, are not recommended. Rhodium appears to be a satisfactory material for anodes. Tungsten has been entirely satisfactory as an anode material, and was used in all of the experiments described below.

The anode should be large enough to minimize anodic polarization. Using a spiral tungsten wire (0.1 cm diameter) with an effective length of about 30 cm as an anode, no appreciable polarization was evident at currents up to 4 amp.

The anode should be located symmetrically with respect to each of the stem leads to be plated so that, with equal potentials applied between the anode and each lead to be plated, equal currents will flow through each stem lead. Under these conditions the plating rate will be the same for each stem lead. Anodes were located roughly 1 cm from the wires to be electroplated.

If different amounts of Cd-In alloy are desired on emitter and collector leads, this should be accomplished by employing different plating times rather than by applying different potentials to emitter and collector leads. This is done in order to obtain alloy of the same composition on both leads.

An inert atmosphere such as dry nitrogen gas is passed over the surface of the plating bath to minimize oxide formation and air oxidation of monovalent indium.

Several plating baths, protected by a nitrogen atmosphere, have been maintained at 250°C for 1 week without appreciable change in the alloy composition as determined by the flow temperature of alloy plated from the bath.

Relationship between Bath and Plated Alloy Composition

Successive increments of CdCl₂ were added to a fused salt solution consisting of 60% InCl and 40% ZnCl₂ by weight. Bath composition versus plated alloy composition, as determined by EDTA titrations, is shown in Table I for a bath operated at 255°C. Six volts d.c. were applied. Plating currents were about the same in each case. The approximate amounts of Cd-In alloy plated in 10 sec on a 20-mil wire immersed 60 mils into the bath are given in the table. All percentages are by weight.

The cathode area of immersed stem leads increases rapidly as ellipsoidal beads of molten Cd-In alloy are electrodeposited on the immersed stem leads. Under typical operating conditions (60 mil immersion of a 20 mil lead in the preferred bath at 255°C, 6 v d.c. applied) the surface area of the molten Cd-In alloy at the end of a 3-sec plating period is 2 to 3 times as great as the original surface area of the immersed lead. As the area of the molten Cd-In alloy increased during plating, the current drawn (at constant applied voltage) also increased. For this reason accurate measurements of current density were not possible. Current density under the typical operating conditions described above is of the order of 40 amp/cm².

In repeat tests, baths operated under the same conditions as those described above (255°C, 6 v, tungsten anode) showed good reproducibility of deposited alloy composition.

Decrease in deposition rate (amount of alloy deposit obtained in a given time) with increase in cadmium chloride content in the bath, as shown in Table I, is ascribed in part to the fact that the reduction reaction at the cathode involves an increasing proportion of Cd²⁺ ions, which have an equivalent weight only half as great as that of In⁺ ions. As a result, even if the cathode current efficiency does not change, the weight of metal deposited would drop somewhat as the alloy deposit becomes richer in Cd.

Effects of Plating Voltage on Alloy Composition

In experiments where a bath containing 6% CdCl₂, 56% InCl, and 38% ZnCl₂, operated at a temperature of 255°C, was electrolyzed at various potentials

from 1.5 to 12 v, alloys flowing below 130° were obtained in all cases. Analysis showed that alloys plated at 1.5 v contained 24% Cd, 76% In; alloys plated at 6 v contained 27% Cd, 73% In.

Potentials of 10 v or more cause a considerable amount of fuming due to local heating at the cathode.

Anode Reactions and Plating Bath Depletion

Depletion tests on a bath containing 9% CdCl₂, 55% InCl, and 36% ZnCl₂ by weight indicated that about 5 g of Cd-In alloy (equivalent to about 1600 transistor stems having 1 mg of alloy on the emitter lead and 2 mg on the collector lead) can be plated from a 160-g bath before the plating rate decreases noticeably. Plating was done at 260°C using 6 v d.c. Over 7 g of Cd-In alloy was deposited with little change in plated alloy composition, as indicated by flow temperature determinations and by EDTA titrations. Plating current remained essentially constant during depletion tests.

The anode reaction during electrolysis of fused CdCl₂-InCl-ZnCl₂ baths involves oxidation of monovalent In ions to In²⁺ and/or In³⁺ ions. While this reaction decreases the operating life of the bath, it completely eliminates evolution of chlorine gas at the anode, which would be very undesirable in many applications of the bath. The gradual increase in multivalent In ions in the bath during electrolysis leads to lower plating rates.

Tests in which successive increments of InCl₃ were added to a bath consisting of 9% CdCl₂, 55% InCl, and 36% ZnCl₂ indicated that plating rate decreased because the cathode reaction In³⁺ + e⁻ → In²⁺ and/or the cathode reaction In²⁺ + e⁻ → In⁺ competed with the desired reactions In⁺ + e⁻ → In and Cd²⁺ + 2e⁻ → Cd. A solution containing 8% CdCl₂, 46% InCl, 15% InCl₃, and 31% ZnCl₂ plated Cd-In alloy less than half as fast as a bath containing 9% CdCl₂, 55% InCl, and 36% ZnCl₂, although plating currents were about equal.

If indium dichloride is formed at the anode during electrolysis, electrodeposition of 1 g of eutectic alloy (containing 25% Cd, 75% In, by weight) results in oxidation of 1.26 g of In⁺ to In²⁺ at the anode; if InCl₃ is formed, 0.63 g of In⁺ is oxidized to In³⁺. There is considerable evidence (14) that indium dichloride actually exists as In⁺InCl₂.

Cleaning of Stems Plated in the Fused Salt Baths

Stems plated in the fused salt bath can be cleaned by immersion in ZnCl₂-NH₄Cl eutectic flux at about 250°C to remove the thin coating of solidified plating bath on the Cd-In alloy. Stems should be immersed deeper into the flux than they had been immersed in the fused salt bath. Gentle stirring is helpful in removing all of the plating bath from the surface of the Cd-In alloy. The ZnCl₂-NH₄Cl eutectic flux (75% ZnCl₂, 25% NH₄Cl, by weight, mp 180°C) is prepared by heating the mixture of ZnCl₂ and NH₄Cl at about 300°C until a clear solution is formed.

The ZnCl₂-NH₄Cl eutectic flux rinse is followed by successive rinses in 3% acetic acid (3% by volume glacial acetic acid in deionized water), cold

Table I. Effect of bath composition on electrodeposited alloy composition and deposition rate; bath at 255°C; 6 v applied

Bath composition			Deposited alloy	
%CdCl ₂	%InCl	%ZnCl ₂	Cd	
			x100 Cd + In	Composition %Cd
				Approximate quantity, mg
0	60	40	0	95
3	58	39	4	77
6	56	38	8	63
9	55	36	12	50

deionized water, and hot deionized water (about 80°C). Stems are dried in air.

In some applications dilute HCl can be used to remove the thin coating of solidified plating bath from Cd-In alloys. In the presence of dilute HCl the In sponge resulting from disproportionation of the fused salt bath in water is dissolved with evolution of hydrogen gas. Concentrations from 0.01N to 0.1N HCl are suitable.

Analytical Methods

In the presence of water InCl undergoes disproportionation (14,15) to In metal and InCl₃ according to the reaction $3\text{InCl} \xrightarrow{\text{H}_2\text{O}} 2\text{In} + \text{In}^{3+} + 3\text{Cl}^-$. This

reaction is the basis of the disproportionation method for determining the monovalent In content of InCl samples and of CdCl₂-InCl-ZnCl₂ baths.

A weighed sample of InCl or of fused salt bath is placed in stirred water to bring about the disproportionation reaction. The aqueous solution is decanted from the resulting spongy lumps of In metal. The In is melted in a mild flux such as 10% NH₄Cl in glycerol to form a single, dense lump of metal, which is cooled and weighed.

Experiments have indicated that the disproportionation reaction is quantitative. Since both Cd and Zn are more negative than In in the electromotive series (3,16), the presence of CdCl₂ and ZnCl₂ in the fused salt bath does not interfere with the reaction in any way; the resulting In metal is spectroscopically free of Cd and of Zn.

Indium dichloride also undergoes disproportionation (14,15) according to the reaction $3\text{InCl}_2 \xrightarrow{\text{H}_2\text{O}} \text{In} + 2\text{In}^{3+} + 6\text{Cl}^-$.

Since, within the range of alloy compositions from 50% Cd-50% In to 20% Cd-80% In, determination of flow temperature is not suitable for estimating alloy compositions, a procedure was developed for titrating In in the presence of Cd with ethylenediaminetetraacetic acid (EDTA) solution. In this procedure, a modification of that described by Flaschka and Amin (17), the Cd²⁺ is complexed with excess KCN and the In³⁺ is titrated with standard EDTA solution. Cadmium was determined by difference based on the total weight of the Cd-In alloy and based on titration of both Cd²⁺ and In³⁺ with EDTA. No KCN was used during the titration of Cd²⁺ + In³⁺.

No Zn has been detected in spectrographic analyses of Cd-In alloys plated from CdCl₂-InCl-ZnCl₂ baths. Detection limit was 0.0001% for Zn.

Indium Recovery from Depleted Baths

Since the bath containing 6% CdCl₂, 56% InCl, and 38% ZnCl₂ contains 43% In metal by weight, methods of recovery of depleted plating baths have been investigated.

In the method now used the depleted bath is heated to about 280°C and slowly poured into a large beaker containing rapidly stirred deionized water (at room temperature). In the resulting dis-

proportionation reaction, two-thirds of the monovalent In and one-third of the divalent In in the bath is converted to In metal. The aqueous solution is decanted from the In sponge, which is then melted under a flux of NH₄Cl in glycerol to form a single globule of In. The In is allowed to cool until solidified and is rinsed with deionized water. No Zn or Cd was detected in spectrographic analyses of In metal samples recovered in this way. Other impurities were at the same level of concentration as those present in the In metal and in the InCl₃ used to prepare the InCl used in the formulation of the fused salt bath.

The recovered In metal can be used to prepare InCl.

The aqueous solution from the disproportionation reaction, containing Cd²⁺, In³⁺, Zn²⁺, and Cl⁻, can be treated with Zn dust to recover In scrap.

Acknowledgment

The authors gratefully acknowledge the interest and encouragement of T. J. Manns and M. Sadowsky.

Manuscript received Oct. 10, 1956. This paper was prepared for delivery before the Cleveland Meeting, Oct. 1-4, 1956.

Any discussion of this paper will appear in a Discussion Section to be published in the December 1958 JOURNAL.

REFERENCES

1. F. Jirsa, *Z. anorg. u. allgem. Chem.*, **268**, 84 (1952).
2. O. H. Johnson, *Chem. Rev.*, **51**, 431 (1952).
3. W. M. Latimer, "The Oxidation States of the Elements and Their Potentials in Aqueous Solutions," 2nd ed., Prentice-Hall, Inc., New York (1952).
4. W. Betteridge, *Proc. Phys. Soc., London*, **50**, 519 (1938).
5. S. C. Carapella, Jr., and E. A. Peretti, *Trans. Am. Soc. Metals*, **43**, 853 (1951).
6. S. Valentiner, *Z. Metallkunde*, **35**, 250 (1943).
7. C. L. Wilson and O. J. Wick, *Ind. Eng. Chem.*, **29**, 1164 (1937).
8. "Intermediate 'Indalloy' Solders," Indium Corp. of America, New York (1954).
9. R. I. Jaffee and M. G. Weiss, cited in "Indium" by J. R. Mills, R. C. Bell, and R. A. King in "Rare Metals Handbook," edited by C. A. Hampel, pp. 199-200, Reinhold Publishing Corp., New York (1954).
10. R. I. Jaffee and S. M. Weiss, *Materials & Methods*, **36**, (3), 113 (1952).
11. Herrmann, *Z. anorg. Chem.*, **71**, 257 (1911).
12. J. Coyle, *Trans. Electrochem. Soc.*, **85**, 223 (1944).
13. W. J. Hamer, M. S. Malmberg, and B. Rubin, *This Journal*, **103**, 8 (1956).
14. N. V. Sidgwick, "The Chemical Elements and Their Compounds," Vol. I, pp. 458-481, Oxford University Press, London (1950).
15. "Gallium and Indium," Chapter 8 in "Chapters in the Chemistry of the Less Familiar Elements," Vol. I, pp. 13-22, by B. S. Hopkins, Stipes Publishing Co., Champaign, Ill. (1939).
16. T. Moller and B. S. Hopkins, *J. (and Trans.) Electrochem. Soc.*, **93**, 84 (1948).
17. H. Flaschka and A. M. Amin, *Z. anal. Chem.*, **140**, 6 (1953).

The Relationship between Thermal Decomposition in Vacuum and the Macrostructure of Alkaline Earth Carbonates

B. Wolk

Physics Laboratory, Sylvania Electric Products Inc., Bayside, New York

ABSTRACT

The control of quality in electronic tubes processed by production equipment depends on numerous factors. Among these factors are those involving the time and temperature conditions for effective conversion of the cathode coating from the carbonate to the emitting oxide. A technique is described for evaluating the relative thermal decomposition properties of different cathode carbonates under simulated tube processing conditions. Various observations on the relationship between the macrostructure of cathode carbonates and the thermal decomposition behavior are described.

One of the fundamental chemical reactions involved in the processing of a coated cathode tube is the dissociation of the emission carbonate. The temperature range over which this is carried out influences a variety of other phenomena such as crystal growth, evaporation and diffusion of impurity elements in both the base metal and bulk oxide, and the formation of interface compounds. Some preliminary studies of carbonate breakdown have been carried out and this paper reports on the method employed and the results obtained.

Work on the double carbonates (1) (Ba, Sr) CO_3 , and on dolomite (2,3), (Ca, Mg) CO_3 , indicates that a multistep process is involved in the conversion to the corresponding oxides. Studies of magnesite (4), MgCO_3 , decomposition in a variety of gaseous atmospheres revealed the mechanism of the reaction. Wooten (5) has studied decomposition of single carbonates in nitrogen and in hydrogen atmospheres. Investigations of CaCO_3 decomposition (6) and BaCO_3 breakdown (7), as well as double and triple carbonates under vacuum conditions, have also been reported. In no instance have two investigators employed identical techniques for the study of these reactions, and the data reported are not adequate in terms of the objectives in the current program. Among the earliest work attempting to relate thermionic emission with the size of the carbonate was that of Benjamin (8), who reported that small carbonate size favors higher emission levels. Shimazu (9), using small-angle scattering x-ray methods, concluded that small oxide size yields higher emission levels than do larger sizes. Generally the decomposition rate itself is only introduced in terms of its dependency on chemical composition, whereas the growth of the oxide crystal is examined in relation to processing time and temperature conditions. Recently both the carbonate and oxide crystal sizes have been studied in terms of their effect on emission levels. Wright (10) reported that superior emission characteristics can be expected from the smaller oxide crystal size originally produced from larger carbonate crystals. This rela-

tion applies to carbonates precipitated by Na_2CO_3 , but holds only to a lesser extent for different sizes of carbonates prepared by $(\text{NH}_4)_2\text{CO}_3$ precipitation owing to a "wider size distribution" in the latter case.

The several kinds of double and triple carbonates currently in general use differ from one another both chemically and physically. The proper choice of processing schedules for any one of these is invariably dictated by the necessity for obtaining complete breakdown in minimum time without destroying the ability of the coating to respond favorably to subsequent activation. However, qualitative consideration is given to the influence of such factors as coating composition, density, weight, particle size, and even the presence of reducing gases during breakdown.

Here the processing performance of coatings has been studied to establish relations between such properties as particle size, size distribution, particle shape, and coating density. Performance in this case means the relative ease with which thermal decomposition occurs under a set of fixed temperature and time conditions.

The general procedure employs a constant rate of increase in temperature of Pt strips coated with the carbonate. An analysis of the resulting pressure-time-temperature relationships provided by each of the materials ultimately made it possible to introduce a method of ranking the carbonates according to their decomposition performance. In addition to relating this performance to the macrostructure of the carbonates, primarily characterized by Fisher sub-sieve sizer (F.S.S.) measurements, it was also possible to evaluate the unique role of coating density.

Experimental Procedure

A hot-filament ionization gauge technique made possible direct measurement of the pressure of the thermal decomposition products and provided relatively simple data for analysis of the resulting pressure-time-temperature profile. This method provided a practical means for studying carbonates

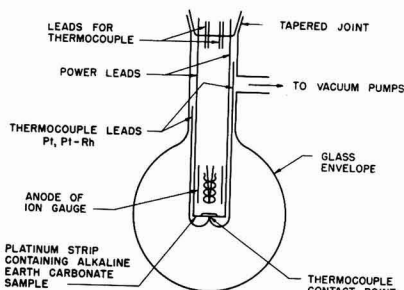


Fig. 1. Vacuum chamber containing sample and ionization gauge.

taken directly from production sources as well as from those prepared here. The apparatus in Fig. 1 contains an ion gauge built into a demountable glass envelope provided with power and thermocouple (Pt, Pt-Rh) leads. The cylindrical anode was of Ta. The glass connection to the oil diffusion pump was located near the upper portion of the envelope. The various carbonates, in standard lacquer suspensions, were sprayed on the central section of 0.002 in. Pt strips. A thermocouple junction was made at the midpoint of the opposite side with 0.004 in. wires. These were welded to 0.020 in. wires of the same materials after the Pt strip was welded securely to the power leads of the demountable stem structure with the coated side facing the ion gauge.

The experimental method had to approximate the breakdown speed normally employed in processing experimental or production tubes to be of greatest value. To do this systematically a servo-controlled linear temperatures scan rate of 13°C/sec was employed. Maximum variation in the rate of temperature rise under these conditions was about $\pm 2\%$. Other essential requirements included rigid control of coating density, a reliable thickness measuring technique, and use of a relatively small mass, thickness and area of the coating under test.

Conventional micrometric methods were replaced by microscopic examination (with a bifilar microscopic eye piece) of the sprayed-coating profile and projection of the resultant image on a ground-glass screen. The calibrated lines and adjustable reference line were projected on the screen simultaneously with the coating profile. This method eliminates uncertainty that might be due to appreciable sample compression, usually about 15%. The largest observable error, about $\pm 5\%$, is an unavoidable consequence of both restricted thickness (about 0.001 in.) and the high degree of surface roughness inherent in low-density coatings, i.e., less than 1 g/cc.

The main reason for employing a small coating thickness was to minimize the thermal gradient through the bulk of the sprayed coating during decomposition. Thinner coatings are more uniform and are less likely to chip away from the Pt strip.

Pressure-Time-Temperature Curves

The usual pressure-time-temperature relation observed when carbonates are heated at linear temperatures scan rates is illustrated in Fig. 2. Starting at room temperature and at a fixed background

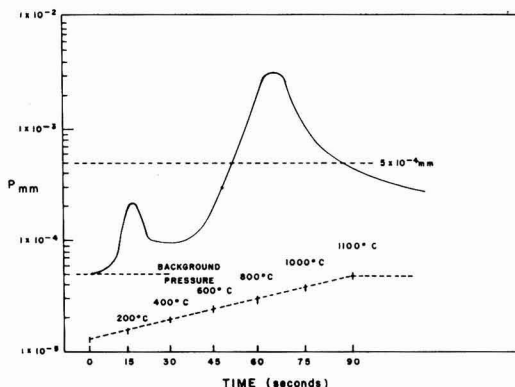


Fig. 2. Typical pressure-time-temperature curves

pressure of 5×10^{-5} mm, the first peak in the pressure-time curve, about 2×10^{-4} mm, occurs as the temperature approaches 200°C due to partial decomposition of the binder. The pressure falls, then starts to rise at about 600°C, and continues until a maximum, usually $1-3 \times 10^{-3}$ mm, is reached at from 800° to 1000°C. From then on, the temperature is permitted to rise to 1100°C and is maintained at that value until the final pressure of 5×10^{-4} mm is reached.

The comparison of the breakdown behavior of various carbonates shown in Table I is based on several characteristics in the decomposition curve just described. Of considerable interest is the temperature at which the maximum pressure occurs. These curves constitute a relative measure of the rate at which decomposition proceeds; they should not, however, be interpreted as true breakdown temperatures. The pressure-time curve width is reported in terms of the number of seconds required for the filament, starting at a temperature equivalent

Table I. Thermal decomposition data obtained for a variety of triple carbonates precipitated under different conditions

Type	Fisher size (μ)	BET size (μ)	Peak press. temp °C	Decomp. time (sec)
C-3	3.05	0.97	871	68.6
C-4 (1829) *	2.76	0.86	867	67.3
C-4 (1698) *	2.63	0.89	863	66.5
C-4 (1903) *	2.55	1.06	868	65.9
C-4 (1904) *	2.40	0.64	869	66.9
C-3,4	2.5	0.16	872	68.3
C-3,4	1.92	0.27	873	71.6
C-3,4	1.41	0.87	860	67.0
C-3,4	13.5	0.63	945	77.7
C-3,4	14.0	1.20	960	76.4
C-10 (1455) *	1.21	0.64	843	66.0
C-10 (1813) *	0.95	0.73	864	67.7
C-10 (1948) *	1.20	0.83	859	66.4
C-3,4	1.9	0.55	864	67.3
C-3,4	1.4	0.26	858	66.3
C-3,4	4.2	1.21	884	69.5
C-3,4	4.0	1.16	883	68.0
C-3,4	5.5	1.3	916	71.0
C-3,4	6.3	1.7	900	69.6

* These samples were obtained from production batches of Sylvania's Towanda Tungsten and Chemical Division. The remaining specimens were laboratory preparations.

lent to a thermocouple emf of 1 mv, to reach a pressure of 5×10^{-4} mm once maximum pressure has been attained. The estimated pumping speed of the system is 3 liters/sec. Conditions affecting pumping speed remain the same from one test to another; consequently the data are strictly comparative. Subsequent experiments showed that the peak pressure reflected primarily the differences in sample weight; the time required to reach the peak reflected primarily differences in the other variables.

Average Particle Size of Carbonates before and after Ball-Milling

It is known that ball milling deagglomerates carbonates in suspension; in this connection Fig. 3 is of interest. Microscopic observations indicate this effect to be especially evident for spherical particles, but much less apparent when the original carbonate is in the form of needlelike particles. However, when deagglomerated suspensions were examined after they had been sprayed on Pt filaments and heated in vacuum to 500°C , the carbonate consisted once again of essentially reagglomerated particles as shown in Fig. 3c. Thus, the similarity between initial and final physical states provided evidence that no permanent alteration in the degree of aggregation results from ball milling.

Routine F.S.S. average particle size determinations reveal a high degree of uniformity among batches of a particular species. However, surface area measurements do not show this same consist-

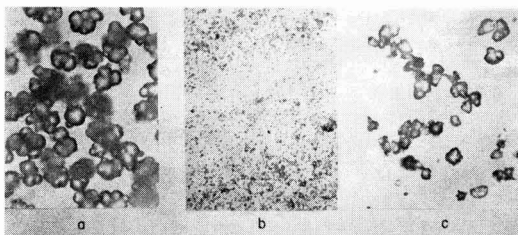


Fig. 3. (a) A large agglomerate specimen of triple carbonate (450 \times); (b) same specimen shown after ball milling (450 \times); (c) same material shown after being sprayed on a platinum filament and heated to 500°C in vacuum (450 \times).

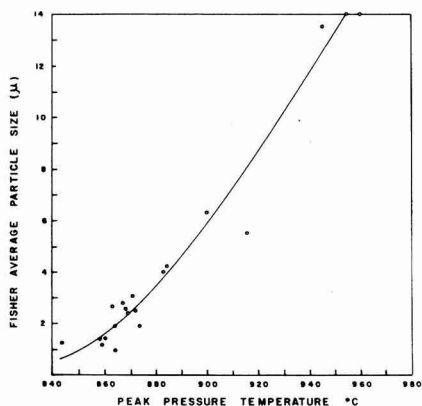


Fig. 4. Relation between decomposition peak-pressure-temperature and average particle size for various triple carbonates.

ency for these same carbonates—a fact presumably due to much greater variation in the microstructure of the surface than in the macrostructure of the carbonate aggregates which the sieve observes. The decomposition-particle size relationship is more generally observed to be consistent with Fisher size values than with particle size values estimated from Brunauer-Emmett-Teller (BET) gas adsorption surface-area measurements.

Some of the original laboratory preparations were based on certain desired BET size ranges obtained under different conditions of precipitation. However, results on the basis of BET analysis were completely different from those based on F.S.S. measurements. Low power microscopic examination confirmed the presence of large aggregates that were influencing the sieve measurements. A series of carbonates prepared at different precipitation temperatures but under otherwise uniform conditions, gave better qualitative agreement between the BET and F.S.S. average particle size values. However, electron microscopic examination using carbon replicas revealed very little difference in the microstructure of these specimens. Differences of a macroscopic nature were confirmed by low power microscopy. Figure 4 illustrates the relation between decomposition (peak pressure) temperature data and the sieve mean particle diameters of several production and laboratory triple carbonates. On the other hand, the absence of correlation between these decomposition data and mean particle diameters based on BET measurements (Table I) points out the lesser importance of the microstructure as a factor in determining the decomposition rate.

Thermal decomposition data and corresponding Fisher values obtained for different lots of the same type of production carbonate were consistently reproducible. This leads one to suspect that reported instances of poor cathode processing reliability are related to factors other than particle size variation. Other possible explanations of observed nonreproducible cathode breakdown performance are discussed later.

Effects of Differences in Coating Density, Weight, and Thickness on Thermal Decomposition of Triple Carbonates

In addition to the fact that small particles decompose more readily than the larger ones, coating density is an influencing factor under certain conditions.

A coating density limit of $1 \text{ g/cc} \pm 0.05$ was maintained throughout the previously described tests because there were no data on the effect of density variation on thermal decomposition. For this reason the study of carbonate decomposition as a function of coating density was included. The relation between bulk density and thermal decomposition was studied on one batch of small-size triple carbonate and one of large size. Table II illustrates two points of considerable interest. First, variations in bulk density for small average particles significantly affect all decomposition characteristics; second, the decomposition of large average particles is unaffected by coating density variations of 30%. The carbon

Table II. Effect of bulk coating density on experimentally observed peak-pressure temperatures for chemically identical carbonates composed of large and small average particle diameters

Fisher average particle size μ	Sample weight $\times 10^3$ g	Sample thickness $\times 10^3$ in.	Coating density g/cc	Temperature ($^{\circ}$ C) at peak pressure
1.85	0.33	1.23	0.895	848
1.85	0.37	1.21	1.02	863
1.85	0.43	1.23	1.17	889
1.85	0.33	1.23	1.17	894
6.3	0.44	1.77	0.83	912
6.3	0.31	1.25	0.83	913
6.3	0.37	1.25	0.99	917
6.3	0.45	1.15	1.30	920

replica electron micrographs reveal no significant difference in their microstructures; the differences are in the sizes of the aggregates.

Peak-pressure temperatures observed for the 1.85 μ (F.S.S.) carbonate were found to be independent of sample weight. Several samples were coated to the same weight and density, then some of the coating was removed from some of the samples. Although the pressure variations during decomposition reflected the lower sample weight, the temperature at peak pressures remained unchanged.

The influence of coating thickness variations was subsequently demonstrated for one small (Fisher mpd = 1.85 μ) and one large particle size (Fisher mpd = 6.3 μ) carbonate; two groups of the 6.3 μ carbonate were sprayed to different coating weights of constant density (0.83 g/cc). The heavier samples were also thicker as indicated by the original dimensions as shown in Table II. By removing approximately one third of the coated area it was possible to eliminate the weight difference. No effect due to thickness differences was noted, since the temperature for peak pressure remained the same as in the original tests. On the other hand, when two groups of small particle size carbonates were sprayed to the same density, but with different thicknesses (0.00121 in. and 0.00137 in.), the peak-pressure temperature was significantly higher for the thicker samples. The thermal decomposition behavior of the smaller particles thus appears to be highly sensitive to both thickness and density variations.

Decomposition of Individual Carbonate Particles

Reduced particle size usually results in increased decomposition, as noted by Bircumshaw and Newman (11) in their studies of the thermal decomposition of ammonium perchlorate. Generally speaking, this is the result of shorter diffusion paths. The special problem of decomposition gas flow impedance due to the relatively small pore dimensions found in coatings composed of small sized particles must be considered. Here the rate of heat transfer by "gaseous conduction" becomes dependent on the dimensions of the pores which make up about 75% of the total volume of a 1 g/cc density coating. For a given spray condition, the packing factor depends largely on such properties as particle size, degree of agglomeration, particle shape, and particle distribution. The random nature of the packing resulting from spraying means that, for a given bulk

density, the smaller particles form a close-packed array. Moreover, this close packing is extremely sensitive to spray conditions and bulk density; consequently breakdown speed is related to both factors. When the pore dimensions produced by larger agglomerates are sufficiently large, the same coating density limitations do not apply and diffusion of the decomposition gases is not so seriously impeded.

Conclusions

1. Despite macrostructure irregularities observed in laboratory and production carbonates, the Fisher size determination method appears to characterize the average particle size in a manner that is related to the thermal decomposition characteristics. Carbonates other than those with needlelike and rod-like forms appear to be highly aggregated. Each portion of any such aggregate is itself composed of still smaller structures which are not yet the ultimate crystallites. This complex microstructure apparently accounts for the large surface area values generally obtained by the BET method.

2. Small aggregates decompose more readily than do the larger aggregates under the experimental conditions described here.

3. Sprayed coatings of normal bulk densities made from carbonates precipitated as rod-shaped, well-ordered crystals exhibit a more sluggish response during thermal decomposition than do the conventional carbonates. The effect is measurable, but, at the same time, can only be explained tentatively on the basis of the higher stability inherent in well-ordered crystals.

4. Ball milling procedures deagglomerate aggregates of spherical carbonate particles, but the shearing forces involved are insufficient to appreciably fracture rods or needles. Subsequent spraying appears to reaggregate those with spherical habits so that the resulting sprayed coating essentially resembles the original macrostructure.

5. Under the conditions of measurement employed, a coating of high density comprised of small size particles alters those decomposition characteristics which normally distinguish the smaller size materials from the larger ones (Table II). Cathodes using larger particles break down more slowly at rates which are relatively insensitive to coating density variations.

6. The observed differences in thermal decomposition between particles of different sizes persist even when the linear temperature scan rates are decreased or increased by factors of two. Such consistent differences can become potentially critical, from a practical point of view, as a direct consequence of the increased tube processing rates and accompanying reduction in the time available for breakdown.

Acknowledgments

The author is indebted to James G. Buck, for the substantial contribution of discussions and suggestions, and to C. F. Tufts, of the Metallurgy Laboratory, for carbon-replica electron photomicrographs of sample materials used in the experiments. The work was supported by U.S. Navy Contracts Nobs-5359 and Nobs-8023.

Manuscript received June 24, 1957. This paper was prepared for delivery before the Washington Meeting, May 12-16, 1957.

Any discussion of this paper will appear in a Discussion Section to be published in the December 1958 JOURNAL.

REFERENCES

1. A. Eisenstein, *J. Appl. Phys.*, **17**, 434 (1946).
2. O. A. Esin, P. V. Gel'd, and S. I. Popel, *J. A. Chem. (Russian)*, **22**, 354 (1949).
3. H. G. F. Wilsdorf and R. A. W. Haul, *Nature*, **167**, 945 (1951).
4. E. Kremer, Solid-State Reactions in Various Atmospheres, University of Innsbruck, Austria. Lecture given at Bayside, December 1953.
5. L. A. Wooten, Bell Lab. Report made to ACS Meeting in 1943.
6. J. Zawadski and S. Bretsznajder, *Bull. intern. acad. polon. sci., Classe Sci. Math. Nat. Ser. A*, **1940-46**, pp. 60-64 (1948).
7. J. J. Lander, *J. Am. Chem. Soc.*, **73**, 5794 (1951).
8. M. Benjamin, R. J. Huck, and R. O. Jenkins, *Proc. Phys. Soc.*, **50**, 345 (1938).
9. J. Shimazu, *J. Phys. Soc. Japan*, **6**, [6] 479 (1951).
10. D. A. Wright, *Le Vide*, **51**, 58 (1954).
11. L. L. Bircumshaw and B. H. Newman, *Proc. Roy. Soc. A*, **227**, pt. 1, 115, pt. 2, 228 (1955).

12. F. Feakes, Quarterly Report of H₂O₂ Laboratories Prep. for ONR Contract No. N5 ori-07819 Sept. 1955, MIT.

APPENDIX

A series of reproducibility tests was carried out, early in the program, using one of the production triple carbonates. The batches of coated filaments were prepared at different times from individually ball-milled suspensions of the same powder. The two coatings differed with respect to their bulk densities by 4.3%. The sample weights had a 2.2% difference, and the coating thickness variation was 2.5%. Examination of the pressure-time curves for six samples in each test batch revealed that the average peak pressures were $1.82 \times 10^{-3} \pm 0.05 \times 10^{-3}$ mm and $1.83 \times 10^{-3} \pm 0.09 \times 10^{-3}$ mm, respectively. The corresponding average temperatures at these pressure peaks were 878° and 876°C. The decomposition times (see text) were 70.6 and 67.3 sec. While individual results in each batch showed deviations from the average of 1 to 5%, the difference between batches was only about 1%. The production carbonate used in these tests continued to serve as a control material with which the reliability of the over-all test equipment and procedure were checked periodically.

Zone Melting and Crystal Pulling Experiments with AlSb

W. P. Allred, Bernard Paris, and M. Genser¹

Battelle Memorial Institute, Columbus, Ohio

ABSTRACT

It has been found that high-resistivity AlSb ingots result from the zone refining of the compound in Al₂O₃ crucibles. Distribution coefficients of the spectroscopically observed impurities in AlSb were found to be 0.1 and smaller. Resistivity and Hall coefficients have been determined for some single-crystal specimens cut from the zone-melted ingots. Single crystals of AlSb have been grown by pulling from the melt. These crystals exhibited low resistivities. The mobility for holes in the crystals has been found to range between 300 and 500 cm²/v-sec.

Of the nine Group III-V semiconducting inter-metallic compounds, AlSb, GaAs, and InP are of major interest for use in the fabrication of solid-state rectifiers and transistors. A considerable amount of work has been done recently on the purification and growth of single crystals and on the study of the electrical properties of the compounds (1). In this paper, the preparation of AlSb by zone melting and the growth of AlSb crystals by crystal pulling are described.

Zone Melting of AlSb

Zone melting is considerably more difficult to apply to AlSb than to Ge because AlSb tends to wet commercially available crucible materials. A slow reaction between AlSb and graphite at high temperatures results in the formation of Al₄C₃ and free Sb. The continued passage of a molten zone along the length of the melt distributes these reaction products throughout the ingot. Materials other than graphite that have been studied for use as crucibles are BN, Si₃N₄, Ta, MgO, and Al₂O₃. Except for dense

Al₂O₃, these crucibles either reacted with the melt or caused excessive doping of the ingot.

The AlSb was zone melted in the apparatus illustrated in Fig. 1. This arrangement is similar to that used by Schell (2). The wire-wound furnaces provide an ambient temperature of approximately 800°C. Heating of the surroundings prevents cracking of Al₂O₃ boats because of sudden temperature changes during the course of the zone melting and also prevents the condensation of Sb vapor on the

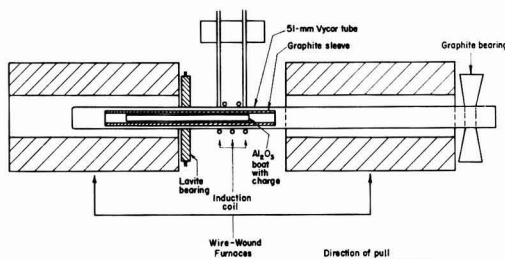


Fig. 1. Apparatus for zone melting AlSb

¹ Present address: International Business Machines, Inc., Poughkeepsie, N. Y.

cold walls of the enclosing Vycor vessel. Special equipment drew the tube containing the graphite sleeve, boat, and contents through the induction coil, returned the tube to start another pass, and counted the number of passes.

The compound was prepared by heating stoichiometric proportions of Al and Sb slightly above the melting point of AlSb. At this temperature, the reaction proceeds rapidly. At the end of the experiment, the ingot of AlSb adheres strongly to the boat; large lumps of AlSb could be cut away from the boat with a SiC wheel.

The Al and Sb used for the preparation of the compound were zone melted prior to use. Spectrographic analysis indicated that the concentration of such impurities as Mg, Si, Fe, and Cu varied in an Al ingot from 1-2 ppm near the front of the ingot to 10-20 ppm near the rear. The Sb contained less than 20 ppm impurities.

The ingots are polycrystalline since the material wets the boat, and crystal growth can be seen to start at the sides of the crucible and proceed toward the center. However, if the last zone-melting pass is carried out slowly (1-2 in./hr) and if the freezing interface is properly shaped (convex into the melt) in the center of the crucible, single crystals can be found which are suitable for Hall specimens. Unfortunately, these large crystallites seldom occur near the front of the boat where the highest resistivity material is found.

Resistivity profiles were measured by the four-probe method. Resistivities determined by this method are generally an order of magnitude greater than those measured on single-crystal Hall specimens. This is thought to be caused by the grain boundary resistance of the zone-melted polycrystalline ingot.

Figure 2 is the resistivity profile of a typical zone-melted ingot. The resistivity decreases from over 10^8 ohm-cm at the front to 10^{-1} ohm-cm at the rear. The entire ingot was *p*-type, as shown by the sign

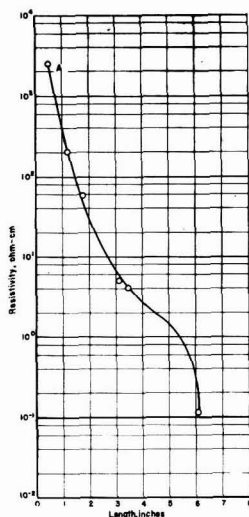


Fig. 2. Resistivity profile of an ingot of AlSb after twenty zone-melting passes.

Table I. Electrical properties of some single-crystal specimens cut from a zone-refined AlSb ingot

Specimen No.	Resistivity, ohm-cm	Hall coefficient, cm ³ /coulomb	Hall mobility, cm ² /v-sec	N _h holes/cm ³
H-1	5.5	1650	250	4.3×10^{18}
H-2	3.0	1100	310	6.5×10^{18}
H-3	1.6	530	280	1.3×10^{19}
H-4	1.0	360	310	2.0×10^{19}
H-5	0.15	79	450	9.0×10^{18}
H-6	0.35	190	460	3.8×10^{19}

of the thermoelectric effect. This ingot was given 20 passes of zone melting; the zone width was about 5 cm and the ingot length was 20 cm.

The resistivity profiles of many zone-melted ingots were shaped as in Fig. 2. However, the resistivities of the front portion of the ingot varied between 10 ohm-cm and more than 10^4 ohm-cm. These variations in resistivity profiles may be attributed to the variation in purity of the Al used in preparing the ingots. Likewise, because Al of higher purity was used in preparing the compound prior to zone melting, the considerably higher resistivities which were observed over those reported by Schell may be explained. Spectrographic analyses of specimens of the compound cut from the front, center, and rear regions of a zone-melted ingot revealed Mg in a concentration of 2 ppm in the rear of the ingot. It is known that the boats used for the zone melting contained a few tenths of a per cent of MgO. This could be the source of the Mg in the ingot.

Table I shows some typical resistivities and Hall coefficients determined on single-crystal specimens cut from a zone-refined ingot. Samples were cut from the front (first to crystallize) half of the ingot with H-1 being the sample nearest the front of the Al₂O₃ boat. The general decrease in Hall mobility as the resistivity increases suggests that the extremely high-resistivity material often observed near the front of the ingot may be due to compensation. The resistivity and Hall coefficient of Specimens H-2, H-3, and H-4 were determined as a function of temperature (Fig. 3 and 4).

Distribution Coefficients of Some Impurities in AlSb

Impurities normally found in the Al were studied to determine if the high-resistivity material observed in the zone-refined ingots was the result of compensation due to an *n*-type impurity with a distribution coefficient greater than unity. Pfann's equation (3) describes the distribution of a solute along the length of a zone-melted ingot after one pass, when the solute is added to the first zone.¹ The equation is

$$C = kC_0 e^{-kx/L}$$

where *C* is the concentration of solute in the solid, *k* is the distribution coefficient, *C*₀ is the concentration of solute added to the first zone, *L* is the zone width, and *x* is the distance along the ingot. In cases where *k* is small, the exponential reduces to unity and *k* can be determined simply as the ratio of the concentration in the solid to the initial liquid

¹ This process is referred to as "zone leveling".

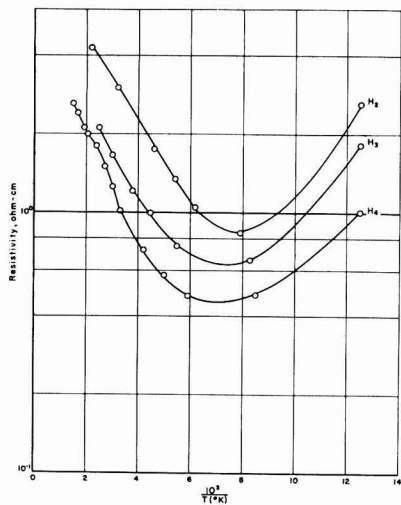


Fig. 3. Variation of resistivity of zone-melted AISb with reciprocal temperature.

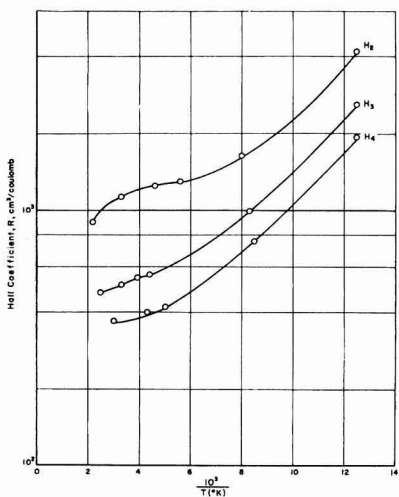


Fig. 4. Variation of Hall coefficient of zone-melted AISb with reciprocal temperature.

concentration. Where k is appreciable (>0.01), the concentration of solute will be higher in the first zone and will decrease toward the rear of the ingot. By plotting $\ln C$ as a function of x/L , the negative of the slope of the line is the distribution coefficient.

In impure AISb, the following impurities are usually observed spectrographically: Mg, Si, Fe, Cu, B, Ag, Pb, V, Ni, Mn, Ti. Therefore, these metals were added to the front zone in a zone-leveling experiment. Specimens of the doped ingot were analyzed spectrographically and the distribution coefficients were determined as above. Order of magnitude values for k were obtained and are given in Table II.

The distribution coefficients of Mg, Si, Fe, and Cu which are usually present in a few ppm are significantly less than one and, hence, these impurities

Table II. Approximate distribution coefficients of some impurity elements in AISb

Element	Distribution coefficient, k
Mg	0.1
Si	0.1
Cu	0.02-0.1
Fe	0.01-0.1
B	0.01-0.02
Ag	0.1
Pb	<0.01
V	<0.01
Ni	<0.01
Mn	<0.01
Ti	<0.01

segregate to the rear of the ingot. The other impurities listed in the table are usually present in smaller concentrations. They also segregate to the rear of the ingot. It is important that such transition elements as V and Ti have a small distribution coefficient and segregate to the rear of the ingot. If such elements segregated to the front of the ingot, they could cause the high resistivity in the AISb, as do Fe and Co in Ge (4).

Unfortunately, elements such as Se and Te cannot be studied by the spectrographic technique. These elements are donor elements in AISb and if they moved to the front of the ingot in zone melting, they could compensate for the acceptor impurities yielding a high-resistivity region. Crystal pulling work with these elements has shown qualitatively that their distribution coefficients are less than unity.

Effects of Dissociation of AISb at the Melting Point on the Resistivity

The effects of the dissociation of the compound at the melting point were investigated. It could be hypothesized, for example, that some dissociation in the liquid would occur. Since at the melting point of the compound the free Sb would have a higher vapor pressure than the Al, the melt could become rich in Al if the Sb continued to escape. In a crystal pulling furnace, for example, it is difficult to maintain a high, even temperature in an enclosed system. In fact, in crystal pulling work traces of free metal, presumably Al, have been observed in the crucible after a crystal is withdrawn.

An experiment was carried out in which the melt was doped indirectly with an excess of Al. The ingot of aluminum antimonide was zone melted in an Al_2O_3 boat inclosed in a Vycor tube. The temperature of the entire system was the usual $800^\circ C$. Prior to the final pass, the temperature was lowered to $450^\circ C$, a condition that permitted the condensation of Sb. The net result was the enrichment of the melt with Al. Figure 5 shows the resistivity profile of this ingot. Some decrease in resistivity is apparent. However, the decrease is not so large as might be expected. Ingots with no higher resistivities after a similar number of passes of zone melting at $800^\circ C$ ambient temperature have been prepared. The experiment suggests that Al is quite insoluble in the solid compound.

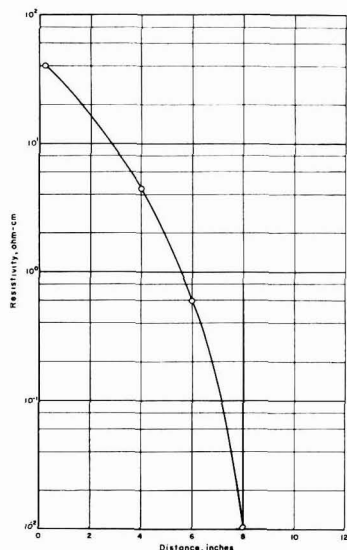


Fig. 5. Resistivity profile of a zone-refined AlSb ingot doped with Al.

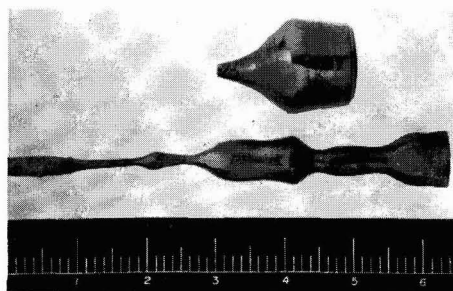


Fig. 6. Crystals of AlSb grown from the melt

Growth of Crystals of AlSb

Single crystals of AlSb were grown in a typical crystal pulling apparatus by the Czochralski technique. Because oxide on the surface of molten AlSb could nucleate the development of new crystals, the melt was skimmed with an Al_2O_3 probe to clear the surface for crystal growth. Figure 6 shows a photograph of typical AlSb crystals grown from the melt. When crystals were pulled from the melt, only low-resistivity *p*-type crystals resulted. In some of the experiments, the AlSb was melted in pure graphite crucibles. Although graphite boats will not suffice for zone melting, graphite crucibles are satisfactory for crystal pulling, provided the temperature of the melt does not greatly exceed the melting point of the compound for long periods of time.

Crystals pulled from zone-refined AlSb exhibited slightly higher mobilities than did crystals pulled from melts prepared directly from the elements.

Likewise, the pulled crystals exhibited higher mobilities than did crystals prepared by zone melting, even though the zone-refined crystals were of higher resistivity.

Failure to pull higher resistivity crystals from zone-refined AlSb was surprising, in view of the zone-melting work where it was observed that excess Al is not greatly soluble in solid AlSb. Spectrographic analysis of a portion of the crystal pulled from an Al_2O_3 crucible showed the presence of Mg and Si. Thus, it is likely that impurities are being introduced by the crucible. The graphite crucible likewise probably introduces impurities into the melt. For example it has been found that a solid solution between AlSb and Al_3C_2 forms on the surface of the graphite in contact with the melt.

An experiment was carried out in which a crystal was drawn from a melt of aluminum antimonide containing an excess of Sb. The excess of Sb was such that, as it was removed from the melt by volatilization, the melt composition passed through the regions of excess Sb, stoichiometry, and finally excess Al, as the crystal was withdrawn. However, the resulting crystal exhibited no resistivity maximum, which would have been expected if stoichiometry effects were controlling the crystal resistivity.

Conclusions

From the work reported here, it can be seen that most impurities found in AlSb segregate readily to the rear during zone refining. Single crystals can be grown by the Czochralski technique. However, the growth of high purity crystals seems to be limited by the purity of the alumina crucible and to the purity of the Al rather than by the effect of deviations from stoichiometry, since both excess Al and Sb are apparently insoluble in AlSb.

Acknowledgment

The authors wish to acknowledge the advice and suggestions of H. L. Goering, Chief of the Physical Chemistry Division. The comments of A. C. Beer are also appreciated. This work was supported by the Wright Air Development Center, Air Research and Development Command, United States Air Force.

Manuscript received Jan. 31, 1957. This paper was prepared for delivery before the Pittsburgh Meeting, Oct. 9-13, 1955.

Any discussion of this paper will appear in a Discussion Section to be published in the December 1958 JOURNAL.

REFERENCES

1. See papers by H. Welker, especially *Physica*, **20**, 893 (1954). For early work on AlSb see R. K. Willardson, A. C. Beer, and A. E. Middleton, *This Journal*, **101**, 354 (1954).
2. H. A. Schell, *Z. Metallkunde*, **46**, 58 (1955).
3. W. G. Pfann, *J. Metals*, **4**, 747 (1952).
4. W. W. Tyler, H. H. Woodbury, and R. Newman, *Phys. Rev.*, **94**, 1419 (1954).

Transport Numbers in Pure Fused Salts

Lead Chloride, Lead Bromide, Thallous Chloride, and Silver Nitrate

Richard W. Laity¹ and Frederick R. Duke

Institute for Atomic Research and Department of Chemistry, Iowa State College, Ames, Iowa

ABSTRACT

The application of the authors' moving bubble cell to the measurement of transport numbers in four pure fused salts is described. From the experimental results it is shown that the anion carries approximately three-fourths of the current in lead chloride, and one-fourth in silver nitrate. Except for lead bromide, in which this figure increases by about 3% when the temperature is raised 100°C, little, if any, temperature dependence is observed.

A radiotracer experiment in fused lead chloride is shown to indicate that long-lived complex anions do not carry any appreciable fraction of the current in this salt. The limitations of the method used are discussed.

The authors' method for measuring the transference numbers of the ions in pure molten salts has already been described (1, 2). The present paper deals with the application of this procedure, or slight modifications of it, to four different salts.

A recent paper by Bloom and Doull described a cell for measuring transport numbers in fused salts in which the possibility of the results being influenced by flow of the liquid under gravity is minimized by making the whole system horizontal (3). The transport numbers for PbCl₂ reported by Bloom and Doull, however, correspond to only a small fraction as much PbCl₂ being transferred from catholyte to anolyte per faraday as was observed in the author's moving bubble cell. Lorenz and Janz (4) have shown that leakage through the membrane was very likely in the experiment of Bloom and Doull, and at the same time point out some limitations of the moving bubble cell; chiefly these limitations center around the fact that certain salts in some types of capillaries form "sticky" bubbles which do not move under small pressure differentials. They showed, however, that PbCl₂ was not one of these salts.

Sundheim (5) has pointed out that the salt can gain no net momentum from the electrode processes, and he further states correctly that, regardless of the nature of complex ions which might be present, $t^+ = M_+ / (M^+ + M_-)$ providing no momentum is transferred to the cell. His view that no momentum is transferred to the cell appears to be an extreme one, since, with no net preferential adsorption of one ion, there could still be frictional interaction between an anion tending to move and an anion held to the surface; the same sort of interaction between cations might be expected.

It was pointed out previously that in order to calculate transport numbers from the data obtained in measurements of this type it is necessary to assume formulas for the current-carrying ions. In the

light of no evidence to the contrary, the simplest formulas, e.g., Pb⁺⁺ and Cl⁻, were assumed.

Experimental

Materials.—Fisher certified reagent PbCl₂ was used. In addition, PbCl₂ containing labeled cation was prepared by dissolving thorium B (Pb²¹²) in nitric acid, adding PbN carrier and precipitating with HCl. The salt was recrystallized from 0.01N HCl, filtered, and dried at 110°C.

Fisher purified PbBr₂ was recrystallized twice from 0.1N HBr. The dried product melted sharply at 370°C.

Fisher purified thallium (ous) chloride was recrystallized from 0.01 HCl. Spectrographic analysis revealed no appreciable amounts of metal impurities.

"Bakers Analyzed" AgNO₃ was recrystallized from water.

The lead metal used for electrodes was "Bakers Analyzed" reagent grade. Thallium electrodes were of Sargent CP Tl metal. Silver electrodes were plated onto the tungsten wires in the cell from an aqueous cyanide bath, using Fisher certified reagent silver metal as anodes in the electroplating.

Apparatus.—The moving bubble cell and accompanying apparatus have already been described (1, 2). These were used in unmodified form in the experiments on PbCl₂, PbBr₂, and TlCl. In the tracer experiment on PbCl₂ a much smaller version was used. The electrode compartments were again joined by a 10-mm tube containing an "ultrafine" porosity fritted Pyrex disk, but no capillary tube was used in the smaller cell. The moving bubble cell was modified only slightly for the work on AgNO₃. In these experiments one vertical arm of the cell was fitted with a glass stopper at the top so that the electrolyte could be sealed tightly into that compartment.

Procedure.—The procedure already described for PbCl₂ was used for PbBr₂ and for TlCl (1, 2). In the case of PbBr₂ an unfavorable combination of

¹ Present address: Department of Chemistry, Princeton University, Princeton, New Jersey.

surface properties and viscosity prevented rapid equilibration of the liquid levels below about 480°C. At higher temperatures, however, good reproducibility was obtained. Thallium chloride was found to undergo a slow hydrolysis or exchange reaction with oxygen on standing molten in the cell. The progress of this conversion to Tl_2O could be followed by noting the change with time of the rate and, eventually, the direction of bubble movement for a given current. A corresponding increase in the activation energy of conductivity from about 3.4 to 10.1 kcal was observed during a 48-hr period. For this reason the salt was freshly purified before filling each cell, and only the initial runs were considered valid. Excellent reproducibility was obtained in this way from one cell to the next.

Rather than test each salt with a variety of membranes, as had been done for $PbCl_2$, the "activation energy of conductivity" criterion proposed earlier (2) was applied to determine whether the membrane might be affecting the mechanism of the conductivity process in each case. This was done by allowing the furnace to cool slowly while measuring the resistance of the transport cell containing the salt with a 1000-cycle conductivity bridge. The slope of $\log 1/R$ vs. $1/T$ was then compared with literature values for cells without membranes.

Silver nitrate was the first salt for which the use of solid electrodes was required. This introduced the problem of keeping the silver "trees," which rapidly grew out from the cathode during electrolysis, from growing right into the anode compartment before sufficient current to make a measurement has been passed. The problem was solved when it was found that superimposing a 60-cycle alternating current of about 350 ma on the 25 ma direct current used for the electrolysis changed the nature of the growth to a bushy deposit which grew out much more slowly. A further modification in these measurements was the stoppering of one compartment of the cell. The purpose of this was to increase the sensitivity of the measurements by magnifying the effect of any volume change developing during electrolysis, the bubble movement being forced in this case by a pressure difference rather than by gravity flow. This procedure was necessitated by the fact that no appreciable bubble movement could be observed for $AgNO_3$ in an unstoppered cell. In the stoppered cell, however, it was found that the passage of current caused a slight initial displacement of the bubble away from the stoppered compartment, after which the bubble came to rest and showed no further tendency to move. The initial displacement was, of course, due to the expansion of liquid in the stoppered side caused by the electrical heating as could be shown by passing a-c current only. This observation established the fact that the bubble was indeed sensitive to small volume changes, so that the accumulating liquid was not escaping back through the membrane, as had been suspected at first. The subsequent stoppering of the bubble when the heating effect reached a steady state thus proved that in $AgNO_3$ the transport numbers happened to have just those values for which the volume of salt accumulating in the

anode compartment is equal to the volume of Ag being transferred from anode to cathode in the temperature range studied. The accuracy of the measurements was, however, considerably reduced by the modifications imposed. The small d-c currents used meant less electrolysis per unit time, while the sealed compartment greatly increased the sensitivity of the bubble to small thermal fluctuations in the furnace.

In the tracer experiment on $PbCl_2$, two identical cells of the small type described above were placed close together in a sand bath inside the furnace. Each cell contained lead electrodes and molten lead chloride in the usual way. The system was allowed to stand several hours at constant temperature, so that thermal and gravitational equilibrium of the electrolyte in each compartment was assured. A few hundred milligrams of the labeled $PbCl_2$ were now introduced into one compartment of each cell. The system was again left standing for about half an hour, a period which was found adequate to permit the labeled salt to become uniformly distributed throughout the compartments containing it. A direct current of about 0.3 amp was now passed through one cell, while an equal alternating current was passed through the other, the electrode in contact with the labeled salt being the cathode in the d-c cell. After about an hour of electrolysis the cells were removed from the furnace, chilled, and broken open at the membrane. The salt in each compartment was dissolved in a solution of sodium acetate and acetic acid. Aliquots of each solution were treated with excess HCl and the resulting precipitates of $PbCl_2$ collected on filter paper, weighed, and counted with a Geiger counter by standard methods.

Results and Discussion

The results of transport number determinations on the four salts are summarized in Table I. The figures for $PbCl_2$ represent no new measurements, but are included here for purposes of comparison. The second column in the table, headed E_m , gives the activation energy of conductivity found for these membrane-containing cells over at least a 70° temperature range encompassing the temperatures of the transport measurements, which are listed in the

Table I. Results of transport number determinations

Salt	E_m kcal	E_n kcal	T_f °C	No. of expts.	t_- (avg.)	t_+
$PbCl_2$	3.9	3.5 ^a	565	22	0.758 ± 0.014	0.242
			635	7	0.757 ± 0.009	0.243
$PbBr_2$	4.1	4.1 ^b	500	11	0.653 ± 0.013	0.347
			600	5	0.674 ± 0.003	0.326
			475	3	0.496 ± 0.004	0.504
$TlCl$	3.4	3.0 ^c	505	2	0.492 ± 0.001	0.508
			525	2	0.493 ± 0.000	0.507
			225	2	0.24 ± 0.05	0.76
			275	2	0.24 ± 0.05	0.76

^a H. Bloom and E. Heymann, *Proc. Roy. Soc. (London)*, **A188**, 392 (1947).

^b "International Critical Tables," Vol. VI, p. 148, McGraw-Hill Book Co., Inc., New York, (1926).

^c P. Drossbach, "Electrochemie geschmolzener Salze," p. 73, Julius Springer, Berlin, (1938).

^d J. Byrne, H. Fleming, and F. E. W. Wetmore, *Can. J. Chem.*, **30**, 922 (1952).

fourth column under T_i . Values of E_m are probably accurate to better than ± 0.5 kcal. In column three, headed E_m , are listed the activation energies found for the same salts in conductivity cells with no membranes, as calculated from data in the references cited. The transport numbers found for the negative ions, t_- , are listed in the sixth column along with the average deviation for the number of experiments shown in column five. The cationic transport number t_+ ($= 1 - t_-$) is also tabulated in the last column for discussion purposes.

In the tracer experiment less than 2% of the labeled cations were found to have diffused into the opposite compartment in the blank (a-c) cell, showing the diffusion correction to be small for this method. The activity found in the anode compartment of the d-c cell, however, represented an even smaller fraction of the total activity. This is exactly the result to be expected for a salt in which a negligible fraction of the current is carried by complex anionic species, since the electrolytic migration of cations carries some of the diffusing activity back into the cathode compartment. If, on the other hand, an appreciable fraction of the ions passing through the membrane from catholyte to anolyte consisted of lead ions bonded to chloride, then the amount of activity found in the anode compartment should have exceeded that found for the blank run. The results of this experiment were sufficiently accurate to warrant the conclusion that such lead-containing anions carried less than 1% of the total current in this experiment on pure PbCl_2 at 550°C.

It should first be pointed out that tracer experiments on PbCl_2 very similar to the type described here had already been carried out by Wirths (7). His results also indicated the lack of nondissociating current-carrying complex anions, but the experimental error was too large to permit the definite conclusion. Wirth's paper also includes data on PbCl_2 -KCl mixtures which seem to bear out the observation of complex anions in the more dilute (in PbCl_2) mixtures. Again, however, the deviations seem extraordinarily large for this type of measurement. Since it is highly probable that equilibration among the possible anionic and cationic radioactive

species is very rapid under the conditions of the experiment, and since the average residence time in the membrane is of the order of 10 sec or longer, the probability of a complex anion, even though it exists, getting through the membrane is exceedingly small unless the equilibrium concentration of such complex ions is such as to cause the gross migration of the lead ions toward the anode. Thus, the radio-tracer method at such high temperatures would be expected to measure the net motion of lead ions toward the cathode, unless the melt contains anionic complexes of unexpectedly long life. The results of the authors' experiments, as well as those of Wirth, therefore, still leave open to a considerable extent the question of the existence of complexes in the pure salt.

The transport numbers obtained indicate roughly that the larger the ion, the less mobile it is; the bromide ion, for example, carries less current relative to lead ion than does chloride. More striking is the effect of the charge on the ion, the relatively small Pb^{2+} carrying less current than even the very large bromide ion; in the cases of the univalent salts, however, the cations compete well with the anions. Aside from pointing out these obvious indications, the authors feel that much more data are needed before attempting to arrive at a theory for electrical conductivity in fused salts.

Manuscript received Feb. 11, 1957. Contribution No. 593; work was performed in the Ames Laboratory of the U. S. Atomic Energy Commission.

Any discussion of this paper will appear in a Discussion Section to be published in the December 1958 JOURNAL.

REFERENCES

1. F. R. Duke and R. W. Laity, *J. Am. Chem. Soc.*, **76**, 4046 (1954).
2. F. R. Duke and R. W. Laity, *J. Phys. Chem.*, **59**, 549 (1955).
3. H. Bloom and N. J. Doull, *ibid.*, **60**, 620 (1956).
4. M. R. Lorenz and G. Janz, Armed Services Technical Information Agency Technical Note 57-240, ASTIA Document Service Center, Dayton 2, Ohio, 1957.
5. B. R. Sundheim, *J. Phys. Chem.*, **60**, 1381 (1956).
6. R. Lorenz and W. Ruckstuhl, *Z. Anorg. Chem.*, **58**, 41 (1907).
7. G. Wirths, *Z. Elektrochem.*, **43**, 486 (1937).

Lead Dioxide Anode for Commercial Use

J. C. Grigger, H. C. Miller, and F. D. Loomis

Research and Development Department, Whitmarsh Research Laboratories,
Pennsalt Chemicals Corporation, Wyndmoor, Pennsylvania

ABSTRACT

Results are presented on one phase of a research carried out under an Office of Naval Research contract for the development of an electrode to replace platinum in the perchlorate cell. Electrodeposition of massive lead dioxide is preferably carried out from a lead nitrate bath. Uniquely, anodic deposition on tantalum is possible without polarization or erosion of the base. In the subsequent anodic process use, this tantalum acts as a polarized, inert filler. Sprayed silver permits the formation of an operable, low resistance current contact to the lead dioxide. Operation of a 100 amp perchlorate cell with a lead dioxide anode is described. Current efficiency of the lead dioxide anode is compared to platinum, and the effect of $K_2S_2O_8$ addition is shown.

The chemical and electrical properties of PbO_2 suggest that it should be an ideal material for anodes in electrolytic processes. With a resistivity as low as 40 to 50×10^{-11} ohm-cm, it is a better electrical conductor than many metals, and a much better conductor than carbon or graphite. Chemically, PbO_2 is inert to most oxidizing agents and strong acids. Although it has been suggested as an anode material for several electrolytic processes (1-7), up to the present time no commercially practical anode has been advanced. Electrodes reported to date have been weak; they have been formed in odd shapes difficult to adapt to commercial cells, and methods of making the electrical contact have not been satisfactory.

The purpose of this investigation was to develop a practical PbO_2 anode that could be used in industrial electrolytic processes. It was hoped that a suitable electrode would be developed that would replace Pt in the perchlorate cell.

Experimental

Electrodeposition of Massive PbO_2

Several baths (3, 8, 9) are known for the electrodeposition of PbO_2 on common metals. The compositions of three bath types modified to give improved PbO_2 deposits are shown in Table I. In this work, the $Pb(NO_3)_2$ bath was preferred because it gives the highest quality of deposit. The addition of copper nitrate to this bath serves to suppress Pb deposition on the cathode, which is preferably carbon or graphite. In order to deposit PbO_2 of high strength, density, and surface smoothness, an addition agent is necessary such as Igepal CO-880¹ which is a non-ionic surface-active agent of the class of "alkyl phenoxy polyoxyethylene ethanol." Addition to the bath of a natural hydrophilic colloid such as gelatin resulted in the formation of a PbO_2 deposit with a high surface smoothness, but which was very weak

¹ Trade Name of Antara Chemical Division of General Dyestuff Corp.

Table I. Lead dioxide plating baths

1. Alkaline lead tartrate
100 g potassium sodium tartrate, $KNaC_4H_4O_6 \cdot 4H_2O$
50 g sodium hydroxide, NaOH
96 g lead oxide, PbO
Dissolve in the order listed in distilled water to make 2 liters of solution. Heat to 60°C to complete solution of lead oxide. Cool and filter through sintered glass. Bath pH is about 13.
2. Lead perchlorate
108 ml of 60% perchloric acid (100 g $HClO_4$)
167 ml distilled water
111.0 g lead oxide, PbO
Dissolve the lead oxide in the diluted perchloric acid. Make up to 2 liters with distilled water. Heat to boiling for 2-3 min to dissolve any white precipitate. Cool and use. Bath pH is about 5.
3. Lead nitrate
269 ml of 69.9% nitric acid (266.5 g HNO_3)
1000 ml distilled water
472 g lead oxide, PbO
Add the lead oxide slowly to the diluted nitric acid with stirring. Dilute to 2 liters and heat to 75°C with stirring. Cool and filter through sintered glass. To this bath add:
Cu $(NO_3)_2 \cdot 3H_2O$ —0.75 g/l
Igepal CO-880*—0.75 g/l
Bath pH is about 3.5.

* Trade Name of Antara Chemical Division of General Dyestuff Corp.

and was laced throughout its cross section with many fine fissures.

Using the acid baths mentioned above, it is difficult to form good deposits on thin attackable base sheets because of the serious anodic dissolution of the metal base. This problem was overcome by using Ta as the base metal. Sound, adherent deposits of PbO_2 2 cm or more in thickness could be formed without any signs of erosion of the base Ta. This plating on Ta was unexpected, since Ta polarizes in most electrolytes when operated as the anode.

Electrodeposits of PbO_2 were made readily on Ta wire, rod, and sheet without any nodular growth, using the $Pb(NO_3)_2$ bath at an anode current density

of 0.016-0.032 amp/cm² (15-30 amp/ft²) and a temperature of 70°C. Figure 1 shows a rod of massive PbO₂ formed on a single wire. The wire core was withdrawn by a sharp pull with pliers. In plating flat base-free deposits by blanking off one side of the starting sheet and stripping away this base after a thick deposit had formed, it was difficult to secure unbroken specimens. Therefore, this approach was discontinued in favor of plating on permanent base sheets.

Flat, massive PbO₂ deposits of surprising strength were made by plating on both sides of rectangular sections of Ta screen in the mesh range of 10-50. The use of baffles around the edges of flat, rectangular anodes permitted the formation of nodular free deposits to within rather close tolerances, as shown in Fig. 2. Using a 14 mesh (0.064 cm wire) Ta screen, a PbO₂ electrode measuring 36.8 x 8.9 x 1.6 cm and weighing 4500 g was plated in 142½ hr from the Pb(NO₃)₂ bath. Current was maintained at 0.016 amp/cm² on the anode and the bath temperature at 70°C throughout the electrolysis.

If the pH of the nitrate plating bath is not carefully controlled, the bath drifts strongly acid during electrolysis and is very corrosive to all of the common metals. However, by very careful maintenance of the pH in the range of about 2-4 during electrolysis by the frequent addition of lead oxide, and by protecting the base metal at the surface of the electrolyte, it is possible to plate PbO₂ on such metals as Ni and Fe. Even with these precautions, the base is slowly eroded away and by the time a thick plate has formed most of the base metal (in contrast to Ta) will have been eroded away, leaving voids (which are not always objectionable) in the center of the PbO₂ deposit.

Current Contacts to PbO₂ Anode

Whenever PbO₂ with a conventional Cu current contact is used as anode in electrolytic cells, severe

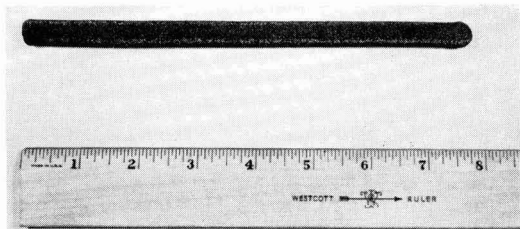


Fig. 1. Lead dioxide rod formed on a wire (#20 B&S); wire core withdrawn.

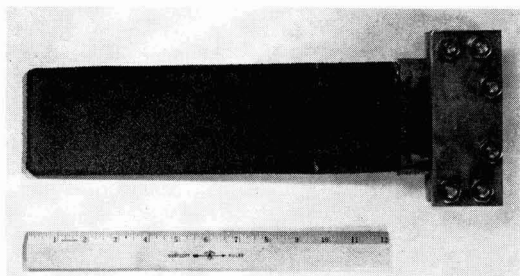


Fig. 2. Massive PbO₂ plated on a Ta screen base, and having a sprayed Cu over Ag current contact.

Table II. Contact resistance of electrodeposited PbO₂ to various metals sprayed thereon

Metal	Contact potential at 1 amp Volts
Tin	0.65
Lead	0.52
Copper	0.04
18-8 Stainless steel	0.69
Zinc	0.5
Aluminum	0.19
Silver	0.0002
Copper over silver	0.0002
Tin over silver	0.0002
Aluminum over silver	0.0002

heating is observed in the contact area. If Ag current contacts are used, no heating occurs. The contact resistance between a number of the common metals and lead dioxide was measured² and it was found that all metals tested with the exception of Ag show high contact resistance to PbO₂ as seen in Table II. It is suggested that the resistance is caused by an oxide layer forming between the contact metal and the PbO₂. Most metal oxides being poor electrical conductors show high resistance. Silver, on the other hand, forms a conducting oxide and therefore has a low contact resistance.

A coating of Ag only 0.002 cm or less in thickness applied by a metal spray technique was sufficient to produce low resistance and to overcome completely the heating previously observed in these electrode connections. In order to protect the Ag and to provide a rugged electrical contact to the PbO₂, the Ag-coated area is sprayed with a heavy layer of Cu, 0.16 cm or more in thickness. Preferably, the Ag and Cu are sprayed to form a jacket over the top end of the PbO₂ electrode, as in Fig. 2. The combination is sufficiently adherent to the base oxide so that it can be machined to fit in a mechanical current contact or it can be soldered directly to the power bus without injury to the PbO₂.

Testing the PbO₂ Anodes

Electrodes formed by plating a thin coat of PbO₂, 0.04 cm or less, on a base metal proved unsatisfactory when used as anode in a perchlorate cell. With such a thin coating on Ta there was poor electrical contact and poor adhesion. The PbO₂ coating on Ni and other base metals proved to be extremely porous and did not protect the base metal from rapid anodic erosion when used in the perchlorate cell.

Thick PbO₂ deposits, 0.16 cm or more, on Ta proved to be efficient anodes in the perchlorate cells. The Ta base polarizes rapidly and then acts as an inert filler. Thick deposits on Fe and Ni also proved satisfactory after they had operated sufficiently long to leach out all traces of the base metal that were left after the original plating operation. It is, therefore, desirable when electrodepositing PbO₂ on metals such as Fe and Ni, to keep the weight of the base to a minimum.

² Test specimens were prepared by spray coating 2.5 cm of each end of electrodeposited PbO₂ rods about 1 cm in diameter and 10 cm long with the given metal. The rods were clamped at the metal coated ends and 1 amp was passed from a direct current source. The potentials across the metal-PbO₂ contact were measured on a potentiometer using manual pressure test probes.

Table III. Current efficiencies in electrolysis of NaClO_3 with PbO_2 and Pt anodes (no additives)

Anode	Test No.	NaClO ₃ conc. range over which eff. is calculated		Current efficiency, %
		Initial g/l	Final g/l	
Pt	1	602	100	85.2
		293	39.8	82.4
	2	602	100	87.4
PbO ₂	1	197.6	3.9	65.4
		606	100	75.0
		198	1.8	27.1
	2	612	100	61.2
		186	49.1	33.9

Anode current density = 0.3 amp/cm²; cell temperature = 25°-35°C; cell potential = 5-6.5 v.

Table IV. Effect of $\text{K}_2\text{S}_2\text{O}_8$ additive on current efficiency in electrolysis of NaClO_3 with PbO_2 anode

g $\text{K}_2\text{S}_2\text{O}_8$ per liter of electrolyte	Test No.	NaClO ₃ conc. range over which eff. is calculated		Current efficiency, %
		Initial g/l	Final g/l	
2.08	1	606	7.1	73.3
		204	7.1	52.0
2.08	2	606	30.3	68.2
		200	44.9	49.2
None	1	606	28.9	46.5
		200	28.9	27.1
		126	28.9	20.3
None	2	606	31.0	43.4
		200	31.0	30.5
		128.4	31.0	22.9

Anode current density = 0.3 amp/cm²; cell temperature = 25°-35°C; cell potential = 5-6.5 v.

The large PbO_2 electrode formed on the Ta screen, and described above, was used with a sprayed Cu over Ag contact in a 100 amp perchlorate cell at a current density of 0.28 amp/cm² and a temperature of 30°-50°C. The cathodes were type 430 stainless steel and the electrolyte was 5 liters of NaClO_3 solution having an initial concentration of 600 g/l. This cell was operated for 24 batches for a total running time of 860 hr without noticeable erosion of the anode, and with less than 0.25 ppm of Pb in the recovered NaClO_3 .

The current efficiency of PbO_2 anodes in the conversion of chlorate to perchlorate, although less

than that of Pt, is reasonably high when the concentration of NaClO_3 in the electrolyte is above 100 g/l. Below this concentration of chlorate, the current efficiency drops sharply. In Table III, the current efficiencies of PbO_2 and Pt anodes are compared for various chlorate concentration ranges when operated in 10-amp cells.

In order to obtain higher current efficiencies with the PbO_2 anode, especially in the lower chlorate concentration range, the use of additives becomes necessary. Sugino (10) has reported using NaF additive at a concentration of 2 g/l. In the present work, $\text{K}_2\text{S}_2\text{O}_8$ was found (11) to be even more effective, and the increase in current efficiency due to this additive is shown in Table IV.

Acknowledgments

This paper includes the results of one phase of a research carried out under the Office of Naval Research Contracts Nonr 372(00) (2/19/51-8/31/51) and Nonr 807(00) (2/1/52-1/31/54).

The authors wish to express their thanks to J. F. Gall under whose supervision this work was done, and to E. Eitelman and W. Barry for their excellent assistance in the laboratory work.

Manuscript received June 24, 1957.

Any discussion of this paper will appear in a Discussion Section to be published in the December 1958 JOURNAL.

REFERENCES

1. J. Mizuguchi, *J. Electrochem. Soc. Japan*, **17**, 294 (1949).
2. J. Mizuguchi, *ibid.*, **17**, 258 (1949).
3. G. Angel and H. Mellquist, *Z. Elektrochem.*, **40**, 702 (1934).
4. E. Andreoli, U. S. Pat. 598,193, Feb. 1, 1898.
5. V. Engelhardt and M. Huth (to Siemens & Halske, A.-G.) U. S. Pat. 935,250, Sept. 28, 1909.
6. M. Huth (to Siemens & Halske, A.-G.) U. S. Pat. 1,043,937, Nov. 12, 1912.
7. K. Sugino and M. Yamashita, *J. Electrochem. Soc. Japan*, **15**, 61 (1947).
8. Y. Kato and K. Koizumi, *J. Electrochem. Assoc. (Japan)*, **2**, 309 (1934).
9. F. Mathers, *Trans. Am. Electrochem. Soc.*, **17**, 261 (1910).
10. K. Sugino, *Bull. Chem. Soc. Japan*, **23**, 115 (1950).
11. H. C. Miller and J. C. Grigger, U. S. Pat. 2,813,825, Nov. 19, 1957.

Enhanced Surface Reactions

II. Oxygen Adsorption on Several Metals

Manfred J. D. Low

Nichols Laboratory, New York University, New York, New York

Recently, interesting experiments have been reported (1, 2) on the influence of high-frequency induced gaseous discharges on rates of chemisorption. In a previous paper (3) the enhancement of the rate and extent of adsorption in four adsorbate-adsorbent systems were reported, and a general mechanism was proposed. That investigation was extended to the adsorption of oxygen on seven metals and is here reported.

Experimental

A Tesla coil was applied in a manner previously described (3) to a standard constant volume adsorption system. Over desired periods of time a continuous discharge barely visible in a darkened room could be caused to persist. It was found that, under the conditions prevailing in actual runs, but in the absence of the adsorbent, the discharge had no noticeable effect on the pressure of the system.

The adsorption of tank oxygen on the following adsorbents is described: (a) 3.07 g gold foil "cohesive cylinders"; (b) 14.23 g C.P. aluminum foil; (c) 136 g N.F. 20 mesh iron filings; (d) 28 g 200 mesh 99.8% Mo powder; (e) 28 g 200 mesh Ni-free C.P. Co powder; (f) 42 g "Baker Analyzed" Cu foil; (g) 18 g "Baker Purified" 30 mesh Mg powder. In order to preclude any effects due to adsorbed hydrogen, the metals were not cleaned by the customary hydrogen reduction and evacuation procedure, but were merely degassed. It was found that a pressure of 10^{-6} mm Hg, or less, could be obtained and maintained by pumping at $400^{\circ} \pm 10^{\circ} \text{C}$ for 16 hr for all metals except gold, which required 170 hr until release of gas ceased. The adsorption of oxygen was thus measured on surfaces covered partially or wholly with oxide films.

Results and Discussion

Gold.—Slight, instantaneous up-takes of oxygen were detected at 0° , 100° , 147° , and 257°C at oxygen pressures of 39-46 mm Hg. An estimate of the amount adsorbed was obtained by pumping, at the adsorption temperature, in 4 min to 10^{-4} mm Hg after the Au had been in contact with oxygen for periods up to 5 hr, and then heating the adsorbent to 400°C . Desorption of gas was detected at approximately 350° during the heating. Pressure increases of up to 0.94 mm Hg within the system indicated that about 0.02 ml NTP of gas had been

evolved. It was concluded that a small amount of oxygen was strongly adsorbed by the Au under the conditions of the experiments, and that at least a part of it remained on the solid while the pressure was decreased and was caused to desorb under the influence of increasing temperature. Causing a discharge in the oxygen for periods up to 4 hr after the adsorption process had taken place had no effect on the oxygen take-up.

Molybdenum, copper, magnesium, aluminum.—Figure 1 is a plot of the data of experiments on the adsorption of oxygen by Mo and by Co. The enhancement in the rate of adsorption on causing the discharge ("ON") is quite detectable and remarkably large in view of the small energizing action of the Tesla coil. On stopping the discharge ("OFF"), the adsorption is seen to approximate its previous rate.

A much larger enhancement is depicted by curve I of Fig. 2, showing the adsorption of oxygen on Mg. At P the adsorbent was heated to 400°C and evacuated for 16 hr to a final pressure of 10^{-6} mm Hg. The experiment described by curve II was then made. It is seen that the rate, extent, and enhancement of adsorption are smaller than those shown by

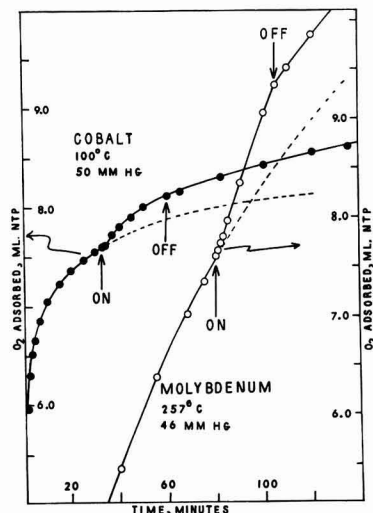


Fig. 1. Adsorption of oxygen on Co and on Mo

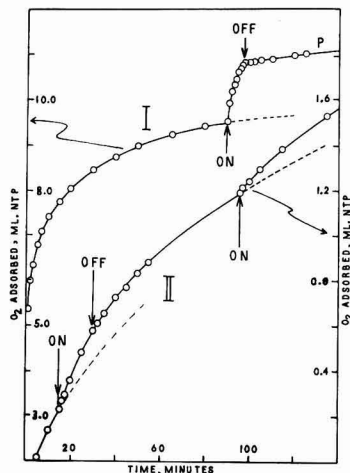


Fig. 2. Adsorption of oxygen on Mg at 100°C, 46 mm Hg

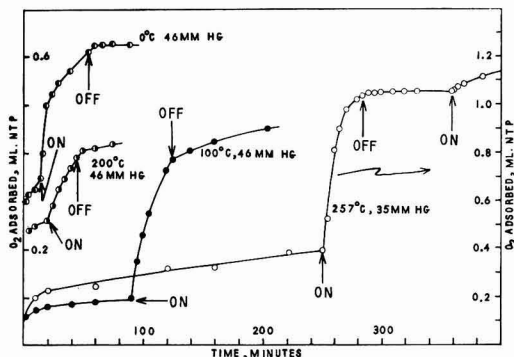


Fig. 3. Adsorption of oxygen on Al

curve I. At the end of the experiments the metal had taken on a deep blue sheen confined to the surface of the adsorbent, and a transparent deep blue coating had appeared on the walls of the adsorbent chamber.

In Fig. 3 the enhanced adsorption of oxygen on Al is shown. The data of four consecutive experiments made at 257°, 100°, 0°, and 200°C in that order are shown, the metal having been pumped at 400° for 16 hr to 10^{-6} mm Hg after each experiment. It is seen that the adsorption rate falls off in a relatively short time, and that adsorption may be caused to occur on almost "saturated" surfaces.

Iron and copper.—Figure 4 shows two plots of adsorption of oxygen on Fe at 257°C. Curve I is an experiment with a fresh surface and curve II after this same adsorbent had been pumped on at 400° for 16 hr to 10^{-6} mm Hg. Desorption, manifested by an increase in system pressure, was found when the discharge was caused, shown by curve I. A slight enhancement effect, however, was detected during the second run, shown by curve II.

A more pronounced desorption effect was found to occur with Cu, Fig. 5. The magnitude of the measured effect is shown by the system pressure-time plot II of that figure.

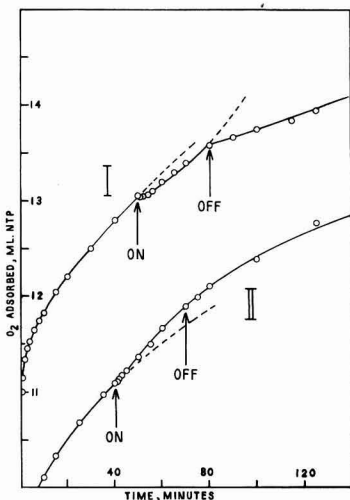


Fig. 4. Adsorption of oxygen on Fe at 257°C, 50 mm Hg

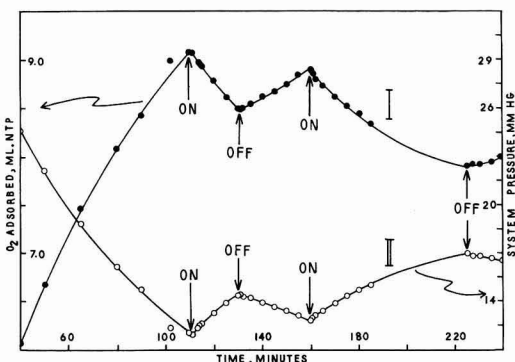
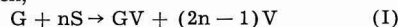


Fig. 5. Adsorption of oxygen on Cu at 257°C, 50 mm Hg

General theory.—A general theory capable of accounting for enhancement of chemisorption, oxidation, and other phenomena, by activation of heterogeneous systems was presented previously (3). It was suggested that the relatively large effects instigated by a minute activating disturbance in the gas phase occur via a branching chain mechanism. If an active particle, G, strikes a surface atom, S, a "dissociation" of the latter may occur with formation of adsorption sites, V, the over-all process being written,



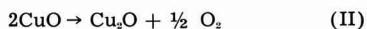
The remaining $(2n - 1)$ sites may be active for further adsorption, causing enhancement, or may suffer bimolecular decay (4). It is suggested that this mechanism is operative in all cases described, with the exception of Au. The enhancements of adsorption which were detected, especially in the case of the almost "saturated" Al surfaces, together with previously discussed enhancement effects (3), tend to support this theory, which is also capable of explaining the interesting desorption phenomena described above.

The oxidation of Cu in activated oxygen has been studied by Dravnieks (5,6) in the pressure range

0.5-2.0 mm Hg and at temperatures ranging from 500° to 690°C. Enhancements of oxygen up-take were found to occur at 0.5, 1.0, and 2.0 mm Hg at 500°C, and at 0.5 mm at 600° and 690°C. At higher pressures at the last two temperatures, however, the enhancement disappeared, and at 2.0 mm and 600°C a retardation in oxygen up-take was found. At 500°C the oxidation curves, plotted according to the parabolic rate law, appeared as two straight lines with an intermediate region of rapidly changing slope. The first parabolic rate was identified with oxidation to Cu_2O , the region of rapidly changing slope with beginning of precipitation of CuO on the surface of the Cu_2O , and the second parabolic region with oxidation occurring in the presence of both oxides. At higher temperatures the oxidation curves could not be resolved into two distinct parabolas. The observations that activation may accelerate or retard the oxidation and may change the composition of the oxide scale were explained in terms of lower permeability of CuO than Cu_2O to reactants, and of rate of precipitation of CuO .

Tylecote (7) found that the CuO content of scales formed on high purity Cu in dry air increased with reduction in temperature from 7% at 850°C to about 100% at 420°C, and that for the majority of temperatures, the CuO content decreased to a constant temperature dependent value as the film increased in thickness. Under the conditions of the experiments reported here, it may be expected, then, that a film of CuO formed on the Cu surface. Similarly, the retardations noted by Dravnieks occurred under conditions at which CuO would predominate, whereas enhancement was found when Cu_2O would predominate.

It is suggested the evolution of gas observed during activation was caused by the transition,



Because the observed effect was large in comparison to the magnitude of the stimulus, it may be postulated that a chain disturbance was initiated on the surface, causing unstable CuO to give up oxygen. The initial step of the mechanism may be the collision of an active oxygen particle, perhaps a metastable oxygen molecule (8), with a surface CuO , causing reaction (II) to occur. The local disturbance then spreads through the film, permitting the gas evolution to occur. The chain propagator may be activated CuO -oxygen complexes, Cu atoms, or the oxygen atoms produced by the process.

The action of active oxygen on iron may be explained similarly by an enhanced transition of a surface film (9) of $\gamma\text{-Fe}_2\text{O}_3$ to cubic Fe_3O_4 with attendant release of oxygen when $\gamma\text{-Fe}_2\text{O}_3$ predominates. At higher Fe_3O_4 concentrations, the normal enhancement effect occurs (Fig. 4).

The influence of active oxygen on Cu and Fe , at least, is thus twofold if more than one oxide can be formed. (A) If a change in oxidation state can occur, that change may be enhanced by causing an increase in the active particle concentration. The effect appears as an actual gas evolution, as described above, or as a retardation of oxidation rate resulting, in either case, in a change in the oxide composition. (B) If no change in oxidation state is possible, or if such a change has occurred, then an enhancement of oxygen adsorption may occur, probably via the site-creating mechanism (I). It seems plausible that an enhancement of adsorption occurs simultaneously with the enhanced change of oxidation state, but may be overshadowed by the latter.

The relatively large enhancements detected (1-3) and the generality of the effect lend credence to the proposed theory. A similar high degree of plausibility is inferred for the application of that theory to the retardation effect. The proposed generation of sites for the enhancement of chemisorption as well as the retardation or enhanced transition of oxidation states must be considered to be operative through a self-perpetuating surface disturbance, of electronic or particulate nature, of considerable chain-length in order to explain the relatively large effects instigated by a small stimulus.

Manuscript received May 29, 1957.

Any discussion of this paper will appear in a Discussion Section to be published in the December 1958 JOURNAL.

REFERENCES

1. H.-J. Engell and K. Hauffe, *Z. Elektrochem.*, **57**, 773 (1953).
2. T. J. Gray and P. W. Darby, *J. Phys. Chem.*, **60**, 209 (1956).
3. M. J. D. Low and H. A. Taylor, *This Journal*, **104**, 439 (1957).
4. H. A. Taylor and N. Thon, *J. Am. Chem. Soc.*, **74**, 4169 (1952).
5. A. Dravnieks, *ibid.*, **72**, 3761 (1950).
6. A. Dravnieks, *J. Phys. Colloid Chem.*, **55**, 540 (1951).
7. R. F. Tylecote, *Metallurgia*, **53**, 191 (1956).
8. S. N. Fouer and R. L. Hudson, *J. Chem. Phys.*, **25**, 601 (1956).
9. D. E. Davies and U. R. Evans, *J. Chem. Soc.*, **1956**, 4373.

Photodeposition of Luminescent Screens

M. Sadowsky and P. D. Payne, Jr.

Lansdale Tube Division, Philco Corporation, Lansdale, Pennsylvania

In the Philco color tube, the phosphor is deposited (1) as a line array on the inside surface of the cathode ray tube bulb panel. The array consists of red-, blue-, and green-emitting phosphor stripes,

between each line of which there is a black, non-luminescent line (2,3). The screen is backed by a reflective film of aluminum, on the back of which is a set of magnesium oxide powder stripes applied in

strict reference to the phosphor lines on the face. These phosphor lines vary in width in a controlled manner between the center and the edge for electrical reasons. The total triplet of red, blue, and green lines plus the three dark guard lines averages 61 mils.

The exact procedure for depositing a color screen is as follows: The bulb is picked up automatically from an indexing conveyor. 200 ml of a clear photoresist solution, containing 25g PVA grade 52-22, and 2.75 g ammonium bichromate dissolved in 600 ml water with 290 ml denatured ethanol, is introduced by a dispenser. The bulb face is flow-coated by tilting and rotating. The excess solution is drained off, and the bulb returned to the conveyor. There it is dried for 35 min using filtered, dried air. It is then placed face down in the projector for a 3½-min exposure through the appropriate line master. It is then returned to the conveyor for automatic flow-coating and drying of the phosphor slurry. 100 ml of a mixture of 80 ml denatured alcohol, 60 ml water, and 50 g phosphor is normally used. Drying takes 13 min. The final step of washing off the unexposed photoresist and phosphor is done on a turntable with water directed against the inside funnel wall and flowing up and across the screen for 1 min. The same procedure is used for guard lines, color lines, and index lines. The screen is treated with 0.5% aqueous lithium hydroxide after the first and second color lines are applied. This prevents subsequently applied phosphors from contaminating the previously applied lines. The suggested mechanism for photofixation is shown in Fig. 1.

When the phosphor slurry is superimposed on the film with its latent image of hardened lines, the water in the phosphor slurry goes into the cross-linked film, softening it for penetration. The alcohol on the other hand tends to remove the water, making it possible to control penetration by proper control of the water-to-alcohol ratio. A compromise is effected between maximum phosphor occlusion (thicker screens) and penetration of the phosphor to the glass which might result in adhesion in the

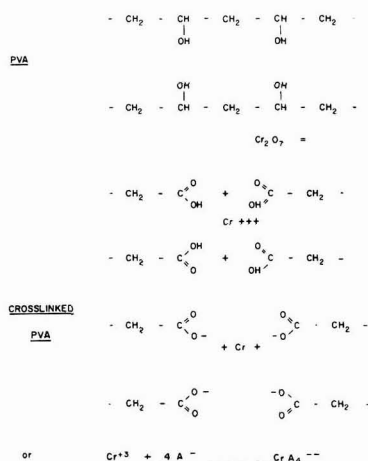


Fig. 1. Suggested mechanism for photofixation of the lines on the screen.

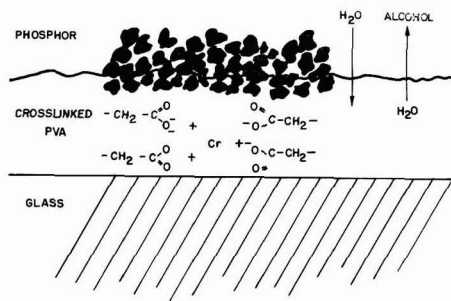


Fig. 2. Mechanism for phosphor imbedment

nonexposed areas. The mechanism for phosphor imbedment is shown in Fig. 2.

The problems encountered in photodeposition of multicomponent screens are: adhesion, control of screen weight, cross contamination and fogging.

To be practical, the process should be a water system, and must also be reasonably fast (short exposure times), must not affect deleteriously the phosphors, MgO, or Al used; agents used must bake off so as not to leave a significant residue in the completed tube, which might damage the cathode.

Addition of H_3PO_4 to the sensitized PVA solution promotes adhesion to the glass, but is difficult to control and deteriorates rapidly with age. Urea formaldehyde gives similar results with slower deterioration. PVA of lower per cent hydrolysis has better adhesion to glass, but is not sufficiently photosensitive. Consistently good adhesion is best obtained by drying the PVA film to equilibrium with air of 1% RH.

Parameters in Control of Screen Weight

Thickness of sensitized PVA film on glass.—As the coating thickness is increased, the total depth of the phosphor layer increases. If exposure takes place from the surface to be coated, through to the glass, too thick a film will result in insufficient light reaching the glass-film interface to provide adequate fixing to the glass. If the exposure time is then increased, the surface to be coated will be insolubilized to such an extent that the phosphor particles will not penetrate it, and a thin screen will result. This effect can be overcome by leaching a portion of the sensitizer out of the surface of the film with a solvent, such as ethyl alcohol, which will dissolve the sensitizer, but not the film.

Phosphor slurry formulation.—A suspension of phosphor in water provides maximum softening of the exposed film, allowing maximum phosphor penetration and screen weight. However, such a slurry is difficult to apply uniformly because it dissolves and carries along much of the unexposed water-soluble portion of the film and dries too slowly. Also, this allows phosphor to reach the glass between the image lines and adhere there. Addition of ethyl alcohol to the slurry reduces its effect on the water-soluble film, and promotes more rapid drying, resulting in a more uniform screen. Addition of the alcohol, however, reduces the penetration of the image lines by the phosphor, causing a

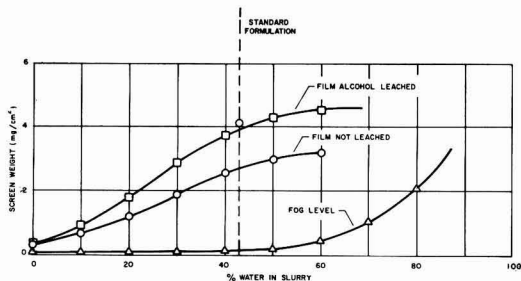


Fig. 3. The screen weight vs. per cent of water in slurry. The three curves show fog level (triangle), film leached with alcohol (square) and film not leached (circle).

drop in screen weight, so these factors are balanced to provide the best combination of screen weight, uniformity, and freedom from fogging between the lines. A typical slurry will contain 80 parts alcohol and 60 parts water by volume, with from 40 to 90 g of phosphor, depending on the particular phosphor used. The weight of phosphor used is set at that value which produces the best flowing characteristics. The compromise is shown on the graph in Fig. 3.

Cross Contamination

Cross contamination is the presence of phosphor of one color in screen lines of another color.

Causes.—(a) Trapping of particles by the PVA line of a previous color which was not thoroughly covered with phosphor; (b) trapping of particles in the rough phosphor surface of a previous line.

Cures.—First, post-harden the PVA to prevent any further phosphor being trapped. Materials used include: titanium lactate, Quilon (chrome organic complex), DMU, glyoxal, diazocyanates, hydroxyadipaldehyde, aqueous ammonium dichromate (exposed to light), heat at 110°C for 15 min. All of these aid in reducing cross-contamination, but none is sufficient.

Retreat the phosphor lines with the same color slurry prior to application of the next color. This works, but is too costly.

Second, coat the screen with an impervious layer (a) lacquer film; this protects completely, but

causes wrinkling of subsequent lines; (b) aqueous potassium silicate; this reduces contamination but produces fog.

Treat the screen with aqueous lithium hydroxide to repel subsequent phosphor. This treatment has produced good results most consistently and is currently in use.

Fog

Fog is the term used to describe phosphor particles which deposit on the glass between the lines and fail to wash off.

Causes.—(a) Electrostatic attraction of particles to the glass; (b) trapping of particles in partially fixed PVA which has dried between the lines after washing.

Cures.—(a) Use of phosphor with few superfines; particles which tend to adhere to bare glass are those of low density and particle size below 1 μ ; (b) prevent penetration of particles through unexposed portion of film to the glass by keeping the water content of the slurry low enough; (c) wash the exposed and coated screen before drying is completed, where very fine particles must be used, and water content must be kept high.

The process described above has been used to make thousands of tubes. The precision is built into the equipment, rather than into hardware incorporated in the tube. The chemical processes are controllable and practical, giving high reproducibility with little more care than is exercised in the preparation of screens for monochrome cathode ray tubes.

Manuscript received June 27, 1957. This paper was prepared for delivery before the Washington Meeting, May 12-16, 1957.

Any discussion of this paper will appear in a Discussion Section to be published in the December 1958 JOURNAL.

REFERENCES

1. M. Sadowsky, *J. (and Trans.) Electrochem. Soc.*, **95**, 112 (1949).
2. H. Colgate, C. Comeau, D. Kelley, D. Payne, and S. Moulton, 1957 IRE National Convention Record, Part 3, pp. 238-241.
3. G. S. Barnett, F. J. Bingley, S. L. Parsons, G. W. Pratt, and M. Sadowsky, *Proc. IRE*, **44** [9], 1115 (1956).

June 1958 Discussion Section

A Discussion Section, covering papers published in the July-December 1957 JOURNALS, is scheduled for publication in the June 1958 issue. Any discussion which did not reach the Editor in time for inclusion in the December 1957 Discussion Section will be included in the June 1958 issue.

Those who plan to contribute remarks for this Discussion Section should submit their comments or questions in triplicate to the Managing Editor of the JOURNAL, 1860 Broadway, New York 23, N. Y., not later than March 3, 1958. All discussion will be forwarded to the author, or authors, for reply before being printed in the JOURNAL.

FUTURE MEETINGS OF The Electrochemical Society



New York, N. Y., April 27, 28, 29, 30, and May 1, 1958

Headquarters at the Statler Hotel

Sessions will be scheduled on

Electric Insulation, Electronics (Luminescence and Semiconductors),
Electrothermics and Metallurgy, Electrothermics and Metallurgy—Semiconductors
Joint Symposium, Electrothermics and Metallurgy—Corrosion Joint Symposium,
Industrial Electrolytics, and Theoretical Electrochemistry (including a symposium
on "Electrokinetic and Membrane Phenomena")

★ ★ ★

Ottawa, Canada, September 28, 29, 30, October 1, and 2, 1958

Headquarters at the Chateau Laurier

Sessions probably will be scheduled on

Batteries, Corrosion, Electrodeposition (including symposia on "Electrodeposition
on Uncommon Metals" and "Chemical and Electropolishing"),

Electronics (Semiconductors), Electro-Organics,
and Electrothermics and Metallurgy

★ ★ ★

Philadelphia, Pa., May 3, 4, 5, 6, and 7, 1959

Headquarters at the Sheraton Hotel

★ ★ ★

Columbus, Ohio, October 18, 19, 20, 21, and 22, 1959

Headquarters at the Deshler-Hilton Hotel

★ ★ ★

Chicago, Ill., May 1, 2, 3, 4, and 5, 1960

Headquarters at the Lasalle Hotel

★ ★ ★

Houston, Texas, October 9, 10, 11, 12, and 13, 1960

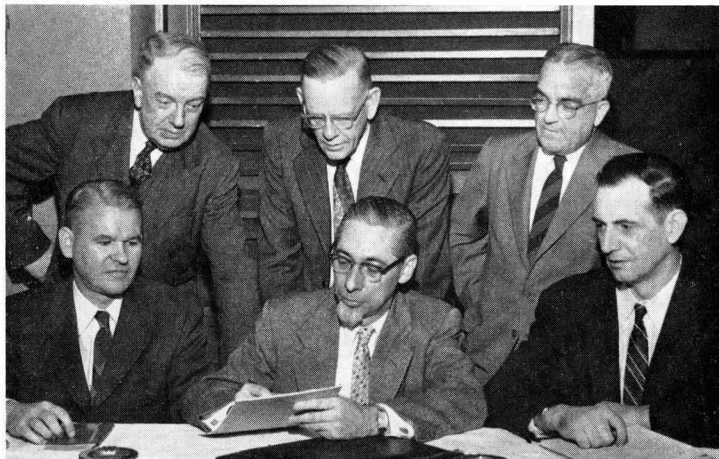
Headquarters at the Shamrock Hotel

★ ★ ★

Papers are now being solicited for the meeting to be held in Ottawa, Canada, September 28-October 2, 1958. Triplicate copies of each abstract (*not exceeding 75 words in length*) are due at the Secretary's Office, 1860 Broadway, New York 23, N. Y., *not later than June 2, 1958* in order to be included in the program. *Please indicate on abstract for which Division's symposium the paper is to be scheduled.* Complete manuscripts should be sent in triplicate to the Managing Editor of the JOURNAL at 1860 Broadway, New York 23, N. Y.



Come to New York in April



Members of the New York Convention Committee. Seated, left to right—H. R. Copson, Chairman, Advisory Committee; F. A. Lowenheim, General Chairman; M. F. Qualey, Chairman, Registration Committee. Standing, left to right—A. C. Loonam, Chairman, Arrangements Committee; K. B. McCain, Chairman, Entertainment Committee; J. L. Everhart, Co-chairman, Publicity Committee. Not shown—F. C. Lang, Chairman, Ladies' Program Committee; C. V. King, Co-chairman, Publicity Committee; L. I. Gilbertson, Chairman, Finance Committee.

There is every reason to expect that the Spring 1958 Convention in New York (April 27-May 1) will continue the recent trend toward bigger and better meetings of the Society. The technical and scientific aspect is, as usual, the responsibility of the various Divisions; complete details will be published in the March issue. Meanwhile, the Convention Committee of the New York Metropolitan Section, under the chairmanship of Dr. F. A. Lowenheim, is maturing plans for a well-rounded social program for the registrants and their ladies.

Headquarters hotel is the Statler, home of many previous meetings of the Society. Reservation cards will be mailed to the membership shortly. *Please note:* the hotel is holding an adequate number of rooms for the Society, but if you fail to mention The Electrochemical Society in your reservation request you may be turned down. Therefore, if writing on your personal or business letterhead, mention The Electrochemical

Society when making your hotel reservation.

Richards Memorial Lecture

One of the highlights of the technical program will be another in the series of memorial lectures in honor of Dr. J. W. Richards. The lecture will be so scheduled that all registrants can attend; no other technical sessions will conflict with it. Dr. Abner Brenner, Chief of the Electrodeposition Section of the National Bureau of Standards and one of the country's outstanding younger electrochemists, will deliver the address.

Mixer

The Committee hopes that as many registrants as possible will take advantage of the opportunity offered to meet their friends and make plans for the week at the "Mixer" on Monday evening, from 8 p. m. to ?. Admission is free—all you need is your registration badge. Beer, soft drinks, and snacks

are "on the house"; a bar also is available.

Have dinner at one of the many fine restaurants New York has to offer; then join your friends at the Mixer for a few hours of sociability.

Luncheons and Banquet

The Society Luncheon is scheduled for Monday noon, April 28. Immediately following luncheon, necessary Society business will be transacted at the Annual Meeting (guaranteed brief) and then a talk of general interest will be heard. Ladies are invited.

Tuesday evening, April 29, a reception in honor of the retiring President will precede the banquet, which will feature the Presidential Address by Dr. Norman Hackerman.

In addition to these principal functions, many of the Divisions are planning Divisional luncheons or other meetings.

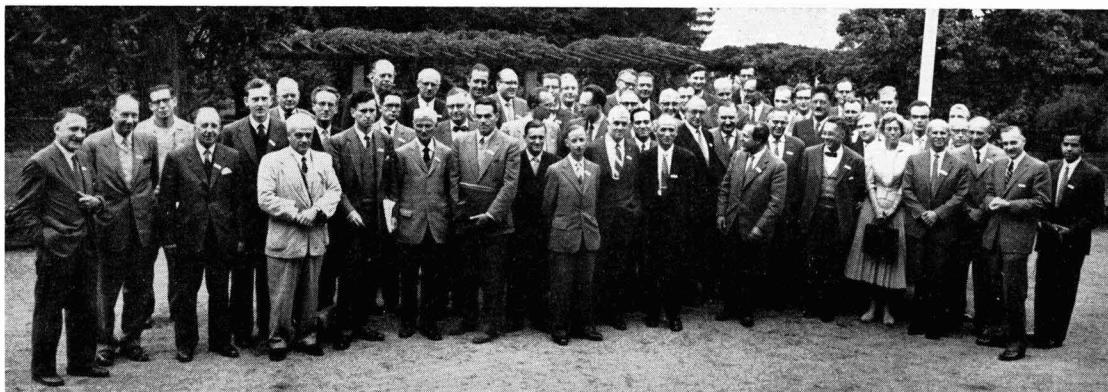
Ladies' Program

The ladies, of course, are invited to the Society Luncheon and the Presidential Reception and Banquet. In addition, a Ladies' Committee, headed by Dr. Frances Lang, is planning such an interesting series of events that we feel quite safe in exhorting you to bring your wife to New York. Luncheon at the Plaza, a boat ride around Manhattan, a visit to the U. N., guided shopping tours along Fifth Avenue, comprise a partial list of what the ladies have in store. In addition, as usual, the ladies will have a headquarters room where they can foregather and have morning coffee, and where expert advice on shopping, lunching, and sightseeing will be available.

Further Details

Watch for the complete program in the March JOURNAL; in the meantime, make your reservation at the Statler in New York for April 27-May 1.

International Symposium on Passivity



International Symposium on Passivity, Schloss Heiligenberg, Jugenheim, West Germany, September 2-7, 1957

The first International Symposium on Passivity, sponsored by The Electrochemical Society, The Deutsche Bunsen Gesellschaft, and the Faraday Society, was held at Jugenheim, West Germany, September 2-7, 1957. It was attended by 55 scientists from this country, Germany, England, France, Italy, Japan, Norway, Holland, and Belgium. One representative attended from Czechoslovakia and one from East Germany. Six Russian scientists were invited, but were unable to come at the last moment because they had applied too late for visas. Their contributed papers arrived, however, and will be published together with other papers and discussion in a special issue of the *Zeitschrift für Elektrochemie*, scheduled to appear early this year.

The Symposium was dedicated to the memory of the late Professor K. F. Bonhoeffer, 1957 Palladium Medalist, who greatly helped in arranging the Symposium, particularly in its initial stages. A commemorative

address on the life and accomplishments of Professor Bonhoeffer was presented to the Symposium by Professor G. M. Schwab of the University of Munich.

Dr. Th. Goldschmidt, President of the Bunsen Gesellschaft, and Professor U. F. Franck, who represented the Bunsen Gesellschaft on the arrangements committee, welcomed the participants. Response was made by Dr. T. P. Hoar representing the Faraday Society, and Dr. H. H. Uhlig representing The Electrochemical Society.

Foreign participants were guests of The Deutsche Bunsen Gesellschaft for the 5½ days of the meeting. The Electrochemical Society, on recommendation of the Committee for Administration of the Corrosion Handbook Fund and by action of the Board of Directors, supported the meeting to the extent of providing for printing and distribution of papers. There were 31 papers prepared for presentation. The lively discussion following each presenta-

tion was facilitated by a running translation of German into English and vice versa, employing earphones and a professional translator. Dr. Franck of the Technische Hochschule at Darmstadt and his co-workers deserve much credit for the smooth operation of the meeting throughout the week.

The seat of the Symposium, Schloss Heiligenberg, made an attractive meeting place. The castle, until recently the residence of the Battenbergs, was the birthplace of the present Queen of Sweden and Lord Louis Mountbatten of Great Britain, and was visited frequently in former times by Queen Victoria. The buildings and acres of surrounding woodland are now part of a Normal School for the Province of Hesse.

The meeting ended with dinner and a wine-tasting party at Eltville on the Rhine where Farbwerke Hoechst A. G. acted as hosts. A second international meeting is hoped for in three to five years.

New United Engineering Center to be Erected in New York City

Plans have been announced for a new \$10,000,000 United Engineering Center to be erected on United Nations Plaza between 47th and 48th Sts., New York City, to serve as the headquarters of 16 National Engineering Societies, with a total membership of about one quarter of a million engineers. The Electrochemical Society is one of 11 Associated Societies which will also occupy space in the new building.

The new building will replace the present 50-year-old Engineering So-

cieties Building at 29 West 39th St. which is now inadequate.

This announcement, made by Dr. Mervin J. Kelly, President of Bell Telephone Labs., who is serving as Chairman of the industrial campaign to raise funds for the new Engineering Center, calls for the occupancy of the building in the fall of 1960. A 20-story tower surrounded by lower structures with landscaped grounds, the Center will not only have facilities for present functions, but provision for continuing growth of the en-

gineering profession. It will include the Engineering Societies Library, and exhibition space in which the rapid advances in engineering will be interpreted for the general public. An engineering Hall of Fame to perpetuate the contributions of distinguished engineers to modern civilization is under consideration. In all there will be about 250,000 square feet of floor space.

The industry campaign which Dr. Kelly heads has a goal of \$5,000,000. Members of the various engineering



The new \$10,000,000 United Engineering Center, to be erected on United Nations Plaza between 47th and 48 Sts., New York City.

societies are expected to contribute \$3,000,000. This money, together with \$2,000,000 which is available in the assets of United Engineering Trustees, Inc., is expected to meet the \$10,000,000 cost of the new building.

Division News

Battery Division

The Battery Division observed its tenth anniversary at the Buffalo Meeting by offering six technical sessions. Two sessions on unconventional types of cells and the Round Table on fuel cells emphasized the expanding concepts being applied to battery investigations and design. Three sessions discussed problems associated with the more familiar cells.

As this is the "off" year, no officers were elected. A short business meeting was held at the Battery Luncheon. The Chairman of the Battery Award Committee, C. K. Morehouse, reported on the nature of the Alessandro Volta Award which has been approved by the Battery Division Executive Committee. The Secretary-Treasurer reported that the Battery Division had a net gain of 23 members for a total of 266 members; and, as of October 1, 1957, the treasury contained \$1380.43 which is an increase of \$521.53 over the 1956 report. Most of our income has resulted from the sale of Extended Abstracts and Bulletins.

Plans for the 1958 meeting in Ottawa are under way.

E. J. Ritchie, *Secretary-Treasurer*

Section News

Mohawk-Hudson Section

The fifth meeting of the Mohawk-Hudson Section was held at the Edison Club, Rexford, N. Y., on November 14, 1957 at 8:00 P. M. The Chairman announced that the Mohawk-Hudson Section had been approved and recognized as a duly constituted section of The Electrochemical Society.

The Section Bylaws were discussed and accepted, pending approval by The Electrochemical Society.

Chairman Schmidt turned the meeting over to J. F. Murphy who introduced the speaker of the evening, W. H. Smith of the General Electric Research Laboratory, who spoke on "Newer Melting Techniques."

A. L. Jenny,
Secretary-Treasurer

India Section

The Seventh Annual Meeting of the Section was held on September 29, 1957 with Dr. M. S. Thacker presiding.

The following Section officers were elected for 1957-58:

Chairman—M. S. Thacker
Vice-Chairman—S. Ramaswamy
Vice-Chairman—K. Srinivas
Treasurer—T. L. Rama Char
Secretary—J. Balachandra, Indian Institute of Science, Bangalore 3, India.

Section dues for 1958 were fixed at Rs. 2.50 as before.

The Chairman made the following nominations:

Bulletin Editorial Committee: M. S. Thacker (Chairman), S. Ramaswamy, K. Srinivas, K. Seshadri, S. Krishnamurthy, J. Balachandra, N. R. Srinivasan, T. L. Rama Char (Editor).

Bulletin Advisory Board: A. Jogarao, K. Rajagopal, P. A. Porecha, S. L. Chawla, H. V. K. Udupa, H. S. Gujral, P. S. Narayana, K. S. Rajagopalan.

Auditing Committee: P. S. Narayana, S. K. Panikkar.

Nominating Committee: K. Rajagopal, H. V. K. Udupa, S. L. Chawla.

The question of creating an Associate Membership of the Section was discussed. The object is to enable nonmembers of the Society to participate in the activities of the India Section as Associate Members, at an annual subscription of Rs. 10. Such members could attend meetings and symposia and receive the *Bulletin*, but would not be entitled to

voting rights. The idea was approved and the Secretary was asked to write to the Society for permission.

It was decided to publish a Special Number covering the proceedings of the India Section Symposium on Electrodeposition and Metal Finishing, held at the Central Electrochemical Research Institute, Karai-kudi, on December 27 and 28, 1957.

J. Balachandra, *Secretary*

Rare Metals Symposium

A Symposium on Rare Metals was held during December 1957 in Bombay by the Indian Institute of Metals in collaboration with the Atomic Energy Commission, India, and the UNESCO.

T. L. Rama Char,
Regional Editor, India

Ontario-Quebec Section

The first meeting of the 1957-58 season was held at McGill University, Montreal, on Friday afternoon, November 15. T. S. Gamble, Section Chairman, welcomed the members and guests and turned the meeting over to John Sumner, Technical Chairman, who introduced the guest speakers—Mr. C. B. Carlson of the technical staff of Lectromelt Furnace Div., McGraw-Edison Co., Pittsburgh, Pa.; and Mr. C. W. Hensen, Field Development Engineer with Refractories Div., Norton Co., Worcester, Mass.

Mr. Carlson's paper, "Modern Electric Pig Iron and Calcium Carbide Practice," covered the mechanical and electrical features of modern Demag low shaft furnaces and discussed the application of such equipment in the manufacture of pig iron and calcium carbide. Mr. Hensen's talk on "Use of High Temperature Refractories" outlined the properties and fabrication of refractories developed for high temperature or corrosive conditions, and discussed the advantages and uses of these special materials. Mr. Hensen followed his talk by a film showing some applications of Norton Rokide Coatings.

L. G. Henry,
Secretary-Treasurer

Philadelphia Section

Dr. Francis P. Bundy of the General Electric Research Lab. spoke, at the November 6 meeting of the Philadelphia Section, on "Super Pressure Research and Diamond Synthesis."

The speaker described the Bridgeman method of generating extremely high pressures. Crystal growth of diamonds and cubic boron nitride was studied at the General Electric

Labs. at pressures up to 100,000 atm. Although considerably smaller than the pressure in the center of the earth (nearly 2,000,000 atm) these pressures are high enough to produce conditions for the growth of artificial diamonds which have properties identical to natural diamonds. Dr. Bundy described some of the technical difficulties of obtaining such high pressures, particularly the problems due to the compressibility of the material of the pressure chamber. The largest diamond crystals produced so far have a diameter of about 0.5 mm, and the largest boron nitride (borazon) crystals of about 1 mm. No seeding for nucleation is necessary in the process developed at G. E. It was particularly interesting to learn about the anisotropic nature of hardness and about the position of borazon and diamond in the absolute hardness scale. Dr. Bundy displayed samples of artificial diamond and borazon.

P. Ruetschi

New Members

In November 1957 the following were approved for membership in The Electrochemical Society by the Admissions Committee:

Active Member Sponsored by a Sustaining Member

Paul E. Lighty, Federal Telecommunication Labs., 500 Washington Ave., Nutley 10, N. J. (Electronics)

Active Members

Ralph N. Adams, University of Kansas; Mail add: 1710 W. 19th Terrace, Lawrence, Kans. (Electro-Organic)

Kristian H. Brandt, 1076 Karesh Ave., Pomona, Calif. (Electric Insulation, Electronics)

Francis J. P. J. Burger, Telegraph Condenser Co. (Canada) Ltd.; Mail add: 74 Highbourne Rd., Toronto 7, Ont., Canada (Corrosion, Electric Insulation)

Luigi Calzavara, Societa Edison, S. Sofia 4199, Venice, Italy (Electrothermics & Metallurgy, Industrial Electrolytic)

E. L. Collins, Chilean Nitrate Sales Corp.; Mail add: 55 Alcott Rd., Mahwah, N. J. (Electronics)

Edward I. Doucette, Bell Telephone Labs., Murray Hill, N. J. (Electronics)

Walter Elsfelder, Silicone Insulation, Inc., 1383 Seabury Ave., Bronx 61, N. Y. (Electric Insulation)

Dorothy P. Enright, Naval Ordnance Lab.; Mail add: 322 Scott Dr., Silver Spring, Md. (Electronics)

Frauke Gries, Mallory Battery Co.; Mail add: 19340 Frazier Dr., Rocky River 16, Ohio (Battery)

Raymond W. Hale, Battelle Memorial Institute, 505 King Ave., Columbus 1, Ohio (Electrothermics & Metallurgy, Industrial Electrolytic)

James M. Hall, Jr., P. R. Mallory & Co., Inc.; Mail add: 4026 N. Graham, Indianapolis, Ind. (Electronics)

Robert L. Hall, Electro Metallurgical Co., 2329 Walnut Blvd., Ashtabula, Ohio (Electrothermics & Metallurgy)

Arnold M. Hartley, University of Illinois, 304 Noyes Lab., Urbana, Ill. (Theoretical Electrochemistry)

William V. Hauck, International Minerals and Chemical Corp.; Mail add: 632 9th St., Apt. 1-B-C, Niagara Falls, N. Y. (Industrial Electrolytic)

MacNeil E. Hertel, American Chrome Co.; Mail add: Box 237, Nye, Mont. (Electrothermics & Metallurgy)

Lee Robinson Hill, Westric Battery Co., 4201 Galapago, Denver, Colo. (Battery)

Herbert F. Hunger, U. S. Army Signal Engineering Labs.; Mail add: 28 Homestead Ave., West Long Branch, N. J. (Battery, Theoretical Electrochemistry)

Fred Kornfeil, U. S. Army Signal Engineering Labs.; Mail add: 365 Lake St., Oakhurst, N. J. (Battery, Theoretical Electrochemistry)

Duncan M. Lamb, Sylvania Electric Products Inc.; Mail add: 33 Orchard St., Towanda, Pa. (Electronics)

Howard Lessoff, Radio Corp. of America, Adv. Components Lab., 64 A St., Needham Heights 94, Mass. (Electrodeposition, Electronics)

Norman H. Morrisette, United Gas Corp., P.O. Box 1407, Shreveport, La. (Battery, Theoretical Electrochemistry)

Walter E. Mutter, I.B.M. Corp., Research Lab., Poughkeepsie, N. Y. (Electronics)

Nels P. Nelson, Jr., Continental Battery and Mfg. Inc.; Mail add: 7422 Eccles Dr., Dallas 17, Texas (Battery, Corrosion)

Ralph H. Nielsen, Wah Chang Corp.,

P.O. Box 366, Albany, Ore. (Electrothermics & Metallurgy)

Thomas P. Nowalk, Westinghouse Electric Corp., Youngwood, Pa. (Electronics)

Egon E. Nurmet, Hanning Electric Co., Ltd.; Mail add: P.O. Box 325, St. John's, Newfoundland, Canada (Battery)

Victor M. Obenhaus, Sprague Electric Co.; Mail add: 65 Meadow St., North Adams, Mass. (Electric Insulation)

Herbert Packer, Mallory Battery Co.; Mail add: 3420 Beachwood Ave., Cleveland Hts. 18, Ohio (Battery)

Raymond W. Reid, Dow Chemical Co.; Mail add: R.F.D. No. 1, Sanford, Mich. (Battery)

Thor N. Rhodin, Jr., Engineering Research Lab., Dupont Experimental Station, Wilmington, Del. (Corrosion)

Newton Schwartz, Bell Telephone Labs., Murray Hill, N. J. (Corrosion, Electric Insulation, Electronics, Theoretical Electrochemistry)

Edward Simon, Transitron Electronic Corp.; Mail add: 5 Nichols Rd., West Peabody, Mass. (Electronics)

Walter R. Spencer, Jr., The Texas Co.; Mail add: R.D. 2, Fishkill, N. Y. (Corrosion)

Minc Stefan, Polskie Tow. Chem.; Mail add: ul. Marszalkowska 55/73 m. 2, Warsaw, Poland (Corrosion, Theoretical Electrochemistry)

Donald Tuomi, T. A. Edison Industries Div. at McGraw Edison, Edison Lab., West Orange, N. J. (Battery, Electronics)

Hans M. Wagner, General Electric Co.; Mail add: 612 Fifth St., Liverpool, N. Y. (Electronics)

Douglas C. Wendell, Jr., Burroughs Corp.; Mail add: 29 Orchard Lane, Berwyn, Pa. (Electrodeposition)

Peter J. Whoriskey, Jr., Raytheon Mfg. Co.; Mail add: 59 Montclair Ave., Roslindale, Mass. (Electronics)

William C. Zeek, Ray-O-Vac Co., 212 E. Washington Ave., Madison 10, Wis. (Battery, Electrodeposition, Theoretical Electrochemistry)

Associate Member

Ronald Enstrom, Metals Research Labs.; Mail add: 716½ Montague St., Niagara Falls, N. Y. (Corrosion)

Student Associate Members

Kamala S. Krishnan, A-17, Indian Institute of Science, Hostel, Bangalore 3, India (Electrodeposition, Electronics, Electrothermics & Metallurgy, Industrial Electrolytic, Theoretical Electrochemistry)

By action of the Board of Directors of the Society, all prospective members must include first year's dues with their applications for membership.

Also, please note that, if sponsors sign the application form itself, processing can be expedited considerably.

Janakiram Sundararajan, Indian Institute of Science, Dept. of General Chemistry, Bangalore 3, India (Corrosion, Electrodeposition, Electronics, Electro-Organic, Theoretical Electrochemistry)

Reinstatements to Active Membership

Klaus K. Berju, Electric Storage Battery Co.; Mail add: 5823 Oxford Ave., Philadelphia 49, Pa. (Battery)

Philip B. Cole, U. S. Naval Ordnance Lab.; Mail add: 12808 Baker Dr., Silver Spring, Md. (Battery)

George B. Diamond, Electro Organic Corp.; Mail add: R. D., Glen Gardner, N. J. (Electro-Organic)

Abraham M. Max, RCA Victor Record Div., Radio Corp. of America; Mail add: 5640 Guilford Ave., Indianapolis 20, Ind. (Electrodeposition, Theoretical Electrochemistry)

Transfers from Student Associate to Active Membership

Irving Galperin, Ind. Rayon Corp.; Mail add: 2026 E. 107 St., Cleveland 6, Ohio (Theoretical Electrochemistry)

Wayne J. Subcasky, Chrysler Corp., Engineering Div.; Mail add: 70 Highland Ave., Highland Park 3, Mich. (Battery, Theoretical Electrochemistry)

Deceased Members

Loren C. Hurd, Basking Ridge, N. J.
Junius D. Edwards, Delray Beach, Fla.

Personals

Gerald L. Moran has been appointed general manager of the Chemical and Metallurgical Div. of Sylvania Electric Products Inc., Towanda, Pa. Mr. Moran had been division chief engineer since 1954.

M. J. Pryor, formerly head of the Basic Physics and Physical Chemistry Branch, Kaiser Aluminum and Chemical Corp., has joined Olin Mathieson Chemical Corp. in New Haven, Conn., as chief of the chemical and physical section, Aluminum Dept., Metallurgical Research Div.

Milton Genser is now technical manager, Electronics Chemicals Div., Merck & Co., Rahway, N. J. He had been with IBM in Poughkeepsie, N. Y.

Alfred D. Gate, formerly technical director at Globe Metallurgical Corp., Beverly, Ohio, recently took a position as technical director with the Beverly Interlake Iron Corp.

Robert E. Shearer has joined the staff of the Research Div. of MSA Research Corp., a subsidiary of Mine Safety Appliances Co., Callery, Pa. Previously he was associated with the Research Dept. of the Union Switch & Signal Div. of Westinghouse Airbrake, Pittsburgh, Pa.

Wendell P. Barrows has had a change in position from chemical engineer, U. S. Naval Gun Factory, to secretary, International Chemical & Metallurgical Supply Corp., Ft. Lauderdale, Fla.

Dodd S. Carr has been appointed director of research for Bart Labs. & Design, Inc., Belleville, N. J. In 1952 he was appointed assistant director of electrochemical research for the Bart Manufacturing Corp. in the fields of electroforming, hard nickel plating on propeller blades, and nickel plating of steel pipes, fittings, and plate. He will continue his work in these fields and report to S. G. Bart, president of the firm.

Horace E. Haring

Horace E. Haring, electrochemical specialist at Bell Telephone Labs., Murray Hill, N. J., died on November 12, 1957 after a short illness. He was 62 years old.

Since 1929 Mr. Haring had been associated with Bell Labs. where he was in charge of research and development in the field of electrochemistry. His work included storage and primary batteries, corrosion, electroplating, electrolytic rectifiers and capacitors, and other devices and processes which function electrochemically.

He made many significant contributions in the electrochemical field and was granted a number of patents for his inventions. Among his outstanding achievements were the lead-calcium alloy storage battery now widely used in the Bell Telephone System; the "sea-water" battery which he developed during World War II for the U. S. Navy; and the bright chromium plating process developed in 1924.

He also invented the Haring cell, and recently was associated with the development of a tantalum solid electrolytic capacitor which has wide applications in communication and military systems.

He was the author of many scientific articles published in professional journals.

In 1946 he received the Naval Ordnance Development Award with Certificate for Exceptional Service in recognition of his "outstanding performance in connection with the

research and development of seawater batteries."

Mr. Haring was born in Delanco, N. J., on August 30, 1895. He received his B. S. degree in 1916 from Franklin and Marshall College, Lancaster, Pa., and his A. M. degree in 1917 from Princeton. After serving as a chemist with the Army Ordnance department during World War I, he joined the National Bureau of Standards in 1919. He joined the technical staff of Bell Labs. in April 1929.

Mr. Haring was a member and a past Vice-President of The Electrochemical Society, and a member of the American Chemical Society.

He is survived by his wife, Edith Miller Haring, and a son, Eugene Miller Haring.

Richard O. Hull

Richard O. Hull, founder and President of R. O. Hull & Co., Inc., died on November 29, 1957 at the age of 52.

One of the world's authorities on electroplating, Mr. Hull has more than 30 patents to his credit pertaining to the plating and testing of tin, copper, zinc, cadmium, and other metals. His invention of the Hull Cell gained him world-wide recognition through its use as the standard control and evaluation method for plating baths.

Mr. Hull was born in Troy, N. Y. He studied at the University of Colorado and graduated with special honors. While doing graduate work at George Washington University in Washington, D. C., he worked for the Bureau of Standards under Dr. William Blum. He became an authority on the deposition of copper while with RCA Victor in Camden, N. J. Mr. Hull joined E. I. duPont Co. in 1933 and became assistant research director of the Electrochemical Dept. before leaving to found his own firm in 1944.

In the past, Mr. Hull supported a number of philanthropic activities including the Engineering Development Fund for aid to students in the field of Chemical Engineering or for Chemical Research at the University of Colorado.

He was active in the Cleveland Section of The Electrochemical Society and was well known by many members throughout the nation. He was also a member of the American Electroplaters Society, British Institute of Metal Finishing, American Chemical Society, American Institute of Chemical Engineers, Alpha Chi Sigma, and Tau Beta Pi.

Mr. Hull is survived by his wife, the former Ann Gregorie Fitz-Simons; two sons, Richard, Jr., and

Harry F.; a daughter, Mrs. Robert C. Platt; six grandchildren; his mother, Mrs. M. M. Hull; a sister, Mrs. D. H. Faires; and a brother, William L. Hull.

News Items

New Patron Member

Olin Mathieson Chemical Corp., Industrial Chemicals Div., Research and Development Dept., Niagara Falls, N. Y., recently became a Patron Member of The Electrochemical Society.

New Sustaining Members

The following recently became Sustaining Members of The Electrochemical Society: International Business Machines Corp., Research Center, Poughkeepsie, N. Y.; Motorola, Inc., Chicago, Ill.; and Superior Tube Co., Norristown, Pa.

1957 Annual Index

The Annual Index for Vol. 104 (1957) of the JOURNAL appears in this issue, pp. i-ix. Reprints of the Index can be obtained about the middle of March by writing to The Electrochemical Society, 1860 Broadway, New York 23, N. Y.

Nominations for 1958 Acheson Award

Charles L. Faust, Chairman of the Acheson Medal Award Committee, would like to receive suggestions for possible candidates for the next Acheson Medal Award, to be made in the fall of 1958.

The procedure to be followed by the membership, taken from the Rules Governing the Award of the Acheson Medal, is given below.

1. Nominations shall be accepted from the membership at large.
 2. All nominations, whether made by a member of the Nominating Committee or by any other member of the Society, must be accompanied by a full record of qualifications of the nominee for the award. Such supporting documents from friends of the candidate or from his organization shall be in order.
 3. The nominator must assume the responsibility for providing the Chairman of the Nominating Committee with nine copies of the supporting documents, one for each member.
- Nominations must be sent to the Chairman not later than March 1 of the year in which the medal is awarded and nominations will be considered closed after that date.

All nominations of candidates for the medal shall be continued in force

for a period of two consecutive awards of the medal. Any unsuccessful candidate may be renominated in the usual manner for any subsequent Medal award.

Correspondence should be addressed to Charles L. Faust, Battelle Memorial Institute, 505 King Ave., Columbus 1, Ohio.

Westinghouse and Gibbs Enshrined in Hall of Fame

On December 1, 1957 more than 1000 persons witnessed the unveiling of bronze busts of George Westinghouse and Josiah Willard Gibbs for the Hall of Fame for Great Americans at New York University, New York City.

Principal speakers were former President Herbert C. Hoover and Dr. Detlev W. Bronk, president of the National Academy of Sciences.

Westinghouse, inventor of the air brake and many electrical devices, and Gibbs, Yale University mathematical physicist who formulated the theory of thermodynamics, are the 84th and 85th distinguished historical figures to be placed in the Hall of Fame. Westinghouse was elected to the shrine in 1955 and Gibbs in 1950.

The Westinghouse bronze, which was donated by the American Society of Mechanical Engineers, is the work of sculptor Edmondo Quattrocchi. The Gibbs bust, a gift of the American Chemical Society, Yale, and several individual donors, was done by Stanley Martineau; a plaque under the bust bears this quotation from Gibbs' writings: "One of the principal objects of theoretical research is to find the point of view from which the subject appears in its greatest simplicity."

George Westinghouse was born in Central Bridge, N. Y., on October 6, 1846, and died in New York City on March 12, 1914. He served as a volunteer in the Union Army during the Civil War and later as an engineer in the Navy.

George Westinghouse was a prolific inventor. When he died there were more than 400 patents to his credit. The manufacturing company he formed at Pittsburgh to produce air brakes and electrical equipment is known today as the Westinghouse Electric Corp.

Josiah Willard Gibbs was born in New Haven, Conn., on February 11, 1839, and died there, April 28, 1903. He was a student at Yale College at 15, where he received his baccalaureate degree in 1858 and his doctorate in 1863. He taught Latin and science for two years at Yale, and then, from 1866 to 1869, he studied in Europe. In 1871 he was appointed professor of mathematical physics at Yale College, where he remained until his death.

Gibbs is remembered primarily for his theory of thermodynamics, which formed the basis for much of modern physical chemistry and chemical engineering.

His principal works in science include "On the Equilibrium of Heterogeneous Substances," "Electrochemical Thermodynamics," "Notes on the Electromagnetic Theory of Light," and "Elementary Principles in Statistical Mechanics."

Gibbs was essentially a student, and a short time before he died he said that were he to live to be as old as Methuselah he would continue to study. He received honorary degrees from universities in the United States and Europe.

Divisions of Union Carbide Among Organizations Receiving 1957 Chemical Engineering Award

For the company's success in pioneering the sodium reduction process for the production of titanium metal sponge, the 1957 Chemical Engineering Achievement Award was presented to Electro Metallurgical Co., Div. of Union Carbide Corp., in New York City on Tuesday, December 3, 1957. The award by *Chemical Engineering*, a McGraw-Hill publication, was given to a group of organizations in recognition of the pioneering application of chemical engineering principles and processes in extractive metallurgy. Union Carbide Nuclear Co. and Oak Ridge National Labs., operated by Union Carbide for the U. S. Atomic Energy Commission, are also among the organizations which received the award. This is the fifth time that divisions of Union Carbide have received the Chemical Engineering Award.

The award for chemical engineering contributions to the extractive

Notice to Members

According to the Constitution of the Society, Article III, Section 9, "Any member delinquent in dues after April 1 of each year shall no longer receive the Society's publications . . ." Such delinquents will not receive the May issue of the JOURNAL. A reminder notice will be mailed to delinquents about the middle of February and a final notice about the middle of March.

metallurgy of atomic age metals was officially presented at a banquet held at the Waldorf-Astoria.

Although *Chemical Engineering* sponsors the award, the award committee consisted of the heads of chemical engineering in all of the educational institutions of the United States, whose courses have been accredited by the American Institute of Chemical Engineers and the Engineers' Council for Professional Development.

E. R. Weidlein Named a Chairman in A.C.S. Building Fund Campaign

Dr. Edward R. Weidlein of Pittsburgh, former president and chairman of the board of trustees of the Mellon Institute, has been named chairman for special and corporate gifts of the American Chemical Society's \$3,000,000 building fund campaign. Dr. Weidlein's duties will be to organize the solicitation of gifts from corporations, foundations and individual friends of the society, according to Professor C. S. Marvel of the University of Illinois, national chairman of the drive.

The fund is to be used for the construction of a new eight-story headquarters on the site of the society's present building at 1155 Sixteenth St., N. W., Washington, D. C.

Gulton Industries Establishes Alkaline Battery Division; Gets U. S. License to Produce, Market SAFT-France Line

Establishment of an Alkaline Battery Div. for the production and marketing of nickel cadmium and nickel iron batteries and associated charging equipment was recently announced by Dr. Leslie K. Gulton, President, Gulton Industries, Inc.

Simultaneously, the company announced that it has been licensed to produce and market alkaline batteries in the United States, under

patent rights held by SAFT-France.

The license includes all production, sales, and distribution rights of SAFT's domestic operations which will be completely integrated into the present marketing structure of Gulton Industries. Gulton immediately will take over the management and operation of the Lodi, N. J., plant, formerly operated by the SAFT Corp. of America.

United Announces New High Purity Aluminum

The United Mineral & Chemical Corp., 16 Hudson St., New York 13, N. Y., recently reported the introduction and availability in the U. S. and Canada of a new aluminum with the very high purity 99.999% minimum. This material was developed and is being produced by the Aluminum-Industrie A. G. of Switzerland.

Properties claimed for the new metal include increased ductility, better light reflecting power, improved electrical conductivity, and higher chemical stability. When anodized, optically purer oxide films result.

Main applications are currently in the fields of semiconductors, catalysis, and chemical analysis.

American Potash & Chemical Corp. to Investigate Manganese Ore Deposits at Batesville, Ark.

American Potash & Chemical Corp. has completed arrangements to conduct exploratory investigations of manganese ore deposits at Batesville, Ark.

The deposits are located in 10,-700 acres of land near Batesville, approximately 100 miles northeast of Little Rock. Mineral rights to the deposits are held by four Arkansas companies, U. S. Manganese Corp., Arkansas Mining and Exploration Co., Miller-Lipp Corp., and Miller-McGee Manganese Corp.

If results of the studies are favorable, present plans include formation of a new company to undertake commercial production, with American Potash holding 55% of the stock.

The Batesville properties have been operated independently by the four Arkansas companies for some years on a small scale for the production of limited quantities of manganese ore.

Manganese dioxide is one of the diversified chemicals produced by the American Potash & Chemical Corp. at its Henderson, Nev., plant by electrolytic methods.

Dow Chemical International Ltd. Opens Sales Office in Hong Kong

A new foreign sales office in Hong Kong has been opened by Dow Chemical International Ltd., an export subsidiary of The Dow Chemical Co.

Eric C. Huggins, who has been appointed manager of the new office, recently served as Far Eastern plastics sales manager with the company's Tokyo, Japan, sales office.

At the same time the export company announced the appointment of Howard C. Visger as manager of the Tokyo office. He succeeds the late H. Lee Clack.

In addition to the two Far Eastern offices, Dow maintains a resident sales supervisor in Sydney, Australia.

Federal Tax Deductions Incurred in Society Activities

Engineers Joint Council has advised us of the following.

The Internal Revenue Service under ruling 55-4, I. R. B. 1955-1 states that a taxpayer "who gives his services gratuitously to an association, contributions to which are deductible" under the relevant provisions of the Code "and who incurs

Manuscripts and Abstracts for Fall 1958 Meeting

Papers are now being solicited for the Fall Meeting of the Society, to be held at the Chateau Laurier in Ottawa, Canada, September 28, 29, 30, October 1, and 2, 1958. Technical sessions probably will be scheduled on Batteries, Corrosion, Electrodeposition (including symposia on "Electrodeposition on Uncommon Metals" and "Chemical and Electropolishing"), Electronics (Semiconductors), Electro-Organics, and Electrothermics and Metallurgy.

To be considered for this meeting, triplicate copies of abstracts (*not to exceed 75 words in length*) must be received at Society Headquarters, 1860 Broadway, New York 23, N. Y., *not later than June 2, 1958. Please indicate on abstract for which Division's symposium the paper is to be scheduled.* Complete manuscripts should be sent in triplicate to the Managing Editor of the JOURNAL at the same address.

* * *

The Spring 1959 Meeting will be held in Philadelphia, Pa., May 3, 4, 5, 6, and 7, 1959, at the Sheraton Hotel. Sessions will be announced in a later issue.

unreimbursed traveling expenses, including the cost of meals and lodging, while away from home in connection with the affairs of the association and at its direction may deduct the amount of such unreimbursed expenses in computing his net income;" subject, however, to the limitation in respect to all gifts made to exempt organizations of our type; namely, that the total amount of such gifts made in any one year may not exceed 20% of the donor's gross income for such year. This limitation means that while such expenses are deductible they are included with other gifts in computing the 20% limitation.

Corrosion Engineers Needed in Larger Industry, A.I.Ch.E. is Told

The need for a corrosion engineer in industrial plants large enough to warrant one was emphasized during a symposium on the subject at the Annual Meeting of the American Institute of Chemical Engineers held in Chicago during December. Four papers comprehensively reviewed the problem and suggested numerous steps to prevent or reduce damage caused by various types of corrosion.

John Halbig, Research Labs., Armco Steel Corp., Middletown, Ohio, told the symposium that "... every plant of large enough size should have at least one engineer keep in touch with developments in the corrosion field. An important part of the plant engineering staff's duties should be to keep abreast of published data and current investigation work. This can be accomplished through technical society publications, committee activities and symposia, and through participation in interplant symposia, local corrosion control activities, supplier sponsored technical meetings, and university short courses.

"There will be times when the plant corrosion engineer will not have all the information he needs in order to cope with a problem. He should realize that many suppliers of materials of construction have research organizations and/or large technical staffs. This should be his first approach for assistance."

In a general review of the corrosion problem, M. G. Fontana, Ohio State University, in a paper titled "Corrosion and Its Manifestations," pointed out that "Too many design engineers seem to take great delight in making parts of as many different metals and alloys as possible. This results in many costly failures that could have been easily avoided." He said that in the design of structures, "equipment life can be pro-

longed or corrosion costs can be reduced through the use of bottom outlets designed to drain completely, readily replaceable or interchangeable parts, standard lengths of tubing, increased thickness in more vulnerable areas, designing to prevent crevices or stagnant areas, and the use of butt-welded instead of riveted joints."

In a paper, "Copper Alloys for Corrosion Resistance," R. V. L. Hall, Bridgeport Brass Co., Bridgeport, Conn., said that copper alloys are being used increasingly to protect other alloys from corrosive conditions, the performance of which alloys is unpredictable, while the performance of copper alloys is predictable.

"As we learn more about the exact conditions in which the various alloys and metals give the best performance," he said, "it should be possible to select combinations of duplex or clad metals which will be economical from the standpoint of long and trouble-free service life. The copper alloys will certainly have their place in this picture because of their generally good corrosive resistance to a wide range of corrosive chemicals, particularly under non-oxidizing conditions."

In a paper, "Stainless Steels for Corrosion Resistance," L. R. Honnaker, DuPont, Wilmington, Del., observed that "the general resistance of stainless steels is only part of the consideration that should be given to the selection and use of stainless steels for chemical process equipment. It is important to consider the possibility of other factors causing unexpected difficulties. Design features that will insure free drainage, ease of cleaning, and elimination of crevices will help to avoid pitting and crevice corrosion. Where acidic conditions are to be handled above ambient temperatures, consideration should be given to the necessity and means of avoiding intergranular corrosion. Finally the non-process or external environments should be considered, particularly with respect to failures by stress-corrosion cracking."

Mr. Honnaker pointed out that stainless steels are widely used for process equipment in the chemical industry and in the past 25 years considerable data have been compiled, and, as a result of this knowledge, failures due to general corrosion (of stainless steel) are now relatively infrequent.

He said that development of fundamental information on the nature of passivity and corrosion resistance is continuing and "there is good rea-

son to believe that stainless alloys of slightly modified compositions having improved corrosion resistance will be available soon."

Books for Asian Students

The Asia Foundation, a nonprofit, nonpolitical organization founded by private American citizens, supports individuals and groups in Asia who are working for the attainment of peace, independence, personal liberty, and social progress. The Foundation maintains 18 offices in Asia which encourage and strengthen these individuals and groups in their work.

In the past two and one-half years, the Foundation's special project, Books For Asian Students, has sent 600,000 selected books to more than 1200 universities, colleges, libraries, and civic groups in Asia. These books were donated by 700 university and college groups, publishers, libraries, and individuals in the United States. The great need for books continues as evidenced by increasing requests.

Your contributions of books will be greatly appreciated. Items in every category on the university and college level, in good condition, published in 1948 or after, and works by standard authors regardless of date, can be sent directly to the following address: Books for Asian Students, 21 Drumm St., San Francisco 11, Calif.

Transportation costs from the donor to San Francisco and thence to Asia will be borne by the Foundation for substantial shipments. Further information for such contributions may be had by writing to the address given above. All contributions are tax exempt.

Book Reviews

Heat and Thermodynamics, by Mark W. Zemansky. Fourth Edition, published by McGraw-Hill Book Co., Inc., New York, 1957. 484 pages, \$7.50.

As do its preceding editions, this revised book by Zemansky provides an excellent text for introductory courses in thermodynamics for students in physics and in engineering. Portions of it would serve equally well for beginning students in chemical thermodynamics, and all of it provides a source book for more advanced chemists looking for a clear exposition of the more physical topics of thermodynamics. The book

starts in the traditional manner with a discussion of temperature (introducing the new Giauque scale), internal energy, and heat. A very extensive discussion of entropy in its many facets then follows. The author has even included brief discussions of entropy and information theory, the basic concepts of entropy flow and the Onsager reciprocal relations in irreversible thermodynamics, and the principle of Caratheodory, as well as classical topics such as the Carnot cycle. The remaining chapters deal with applications to various fields in physics, engineering, and chemistry. To chemists the chapter on low-temperature physics will be particularly useful. This chapter includes an excellent discussion of the background of the third law of thermodynamics, although it does not describe applications to actual chemical problems.

Likewise, while the thermodynamic basis of electrochemistry is clearly delineated, applications to standard chemical problems are not introduced. In short, the theoretical background of chemical thermodynamics is very well expounded but the problems which an electrochemist is most likely to encounter are not examined. This statement should not be construed as a criticism, however. A book of finite length can treat only a finite number of topics. The author, being a physicist, has chosen those topics most nearly allied to physics. For physicists and engineers an excellent text is available; for electrochemists and physical chemists in general, Zemansky's book will continue to serve as a prime reference for the elucidation of the fundamental concepts of thermodynamics.

I. M. Klotz

Corrosion and Wear Handbook for Water Cooled Reactors. Edited by D. J. DePaul. Published by McGraw-Hill Book Co., Inc., New York, 1957. 293 pages, \$6.00.

Although the circulation of water in heated systems is an ancient technique, in nuclear reactors it involves a whole new technology because of the high purity required and the radioactivity induced in corrosion products. Thousands of man-years have been spent in establishing the conditions necessary for successful operation of water-cooled reactors in the vicinity of 500°F. The results of this work are summarized in this handbook, which will naturally become a bible for all designers in this specialized reactor field, in addition

to being of intense interest to all students of corrosion.

The handbook is the sixth in the series on nuclear reactor technology sponsored by the Naval Reactors Branch of the U. S. Atomic Energy Commission, as an outgrowth of the research and development preliminary to the construction of pressurized water reactors for use in naval propulsion systems. The performance of the submarine *Nautilus* attests to the thoroughness of the work reported in the book.

The book begins with a general discussion of ferrous corrosion and the fundamental aspects of friction and wear, then provides detailed descriptions of the approach to corrosion and wear problems and of the equipment used in experimentation. There is a comprehensive tabulation of the basic data obtained for a variety of materials. The second part of the text is devoted to special problems of crevice corrosion, stress corrosion control of corrosion products, and an interpretation of wear performance. The final chapter discusses the manufacturing procedures that are likely to affect corrosion and wear.

In his preface, Admiral Rickover complains that the basic understanding of water technology is still weak. However, there can be no doubt that this book represents a giant stride forward in the engineering application of water as a heat transfer medium.

Morris Kolodney

Announcements from Publishers

"A Basic Laboratory Course in College Chemistry," by J. F. Hazel. Published by John Wiley & Sons, Inc., New York, 1957. 233 pages, \$3.95.

"Systematic Organic Chemistry," by H. C. Muldoon and M. I. Blake. Published by McGraw-Hill Book Co., Inc., New York, 1957. 828 pages, \$7.75.

"Sixth Symposium (International) on Combustion," August 19-24, 1956, Combustion Institute, Yale University, New Haven, Conn. Published by Reinhold Publishing Corp., New York, 1957. 1053 pages, \$28.00.

"Chemical Engineering in the Coal Industry," by W. Forbes-Sharpely.

Published by Pergamon Press Inc., New York, 1956. 141 pages, \$8.50.

"Magnetohydrodynamics." Edited by Dr. Rolf K. M. Landshoff, consulting scientist of the Lockheed Missile Systems division. Published by Stanford University Press, Stanford, Calif., 1957. 115 pages, \$4.00.

The recent outstanding research work of 11 top U. S. and British physicists and astronomers in the new field of magnetohydrodynamics, combining the sciences of fluid flow and electromagnetics, has been compiled in this volume. The book grew out of the talks and discussions at a year-end Lockheed-sponsored symposium attended by 200 leading scientists at the company's missile division laboratories in Palo Alto, Calif.

Magnetohydrodynamics, a new branch of physical science, is a study of how magnetic fields influence and are influenced by ionized gases which are brought about at extremely high temperatures.

Detailed in the book are Some Dimensional Aspects of Hydromagnetic Phenomena, the Build-Up of Large Magnetic Fields Inside Stars, Penetration of a Shock Wave into a Magnetic Field, Dynamics of a Pinched Gas, Scaling Laws as an Aid to Experimental Studies, Experiments on Magnetically Driven Shock Waves (conducted at the U. S. Naval Research Lab., Lockheed Missile Systems division, and AVCO), Shock Waves Passing Through a Magnetic Field Region, Liquid Sodium Instability Experiment, and the Hydro-magnetic Wave Guide.

"Forming of Titanium and Titanium Alloys: Part 1," Titanium Metallurgical Lab., Battelle Memorial Institute, Dept. of Defense, May 1957. Report PB 121917, 247 pages, \$6.25. Order from OTS, U.S. Dept. of Commerce, Washington 25, D. C.

Thirteen major methods of forming titanium sheet were evolved from a survey of the airframe industry to determine the state of the forming art. These are discussed in detail in three sections. One contains accounts of presses preparatory to forming, of equipment and methods commonly used in forming, of heating and stress-relieving treatments for forming, and various formability tests that have been used. Another section contains more detailed descriptions of specific practices for titanium-sheet materials. The final section discusses a number

of forming problems suggested by industry engineers.

"Advanced Materials Technology"

"Advanced Materials Technology," a new publication by The Carborundum Co., features technical information on materials to meet severe or unusual conditions in processing or operation, such as extreme heat, abrasive action, corrosion, or other problems beyond the capabilities of conventional materials.

The first issue gives data on a new self-bonded KT Silicon Carbide which provides "high strength" and other outstanding properties up to 4000°F. "Thermal Shock Problems" are treated; a new improved heating element is discussed and some of the new uses of zirconium are explained. Another feature is a question and answer treatment on ceramic to metal bonds.

General Leslie E. Simon, Vice-President of the company and Director of the Research & Development Div., launches the new publication with an editorial entitled "Looking Ahead in Materials Progress." He says: "The publication of 'Advanced Materials Technology' is an expression of Carborundum's desire to share its knowledge and to participate with all who face the challenge of finding new ways and new materials to meet the increasingly severe and complex demands of today's products and processes."

"Advanced Materials Technology," published by the Research & Development Div. at Niagara Falls, N. Y., is the third of Carborundum's new technical publications. The others are "More Zr Facts" by the Carborundum Metals Co., Akron, N. Y.; and "Carborundum's Refractories" by the Refractories Div., Perth Amboy, N. J.

All of the publications are available upon request to the respective divisions.

AEC Reports on Chemical Research and Reactor Research Available from OTS

The following Atomic Energy Commission reports were released recently for sale to the public through the Office of Technical Services, U. S. Dept. of Commerce, Washington 25, D. C.

"Electrokinetic processes—Nuclear aspects, Quarterly progress report for November 1, 1955-January 31, 1956" (portions deleted), Feb. 1956, 13 pages, 50 cents. (Order KXLX-10021 from OTS.)

"Corrosion of an aluminum-nickel alloy in a reactor test loop," Sept.

1957, 18 pages, 75 cents. (Order ANL-5783 from OTS.)

"Boron-aluminum and boron-uranium-aluminum alloys for reactor application," n.d., 23 pages, \$1.00. (Order ORNL-2149 from OTS.)

"Tantalum annealing and degassing and hardness effects of dissolved gases," May 1957, 39 pages, \$1.25. (Order LA-2136 from OTS.)

"Anodic overpotential for oxide-free zirconium," May 1957, 12 pages, 15 cents. (Order AECU-3467 from OTS.)

"A kinetic study of the fluoride catalyzed nitric acid dissolution of thorium metal," Nov. 1955, 35 pages, 35 cents. (Order HW-40250 from OTS.)

"Kinetics of the reaction between calcium and water vapor," March 1956, 67 pages, 40 cents. (Order ISC-777 from OTS.)

"Caustic fusion of columbite-tantalite concentrates with subsequent separation of niobium and tantalum," Aug. 1956, 29 pages, 25 cents. (Order ISC-796 from OTS.)

"Kinetics of the reaction between magnesium and water vapor," June 1956, 38 pages, \$1.25. (Order ISC-779 from OTS.)

"Mechanism of the diffusion of hydrogen through active and inactive palladium," Nov. 1956, 56 pages, \$1.50. (Order KAPL-1674 from OTS.)

Radiochemical Analysis Handbook Available

A handbook containing information necessary for precise radiochemical analysis of fission and nonfission product activities has been made available for industry use through the Office of Technical Services, U. S. Dept. of Commerce, Washington 25, D. C.

The handbook was prepared under Government contract by Tracerlab, Inc., with the cooperation of the Los Alamos Scientific Lab. Chemistry Group. It appears in two volumes under the general title "Handbook of Radiochemical Analysis." They are:

"Vol. 1: Radiochemical Techniques," May 1953, 152 pages, \$4.00. (Order PB 121690 from OTS.) A prerequisite for the use of the second volume, particularly for those unfamiliar with radiochemical analysis, this book contains information and instructional material for the procedures. Tables, drawings of equipment, and various curves useful in treatment of counting data and identification of functions influencing counting rate determinations are also included.

Advertiser's Index

E. I. du Pont de Nemours & Co. (Inc.)	18C
Enthone, Incorporated	Cover 4
Great Lakes Carbon Corporation	Cover 2
E. H. Sargent & Company	16C

"Vol. 2: Radiochemical Procedures," March 1952, 129 pages, \$3.25. (Order PB 121689 from OTS.) This volume clarifies the chemistry and standardizes the techniques used in analyzing fission product and nonfission product isotopes. Three main chemical tasks are involved: dissolution of the sample with steps to provide for the exchange between active isotopes and added carrier elements; separation of individual activities from the solution; and decontamination and determination of the desired activities. Samples considered are of antimony, barium, cadmium, cerium, cesium, europium, lead, molybdenum, neptunium, plutonium, ruthenium, silver, strontium, tin, uranium, and zirconium.

Employment Situations

Please address replies to box shown, c/o The Electrochemical Society, Inc., 1860 Broadway, New York 23, N. Y.

Position Wanted

Chemist, inorganic, 11 years' experience: Electroplating (copper-acid, alkali; tin-acid, alkali; nickel; chromium), batteries, gelatines, glues, pyrotechny, general physical and chemical commercial testing, seeks position in New Jersey and environs; has held supervisory positions, experienced in analysis, capable of producing new ideas, anxious to forge ahead. *Reply to Box 363.*

Positions Available

Associate Technical Director required for research in secondary battery industry. Background in administration desirable with particular emphasis upon electrochemical research. Physical chemistry valuable. Expanding laboratory offers growth opportunity. *Reply to Box A-274.*

Technical Personnel for research group. Electrochemical and/or physical chemistry background. Project leader level. For expanding research activity in all types of secondary batteries. *Reply to Box A-275.*



The Electrochemical Society

INSTRUCTIONS TO AUTHORS OF PAPERS

Address all correspondence to the Editor,
JOURNAL OF THE ELECTROCHEMICAL SOCIETY,
1860 BROADWAY, NEW YORK 23, N. Y.

FORM

Manuscripts submitted for publication should be in triplicate to expedite review. They should be typewritten, double-spaced, with 2½-4 cm (1-1½ in.) margins.

Title should be brief, followed by the author's name and his business or university connection.

Abstract of about 100 words should state the scope of the paper and give a brief summary of results.

ILLUSTRATIONS

Drawings will be reduced to column width, 8.3 cm (3¼ in.), after reduction should have lettering at least 0.15 cm (1/16 in.) high. Original drawings in India ink on tracing cloth or white paper are preferred. Curves may be drawn on coordinate paper only if the paper is ruled in blue. All lettering must be of lettering-guide quality. See sample drawing on reverse page.

Photographs must be glossy prints and mounted flat.

Captions for all figures must be included on a separate sheet. Captions and figure numbers should not appear in the body of the figure.

General—Figures should be used only when necessary. Omit drawings or photographs of familiar equipment. Figures from other publications are to be used only when the publication is not readily available, and should always be accompanied with written permission for reprinting.

REFERENCES

Literature and patent references should be listed at the end of the paper on a separate sheet, in the order in which they are cited. They should be given in the style adopted by *Chemical Abstracts*. For example:

R. Freas, *Trans. Electrochem. Soc.*, **40**, 109 (1921).

H. T. S. Britton, "Hydrogen Ions," Vol. 1, p. 309, D. Van Nostrand Co., New York (1943).

H. F. Weiss (To Wood Conversion Co.), U. S. Pat. 1,695,445, Dec. 18, 1928.

UNITS OF MEASUREMENT

Metric units should be used throughout but, where desirable, English units may be given in parentheses.

Corrosion rates in the metric system should preferably be expressed as milligrams per square decimeter per day (mdd), and in the English system as inches penetration per year (ipy).

As regards algebraic signs of potentials, the standard electrode potential for $\text{Zn} \rightarrow \text{Zn}^{++} + 2e$ is negative; for $\text{Cu} \rightarrow \text{Cu}^{++} + 2e$, positive.

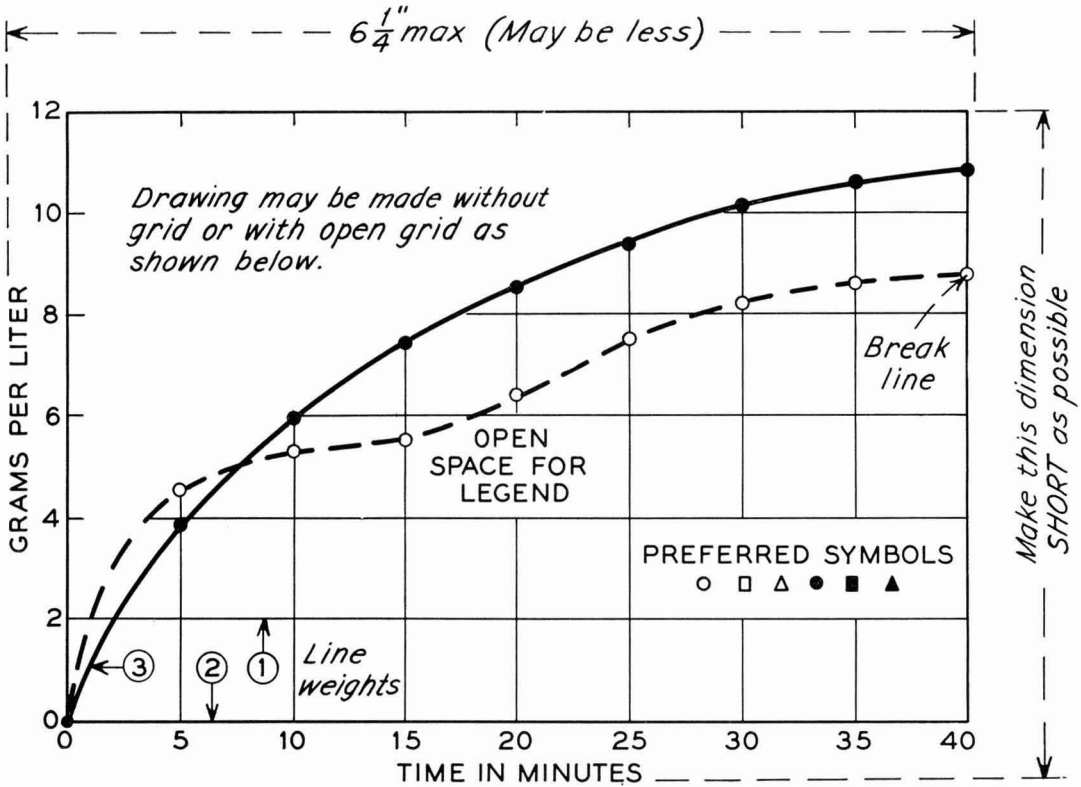
ABBREVIATIONS

Abbreviations should conform with the American Standards Association's list of "Abbreviations for Scientific and Engineering Terms."

GENERAL

Authors should be as brief as is consistent with clarity, and must omit all material which can be regarded as familiar to specialists in the particular field.

The use of proprietary names, trade-marks, and trade names should be avoided if possible. If used, these should be capitalized so that the owner's legal rights are not jeopardized.



Remarks: Line weight ② is used for borders and zero lines. When several curves are shown, each may be numbered and described in the caption. Lettering is approx. $\frac{1}{8}"$.

SAMPLE CURVE DRAWING FOR REDUCTION TO $\frac{1}{2}$ SIZE

The Electrochemical Society

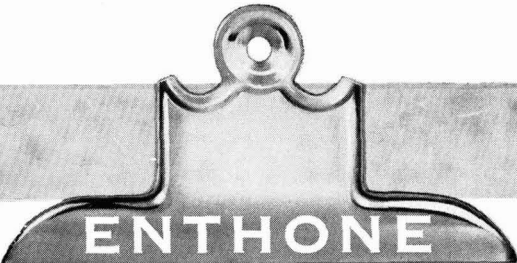
Patron Members

Aluminum Co. of Canada, Ltd., Montreal, Que., Canada
International Nickel Co., Inc., New York, N. Y.
Olin Mathieson Chemical Corp., Niagara Falls, N. Y.
Industrial Chemicals Div., Research and
Development Dept.
Union Carbide Corp., Divisions:
Electro Metallurgical Co., New York, N. Y.
National Carbon Co., New York, N. Y.
Westinghouse Electric Corp., Pittsburgh, Pa.

Sustaining Members

Air Reduction Co., Inc., New York, N. Y.
Ajax Electro Metallurgical Corp., Philadelphia, Pa.
Allied Chemical & Dye Corp.
General Chemical Div., Morristown, N. J.
Solvay Process Div., Syracuse, N. Y. (3 memberships)
Alloy Steel Products Co., Inc., Linden, N. J.
Aluminum Co. of America, New Kensington, Pa.
American Machine & Foundry Co., Raleigh, N. C.
American Metal Co., Ltd., New York, N. Y.
American Platinum Works, Newark, N. J. (2 memberships)
American Potash & Chemical Corp., Los Angeles, Calif.
(2 memberships)
American Zinc Co. of Illinois, East St. Louis, Ill.
American Zinc, Lead & Smelting Co., St. Louis, Mo.
American Zinc Oxide Co., Columbus, Ohio
Auto City Plating Co. Foundation, Detroit, Mich.
Bart Manufacturing Co., Bellville, N. J.
Basic Incorporated, Cleveland, Ohio
Bell Telephone Laboratories, Inc., New York, N. Y. (2 memberships)
Bethlehem Steel Co., Bethlehem, Pa. (2 memberships)
Boeing Airplane Co., Seattle, Wash.
Burgess Battery Co., Freeport, Ill. (4 memberships)
C & D Batteries, Inc., Conshohocken, Pa.
Canadian Industries Ltd., Montreal, Que., Canada
Carborundum Co., Niagara Falls, N. Y.
Chrysler Corp., Detroit, Mich.
Columbia-Southern Chemical Corp., Pittsburgh, Pa.
Consolidated Mining & Smelting Co. of Canada, Ltd.,
Trail, B. C., Canada (2 memberships)
Corning Glass Works, Corning, N. Y.
Cramet, Inc., Chattanooga, Tenn.
Crane Co., Chicago, Ill.
Diamond Alkali Co., Painesville, Ohio (2 memberships)
Dow Chemical Co., Midland, Mich.
Wilbur B. Driver Co., Newark, N. J. (2 memberships)
E. I. du Pont de Nemours & Co., Inc., Wilmington, Del.
Eagle-Picher Co., Chemical Div., Joplin, Mo.
Eaton Manufacturing Co., Stamping Div., Cleveland, Ohio
Electric Auto-Lite Co., Toledo, Ohio
Electric Storage Battery Co., Philadelphia, Pa.
The Eppley Laboratory, Inc., Newport, R. I. (2 memberships)
Federal Telecommunication Labs., Nutley, N. J.
Food Machinery & Chemical Corp.
Becco Chemical Div., Buffalo, N. Y.
Westvaco Chlor-Alkali Div., South Charleston, W. Va.
Ford Motor Co., Dearborn, Mich.
General Electric Co., Schenectady, N. Y.
Chemistry & Chemical Engineering
Component, General Engineering Lab.
Chemistry Research Dept.
Metallurgy & Ceramics Research Dept.
General Motors Corp., Guide Lamp Div., Anderson, Ind.
Research Laboratories Div., Detroit, Mich.

Brown-Lipe-Chapin Div., Syracuse, N. Y. (2 memberships)
Gillette Safety Razor Co., Boston, Mass.
Gould-National Batteries, Inc., Depew, N. Y.
Graham, Crowley & Associates, Inc., Chicago, Ill.
Great Lakes Carbon Corp., New York, N. Y.
Hanson-Van Winkle-Munning Co., Matawan, N. J. (3 memberships)
Harshaw Chemical Co., Cleveland, Ohio (2 memberships)
Hercules Powder Co., Wilmington, Del.
Hooker Electrochemical Co., Niagara Falls, N. Y. (3 memberships)
Houdaille-Hershey Corp., Detroit, Mich.
International Business Machines Corp.,
Poughkeepsie, N. Y.
International Minerals & Chemical Corp., Chicago, Ill.
Jones & Laughlin Steel Corp., Pittsburgh, Pa.
K. W. Battery Co., Skokie, Ind.
Kaiser Aluminum & Chemical Corp.
Chemical Research Dept., Permanente, Calif.
Div. of Metallurgical Research, Spokane, Wash.
Libbey-Owens-Ford Glass Co., Toledo, Ohio
P. R. Mallory & Co., Indianapolis, Ind.
McGean Chemical Co., Cleveland, Ohio
Merck & Co., Inc., Rahway, N. J.
Metal & Thermit Corp., Detroit, Mich.
Minnesota Mining & Mfg. Co., St. Paul, Minn.
Monsanto Chemical Co., St. Louis, Mo.
Motorola, Inc., Chicago, Ill.
National Cash Register Co., Dayton, Ohio
National Lead Co., New York, N. Y.
National Research Corp., Cambridge, Mass.
Norton Co., Worcester, Mass.
Olin Mathieson Chemical Corp., Niagara Falls, N. Y.
High Energy Fuels Organization (2 memberships)
Pennsalt Chemicals Corp., Philadelphia, Pa.
Philips Laboratories, Inc., Irvington-on-Hudson, N. Y.
Pittsburgh Metallurgical Co., Inc., Niagara Falls, N. Y.
Poor & Co., Promat Div., Waukegan, Ill.
Potash Co. of America, Carlsbad, N. Mex.
Radio Corp. of America, Harrison, N. J.
Ray-O-Vac Co., Madison, Wis.
Raytheon Manufacturing Co., Waltham, Mass.
Reynolds Metals Co., Richmond, Va.
Shawinigan Chemicals Ltd., Montreal, Que., Canada
Speer Carbon Co.
International Graphite & Electrode Div., St. Marys, Pa.
(2 memberships)
Sprague Electric Co., North Adams, Mass.
Stackpole Carbon Co., St. Marys, Pa. (2 memberships)
Stauffer Chemical Co., Henderson, Nev., and New York,
N. Y. (2 memberships)
Sunner Chemical Co., Div. of Miles Laboratories, Inc.,
Elkhart, Ind.
Superior Tube Co., Norristown, Pa.
Sylvania Electric Products Inc., Bayside, N. Y. (2 memberships)
Sarkes Tarzian, Inc., Bloomington, Ind.
Tennessee Products & Chemical Corp., Nashville, Tenn.
Texas Instruments, Inc., Dallas Texas
Titanium Metals Corp. of America, Henderson, Nev.
Udylite Corp., Detroit, Mich. (4 memberships)
Victor Chemical Works, Chicago, Ill.
Wagner Brothers, Inc., Detroit, Mich.
Weirton Steel Co., Weirton, W. Va.
Western Electric Co., Inc., Chicago, Ill.
Wyandotte Chemicals Corp., Wyandotte, Mich.
Yardley Electric Corp., New York, N. Y.



ENTHONE

Which metal do you want to strip?

There's an Enthone metal stripper for most applications:

- ENSTRIP "S"** — an additive for sodium cyanide solutions used to dissolve nickel, copper, gold, silver, zinc, cadmium and alloys of these metals from steel without attacking the base metal in any way.
- ENSTRIP "A"** — a fully-prepared alkaline mixture already containing sodium cyanide, used for the same purpose as Enstrip "S".
- ENSTRIP "Z"** — an alkaline stripper that rapidly strips zinc from steel.
- ENSTRIP 103** — an economical, alkaline electrolytic stripper for removing nickel, copper, brass, zinc, silver, gold, cadmium, tin and lead from steel.
- ENSTRIP CR-5** — a rapid, acid-type dry salt stripper that dissolves heavy deposits of chromium from steel, nickel, copper base alloys, stainless steel and aluminum.
- ENSTRIP "T-L"** — a fast-acting, dry alkaline stripper for dissolving tin, lead, solder alloys, tin-zinc alloys and zinc from steel base metals.
- ENSTRIP 165S** — a neutral dry-additive for acid solutions for quick removal of nickel, tin, lead, zinc, cadmium, iron and aluminum from copper and copper base alloys.
- ENSTRIP L-88** — a completely prepared acid electrolytic stripper for removing copper, nickel, chromium, brass, bronze, iron and white brass from zinc-base die castings.

These eight outstanding strippers are "stock" items in the Enthone line of chemicals for the metal finishing and electroplating industries. In most cases, one of the "Enstrips" will prove to be the answer to your problem. On the other hand, special developments are available from Enthone to meet requirements not covered by the Enstrips featured above. Write us, outlining your needs, and include a sample of your product, if possible. We'll be glad to recommend the best stripping method possible.

Write to Dept. J-2

DISTRIBUTION AND SERVICE THROUGHOUT THE UNITED STATES, CANADA, MEXICO, BRAZIL AND EUROPE

PRODUCTS OF *Enthone* THE SCIENTIFIC SOLUTION OF METAL FINISHING PROBLEMS

ENTHONE

ENTHONE
INCORPORATED

442 ELM STREET, NEW HAVEN 11, CONN.
Metal Finishing Processes • Electroplating Chemicals

SUBSIDIARY OF AMERICAN SMELTING AND REFINING COMPANY